# Study of Molecular Properties using Linear Response Approach to Density Functional Theory

Thesis submitted to the
University of Pune
for the degree of

Doctor of Philosophy
in
Chemistry

by

Sophy Bhasi Kunnappilly

Physical Chemistry Division

National Chemical Laboratory

Pune - 411 008 India

March 2007

# Certificate

This is to certify that the work presented in this thesis entitled, **Study of molecular properties using linear response approach to density functional theory** by, **Sophy Bhasi Kunnappilly**, for the degree of Doctor of Philosophy, was carried out by the candidate under my supervision in the Physical Chemistry Division, National Chemical Laboratory, Pune, India. Any material that has been obtained from other sources has been duly acknowledged in the thesis.

Date:

Place:

**Dr. Sourav Pal**
Thesis Advisor
Physical Chemistry Divison
NCL, Pune, India

# Declaration by the Candidate

I declare that the thesis entitled Study of molecular properties using linear response approach to density functional theory submitted by me for the degree of Doctor of Philosophy is the record of work carried out by me during the period from May 2003 to March 2007 under the guidance of Dr. Sourav Pal, and has not formed the basis for the award of any degree, diploma, associateship, fellowship, titles in this or any other University or other institution of Higher learning.

I further declare that the material obtained from other sources have been duly acknowledged in the thesis.

Signature of Candidate

Date:

**. . . to my parents**

# Acknowledgment

I take this opportunity to thank my research guide, Dr. Pal for his encouragement, support and guidance. He has been a source of inspiration throughout the course of my research in NCL, not to mention the lectures he conducted for all of us added immensely to my knowledge. Besides, he has been a friend and a well wisher.

I am grateful to the Director, NCL for providing the infrastructure and facilities for my research during the course of my PhD. I would like to acknowledge the funds from CSIR and BRNS. Annick has been instumental in introducing me and my work to the deMon community. I thank her for all her help.

Thanks to Kausar, I joined the Chemistry Dept. in the University of Pune where I met few more good friends, Prashant, Subashini, Rahul and Milind. I would always cherish the times I had during my M.Sc. days filled with hard work and fun together. It was nice to meet Vishal and Nikhil. I owe my thanks to Prof. Gadre for opening the doors of Quantum Chemistry to me. I am grateful to Dr. Gejji, my project guide for his support, help and for being a friend.

Chandra, Sailaja, Sharan, Nayana, Ramda, Sham made my stay in NCL comfortable as a junior. The interesting discussions about the calculations and properties I had with Chandra were informative. Sailaja helped me initially with the deMon. Chandra, Sharan and Nayana have been more of a friend than seniors. Maneesha has been more than a friend. I thank her for all the love and care she showers on me. Prashant has always been a dear friend whom I have taken for granted for all kinds of help and running around.

In the last two years of PhD., Akhilesh, Sajeev and Daly added to the list of friends. I never felt Bhakti was a junior, we instantly became friends, and hope the friendship would only grow further. Ideh has been very different from the rest of the people in the lab. A truely interesting personality, she can make even a newcomer comfortable. Shobhana, its been a nice association... guess what?.... lunch time association. Bon appetit and there we go with some new and interesting discussion.

My thanks to Sharan for being such a nice friend, and for inspiring me to write my thesis in Latex, and Prashant for helping me out with details. Akhilesh needs a special mention for his help during compilations and installations with different machines and also for the printing of the thesis.

I enjoyed the company of my juniors Tuhina, Rahul, Arijit, Subrata, Saikat, Sumantra, Lalitha, Deepti, Himadri, Sugata and Nilanjan. I thank Sumantra for his last minute help. I thank all the people who have been behind the scenes in making this thesis possible in this form.

Shyam, you have been my inspiration during my thesis writing days. Thanks for all your support and love. Words won't suffice to thank my family, especially my parents for all the sacrifices, support, love, care and freedom. I dedicate my thesis to them.

March 2007 KBS

Pune

# Contents

# Abstract

Response properties using Kohn-Sham density functional theory (KS-DFT) [1,2] have been studied extensively for the past several decades. As a result, different methods have been proposed to study the response properties of molecules and a vast amount of data for the response electric properties, namely, dipole polarizabilities, first-hyperpolarizabilities etc., of certain prototype molecules is available [3]. Study of molecular response properties can be highly useful in marking out the molecules which could be candidates for applications concerning non-linear optical (NLO) materials [4].

Despite the enormous amount of data available for such properties, the ones using rigorous numerical and analytic methods are mostly available for smaller molecules or use smaller basis sets or both. Rest of the available data uses the crude energy based, finite field approach, which could be highly inaccurate for higher order energy derivatives. There is, therefore, a need to explore computationally feasible methods, which can handle large molecules with reasonable accuracy.

The objective of this thesis is to put forward a computationally simplified implementation of the analytic response approach using the coupled-perturbed Kohn-Sham (CPKS) method in DFT for application to larger molecules in combination with finite-field method. We will focus mainly, on the implementation for response electric properties of the molecules. Additionally, we would like to emphasize the scope of the method proposed by us. Our objectives are the following:

1. Outline a clear method for calculation of the response electric properties viable for application to large molecules.

2. Test our method for studying the response properties of some prototype molecules followed by comparison with benchmark *ab initio* results for understanding the accuracy of our results. The feasibility of our method for stretched internuclear distances will also be explored.

3. Carry out the implementation of our proposed formalism in the deMon, which is a software based on DFT for calculation of polarizability and first-hyperpolarizability of molecules.

4. A further implementation on similar lines for the dipole-quadrupole polarizabilities of molecules.

5. Application for some large molecules using reasonably larger basis sets to showcase the feasibility of our method for larger molecules.

The organization of the dissertation work will be as follows:

**Chapter 1**
In chapter 1, we will review the basic DFT [1] and give some details about the exchange-correlation functionals followed by the response theory for obtaining the molecular response properties. Few of the developments concerning the response approach and response properties in the area of DFT that have already taken place will be reviewed. We will then discuss the motivation for our present work.

**Chapter 2**
In chapter 2, we will give a detailed account of the formalism proposed by us, towards developing a simplified linear response approach to DFT for calculating response electric properties, namely, polarizability and first- hyperpolarizability of molecules [5]. Its implementation in the deMon software will also be discussed. The implementation of our method in the deMon-KS, version 3.5 [6], which we tested for some prototype molecules, namely, HF, BH, CO and $H_2O$ [5], (presented in chapter 3) would be discussed in brief. The details of the recent implementation in deMon2k [7] would also be presented. The advantages of the implementation of our formalism for the molecular response property calculation using DFT would be highlighted in this chapter.

**Chapter 3**
In chapter 3, we will discuss the results of polarizability and first-hyperpolarizability obtained using the deMon-KS. The results for HF and BH molecule at different internuclear distances for different basis sets and exchange-correlation functionals and those for equilibrium geometries of CO and H2O molecule will be thoroughly discussed [5]. We will focus on issues like the behaviour of DFT away from equilibrium bond distances and certain other implications of the results.

**Chapter 4**
In chapter 4, we will present the extension of our method to the calculation of

dipole-quadrupole polarizabilities [8]. The details of the implementation for closed shell cases would be discussed. Also, we will present in this chapter, some results for polarizability and hyperpolarizability from our method in comparison with another approximate CPKS method [9] developed by a research group in Mexico. However, we added the hyperpolarizability module to their program. In this chapter we will also discuss details about their CPKS implementation as against our implementation of the CPKS method to the DFT. Additionally, We would also like to discuss the scope of our proposed formalism for DFT.

**Chapter 5**

In chapter 5, we will study two sets of molecules using our method. The first set of system is Sodium atom clusters of even number [5]. We will study the $Na_2$, $Na_4$, $Na_6$ and $Na_8$ clusters using our method and also compare them with *ab initio* calculations. The second set of molecules is para-nitroaniline and its derivatives, which are a highly interesting set of molecules as they are candidates for NLO materials study. We will compare the results with benchmark *ab initio* calculations. We would discuss the results for the above calculations to emphasize the advantages of our method for property calculations for larger molecules using reasonably large basis sets.

## References

[1] (a) R. G. Parr, W. Yang, *Density Functional Theory of Atoms and Molecules*, Oxford University Press, Oxford, (1989). (b) R. M. Dreizler and E. K. U. Gross, *Density Functional Theory*, Springer- Verlag, New York, (1990).
[2] W. Kohn and L. J. Sham, *Phys. Rev.* **140**, A1133 (1965).
[3] (a) G. Senatore and K. R. Subbaswamy, *Phys. Rev. A* **34**, 3619 (1986). (b) P. G. Jasien and G. Fitzgerald, *J. Chem. Phys.* **93**, 2554 (1990). (c) J. Moullet and J. L. Martins, *J. Chem. Phys.* **92**, 527 (1990). (d) M. K. Harbola, *Chem. Phys. Lett.* **217**, 461 (1994). (e) S. M. Colwell, C. W. Murray, N. C. Handy and R. D. Amos, *Chem. Phys. Lett.* **210**, 261 (1993). (g) J. Guan, P. Duffy, J. T. Carter, D. P. Chong, K. C. Casida, M. E. Casida and M. Wrinn, *J. Chem. Phys.* **98**, 4753 (1993). (h) C. Jamorski, M. E. Casida, and D. R. Salahub, *J. Chem. Phys.* **104**, 5134 (1996).
[4] A. A. Hasanein, In *Modern Nonlinear Optics*, Part 2, M. Evans and S. Kielich, Ed., *Adv. Chem. Phys.* Vol. LXXXV, Wiley, New York (1993).
[5] (a) K. B. Sophy and S. Pal, *J. Chem. Phys.* **118**, 10861 (2003). (b) K. B. Sophy and S. Pal, *J. Mol. Struc.: THEOCHEM* **676**, 89 (2004). (c) S. Pal and K. B. Sophy, *Lect. Series in Comp. and Comp. Sc.* **3**, 142 (2005). (d) K. B. Sophy, P. Calaminici, S. Pal, *J. Chem. Theory Comp.* (2007) (In Press)
[6] (a) A. St-Amant, D.R. Salahub, *Chem. Phys. Lett.* **169**, 387 (1990). (b) A. St-Amant, Ph.D. thesis, University of Montreal (1992). (c) M.E. Casida, C. Daul, A. Goursot, A. Koester, L. Pettersson, E. Proynov, A. St.-Amant, D. Salahub, principal authors, S. Chreties, H. Duarte, N. Godbout, J. Guan, C. Jamorski, M. Leboeuf, V. Malkin, O. Malkina, F. Sim, A. Vela, contributing authors, DEMON-KS version 3.5, DEMON Software, 1998.
[7] deMon2k (Version 1.07, Dec. 2004) Copyright (C) By the National Research Council, Ottawa, Canada, Authors: Andreas M. Koester, Patrizia Calaminici, Roberto Flores, Gerald Geudtner, Annick Goursot, Thomas Heine, Florian Janetzko, Serguei Patchkovskii, J. Ulises Reveles, Alberto Vela and Dennis R. Salahub.
[8] G. Maroulis, *J. Chem. Phys.* **105**, 8467 (1996). (and references therein)
[9] deMon2k (Version 2.2.4, July 2006) Copyright (C) by The International DeMon Developers Community, Authors: Andreas M. Koster, Patrizia Calaminici, Mark E. Casida, Roberto Flores-Moreno, Gerald Geudtner, Annick Goursot, Thomas Heine, Andrei Ipatov, Florian Janetzko, Jorge M. del Campo, Serguei Patchkovskii, J. Ulises Reveles, Alberto Vela and Dennis R. Salahub.

# List of Figures

# List of Tables

Chapter 1

# Introduction

The area of non-linear optics (NLO) has been in the limelight for the past few decades due to the development in the field of laser technology. These developments have further advanced the research on potential NLO materials. As a result, the calculation of molecular response properties have been gaining considerable attention. These calculations can be highly intuitive in giving cue for identification of technologically and mechanically important materials for NLO applications.

Electric properties, in particular, have been studied for a wide variety of atoms, molecules and clusters in the past using a spectrum of different approaches. Density functional theory (DFT) has been widely popular for calculation of electronic structure and properties of such molecules. The popularity is due to the exactness of the theory in principle and the simple working equations due to the use of electron density as a basic variable in the entire framework of the theory. Further, electron correlation effects and basis sets are known to play an important role in the determination of these molecular response properties. However, as the size of the system under study and basis set size increases, it becomes utterly impracticable to use the more rigourous *ab initio* methods. Although, the Hartree-Fock (HF) theory provides an option in terms of computational feasibility it lacks the effects of dynamical electron correlation. DFT on the other hand, can take care of this problem with relative ease. It takes care of the electron-correlation effects and at the same time scales similar to the HF theory in terms of the computational time. This is due to the Kohn-Sham (KS) method in DFT, which further transforms the working equations to single-particle form thus converting the theory into a prac-

tical tool for large scale applications. In this thesis, we present a simplified linear response approach for studying the response electric properties of molecules using KS-DFT.

## 1.1 Wavefunction Theory

Obtaining the solutions of the Schrödinger eigenvalue equations have been the primary goal of quantum mechanics. For an isolated N-electron atomic or molecular system in the Born-Oppenheimer nonrelativistic approximation, this is given by,

$$\hat{H}\Psi = E\Psi \tag{1.1}$$

where, E is the electronic energy, $\Psi$=$\Psi$($x_1$, $x_2$, ... $x_n$) is the wavefunction which describes the state of the N-electron quantum-mechanical system and is a function of the space-spin coordinates, $x_i$, of all the electrons of the system, and H is the Hamiltonian operator which constitutes the following terms:

$$\hat{H} \;=\; -\sum_{i=1}^{N}\frac{1}{2}\nabla_i^2 + \sum_{i=1}^{N}\nu(r_i) + \sum_{i<j}^{N}\frac{1}{r_{ij}} \tag{1.2}$$

where, the first term is, T, the kinetic energy (KE) operator, last term is $V_{ee}$, the electron-electron repulsion energy operator, the middle term is $V_{ne}$, the nuclear-electronic interaction operator, where, the external potential due to the nuclei can be given as,

$$\nu(r_i) = -\sum_{\alpha}\frac{Z_\alpha}{r_{i\alpha}} \tag{1.3}$$

and Eq. 1.2 could be more compactly written as,

$$\hat{H} = \hat{T} + \hat{V}_{ne} + \hat{V}_{ee} \tag{1.4}$$

The total energy is obtained after adding the nuclear-nuclear repulsion energy, $V_{nn}$ to the electronic energy, E after solving the Schodinger equation. The $V_{nn}$ term is a constant for a fixed arrangement of the nuclei and could be added before or after the calculation. When the system is in a state $\Psi$, which may or may not satisfy

the Schrödinger equation, the average of many measurements of the energy or the expectation value of the energy is given by,

$$E[\Psi] = \frac{\langle \Psi | \hat{H} | \Psi \rangle}{\langle \Psi | \Psi \rangle} \tag{1.5}$$

Since, each measurement of energy gives one of the eigenvalues of H, we have,

$$E[\Psi] \geq E_0 \tag{1.6}$$

Thus, energy computed from the guess wavefunction is an upper bound to the true ground state energy, $E_0$. There are different *ab initio* theories namely the more rigourous theories like the coupled-cluster theory (CC), Moeller-Plesset (MP) perturbation theory, configuration interaction (CI) theory, etc., which attempt to solve the Schrödinger equation.

### 1.1.1 Hartree-Fock Theory

Hartree-Fock (HF) theory [1, 2] is the simplest of the *ab initio* methods due to its single-particle equations and is the starting point for understanding the other much complex theories. We describe here the HF theory in brief. The electronic Hamiltonian in the HF framework is,

$$\hat{H} = \hat{T} + \hat{V}_{ne} + J - K \tag{1.7}$$

Although the KE is written in terms of a non-interacting operator for the sake of simplifying the equations, the electrostatic coulomb interaction, J, is obtained in an average manner. The exchange energy term, K, accounts for the interaction between the electrons of parallel spin, however, the interaction between the electrons of opposite spin (correlation energy contribution) is missing in the HF theory. The energy, E is a functional of the wavefunction which is approximated as a single Slater determinant constructed using an orthonormal set of single-electron spin-orbital functions. The method of Lagrange undetermined multipliers is used to solve the HF matrix eigenvalue equation for stationarity of the energy functional.

In the process the spin-orbitals are varied under the constraint that the spin-orbitals form an orthonormal set.

$$\int \Psi(i)\Psi(j) = \delta(ij) \tag{1.8}$$

The Euler-Lagrange equation for stationarity of the energy is,

$$\partial E = \partial\langle\Psi|\hat{H}|\Psi\rangle - E\partial\langle\Psi|\Psi\rangle = 0 \tag{1.9}$$

At the end one thus obtains a Slater determinant corresponding to the best set of spin-orbitals and consequently the minimum energy or the ground state energy of the system. An elaborate discussion of the HF theory could be found in the chapter 3 of the book by Szabo and Ostlund [3]. The alternative to using the 3N-dimensional wavefunction is to use methods based on the electron density. Unlike the wavefunction the electron density not only has a physical significance but is also a measurable quantity.

## 1.2 Density Theory

The idea of using the 3-dimensional electron density as a basic variable for studying an N-electron quantum-chemical system originated in 1920's as a result of the independent works of Thomas and Fermi. The model used statistical considerations to approximate the electronic distribution in an atom and is known as the Thomas-Fermi (TF) model [4, 5]. The original papers were translated into English by March in 1975 [6].

### 1.2.1 Thomas-Fermi Model

In this approximation the electrons are treated as independent particles forming a uniform electron gas and the electron-electron repulsion energy arises solely due to electrostatic interactions. The KE corresponds to a noninteracting system with the electron density, $\rho$(r). The TF energy functional can be written as:

$$E_{TF}[\rho(r)] = C_F \int \rho^{\frac{5}{3}}(r)dr - Z\int \frac{\rho(r)}{r}dr + \frac{1}{2}\int\int \frac{\rho(r_1)\rho(r_2)}{|r_1 - r_2|}dr_1 dr_2 \tag{1.10}$$

and,

$$C_F = \frac{3}{10}(3\pi^2)^{\frac{2}{3}} = 2.871$$

where, the first term is the KE, second term is the external potential and the last term is the classical coulomb energy term. The energy functional is then minimized under the constraint that the electron densities should integrate to the total number of electrons in the system to obtain the ground state electron density of the system.

$$\int \rho(r)dr = N \tag{1.11}$$

The TF method has been used in the past for calculations for atoms and molecules and a quite a bit of literature is available [7, 8, 9]. The early works have been reviewed by Gombas and by March [10, 11]. The applications to atoms and molecules have been reviewed by March (1981) [12]. The TF method was found to give a very crude description of the electron density and the electrostatic potential. Lieb and co-workers have researched the TF method and proved a number of theorems [13, 14, 15, 16]. It was shown that the TF scheme is exact in the limit of infinite nuclear charge.

However, the TF model has a number of deficiencies; some severe ones include the infinite charge density at the nucleus. Also, the charge density does not decay exponentially away from the nucleus of the atom. The method does not account for binding of atoms to give molecules or solids. The model lacks the shell structure in the atom. All these and a few other defects have led to the modification of the model. There were subsequent modifications to the TF model by Dirac, wherein, an exchange term was added to the TF equations [17]. This additional exchange energy term, $K_D$, was given to be,

$$K_D[\rho] = C_x \int \rho^{\frac{4}{3}}(r)dr \tag{1.12}$$

where,

$$C_x = \frac{3}{4}\left(\frac{3}{\pi}\right)^{\frac{1}{3}} = 0.7386$$

This model was called the Thomas-Fermi-Dirac (TFD) model. Von Wiezsacker added a gradient term to the KE term of the TF model. This model came to be

known as Thomas-Fermi-Weizsacker (TFW) model [18]. The review by Lieb on TF and related theories of atoms and molecules could be seen for more information on this topic. Despite the flaws in the TF model, it came to be known as the first approximation to the exact description of the ground state of any system in terms of the density; this turns out to be a density functional description, where, all properties of a system can be expressed in terms of the electron density, $\rho$, i.e. the number of electrons per unit volume, as it varies through space. The charge density or electron density can be expressed in terms of the wave function as:

$$\rho(r_1) = N \int \int |\Psi(x_1, x_2, \ldots, x_N)|^2 ds_1 dx_2 \ldots dx_N \tag{1.13}$$

where, $\rho(r_1)$, is a simple non-negative function of the three variable, x, y, and z, integrating to the total number of electrons, N.

### 1.2.2 The X$\alpha$ Method

Slater proposed a new method called the X$\alpha$ method which is a combination of the HF model and the TFD model [19]. Here, Slater uses the TDF exchange potential with a numerical prefactor, $\alpha$, which appears as a parameter in the theory and employs the KE part of the HF model. He thus put forth a simplification to the integro-differential equations of the HF model. His idea was to keep the KE as in HF model, and instead, apply a statistical approximation to the exchange part of the potential. This corrects the deficiency of the TFD model, and, at the same time, simplifies the HF model drastically. Techniques for solving the X$\alpha$ equations, choosing $\alpha$ values, and many calculated results, are described in detail in the reviews of Slater, Johnson and Connolly, and in the book by Slater [20, 21, 22, 23]. The TFD and the X$\alpha$ methods have been compared in detail by Slater [24] and the article by Gasper [25] justifies the $\alpha$=1 value. The X$\alpha$ method may be regarded as a density functional scheme with neglect of correlation and with approximation to the exchange energy.

### 1.2.3 Density Matrix Theory

If the density contains all the information about the system and can determine all properties, then the first-order reduced density matrix should hold even more information about the system. The formal expression of the first order reduced density matrix or the one-matrix in terms of the wavefunction is:

$$\gamma_1(x_1', x_1) = N \int \Psi^\star(x_1, x_2, \ldots, x_N)\Psi(x_1, x_2, \ldots, x_N)dx_2 dx_3 \ldots dx_N \tag{1.14}$$

The diagonal elements of the one-matrix, $\gamma_1$, are the electron density; as a result the trace of the one-matrix gives the number of electrons of the system, whereas, the second-order density matrix, $\gamma_2$, normalizes to the number of electron pairs. The idea is to have a whole new theory, which can be constructed using density matrices alone. And, since, the basic Hamiltonian has only one-electron and two-electron operators, the first-order and second-order reduced density matrices should suffice for construction of the energy expression where all the terms and the energy itself is a functional of the density matrix. In fact the $\gamma_1$ can be obtained from $\gamma_2$ by quadrature as:

$$\gamma_1(x_1', x_1) = \frac{2}{N-1} \int \gamma_2(x_1' x_2, x_1 x_2)dx_2 \tag{1.15}$$

The reduced density matrices $\gamma_1$ and $\gamma_2$ are co-ordinate space representation of the operator $\hat{\gamma}_1$ and $\hat{\gamma}_2$ acting, respectively, on the one- and two-particle Hilbert spaces. The eigenfunctions of $\hat{\gamma}_1$ are called the natural spin orbitals and the eigenvalues are the occupation numbers. It is because of Eq. 1.15, the second-order density matrix alone, is needed to obtain the energy expression, which can be integrated over spin to get the expression in terms of the spinless density matrices [26, 27, 28]. So, now, the equations need to be minimized with respect to the second-order density matrix only. As a result, a lot of research has been done in the hope to avoid the 4N-dimensional $\Psi$ [29, 30, 31, 32, 33, 34, 35, 36, 37]. Even the HF theory has been reworked in the density matrix language by Lowdin [38]. However, the major obstacle in implementing this idea, was realized pretty much in the beginning. The trial $\gamma_2$ must correspond to some antisymmetric wavefunction, $\Psi$. This is the

N-representability (discussed later) problem for the second-order density matrix.

## 1.3 Density Functional Theory

Despite the TF and other models propagating the use the of electron density based theories, the actual justification for using the electron density as a basic variable and expressing energy as a functional of the ground state electron density came from the landmark papers of Hohenberg and Kohn (HK) in 1964 [39]. The idea of the energy being a functional of the exact ground state electron density was based on the following theorems.

### 1.3.1 The Hohenberg-Kohn Theorems

Hohenberg and Kohn put forth two theorems, the first HK theorem said that, for a non-degenerate ground state of an electronic system the electron density, $\rho$(r), uniquely determines, within a trivial additive constant, the external potential, $\nu$(r). The simple proof for this theorem can be found illustrated on p. 51 of reference [40]. Since $\rho$ determines the number of electrons N (by simple quadrature from eqn. 11) and the $\nu$(r), it fixes the Hamiltonian H of the system and thus determines the ground state wavefunction $\Psi$ and all other electronic properties of the system including the KE, T[$\rho$], potential energy V[$\rho$] and the total energy E[$\rho$]. We now write $E_\nu$ instead of E to make the dependence on $\nu$ explicit.

$$\begin{aligned} E_\nu[\rho] &= T[\rho] + V_{ne}[\rho] + V_{ee}[\rho] \\ &= \int \rho(r)\nu(r)dr + F_{HK}[\rho] \end{aligned} \tag{1.16}$$

Here, the $F_{HK}[\rho]$ is a universal HK functional of $\rho$(r) and is independent of the external potential, $\nu$(r). It depends only on the number of electrons and constitutes,

$$F_{HK}[\rho] = T[\rho] + V_{ee}[\rho] \tag{1.17}$$

The $V_{ee}$ contains the classical repulsion term J[$\rho$],

$$J[\rho] = \frac{1}{2}\int\int \frac{1}{r_{12}}\rho(r_1)\rho(r_2)dr_1dr_2 \tag{1.18}$$

and the non-classical term, the major part of which, is the exchange-correlation energy. Once the form of $F_{HK}[\rho]$ is known, the exact ground state energy of the system could be determined. However, the exact form of the universal HK functional is not known. The first HK theorem is thus merely an existence theorem for the energy functional.

The second HK theorem gives an energy variational principle or a variational bound to the energy functional, which means, for any given trial density, $\tilde{\rho}$(r) such that, $\tilde{\rho}(r) \geq 0$, $\int \tilde{\rho}(r)dr = N$, and $\rho(r)$ is non-negative, the energy functional is always greater than or equal to the exact ground state energy, $E_0$.

It can be seen that the determination of the form of the $F_{HK}[\rho]$ is the crucial part in construction of the energy functional for obtaining the exact ground state energy. Since, the form of the $F_{HK}[\rho]$ is unknown, lot of research has been directed towards finding the best approximation for it in the hope to take advantage of the formal exactness of the theory for obtaining the exact ground state energy of the system.

### 1.3.2 The v- and N-representability problem

When we say that the ground state electron density can give all the electronic properties of the system, the electron density has to be v-representable and all functionals of the density are defined only for v-representable electron densitites. The electron density may or may not be v-representable. An electron density is v-representable if it is associated with an antisymmetric ground state wavefunction of a Hamiltonian of the form in Eq. 1.2, corresponding to an external potential $\nu$(r). It is this unique mapping between the v-representable density, $\rho$(r) and the ground state wavefunction $\Psi$ that facilitates in obtaining all the electronic properties of the state.

From the second HK theorem, we have for all v-representable densities,

$$E_\nu[\rho_0] = E_0 \leq E_\nu[\tilde{\rho}] \tag{1.19}$$

where, $E_\nu[\rho_0]$ is the ground state energy of the Hamiltonian with $\nu$(r) as the external potential and $\rho_0$ the ground state electron density. As mentioned earlier, not all electron densities are v-representable, and infact, many resonable densities have been shown to be non-v-representable by Levy and Lieb in 1982 [41, 42]. This is a serious problem that needs to be countered. It was later discovered that, the electron density in the functionals and the variational principle can be made to satisfy a much weaker condition called the N-representability by formulating the DFT in a different manner. N-representability is a pre-requisite for the v-representability condition and any reasonable density that can be obtained from some antisymmetric wave function is N-representable. The works of Gilbert and Harriman, in particular, could be referred for more details about the N-representability [34, 43].

### 1.3.3 Constrained-search formulation of Levy

The N-representability of the electron density now poses a new problem. We found a one-to-one correspondence between the ground state wave function, $\Psi_0$ and the ground state electron density, $\rho_0$. $\rho_0$ can be obtained from $\Psi_0$ by simple quadrature, but, the reverse is not as trivial, since, the $\rho_0$ can be obtained from an infinite number of antisymmetric wavefunctions, which do not necessarily correspond to any ground state and yet give the same density. The answer is simple [44, 41, 45], and the constrained-search formulation of Levy can be used to understand it. Since, the external potential is a simple functional of the density, we have,

$$E_\nu[\rho] = F_{HK}[\rho] + \int \nu(r)\rho(r)dr \geq E_\nu[\rho_0] \tag{1.20}$$

which means that, among all the wavefunctions giving the ground state density $\rho_0$, only the ground state wavefunction, $\Psi_0$, minimizes the expectation value of $\langle \hat{T} + \hat{V}_{ee} \rangle$.

$$\langle \Psi_{\rho_0} | \hat{T} + \hat{V}_{ee} | \Psi_{\rho_0} \rangle \geq \langle \Psi_0 | \hat{T} + \hat{V}_{ee} | \Psi_0 \rangle = F_{HK}[\rho_0] \tag{1.21}$$

So, we have, $F_{HK}[\rho_0]$, the universal functional of the v-representable density,

$$F_{HK}[\rho_0] = Min\langle\Psi|\hat{T} + \hat{V}_{ee}|\Psi\rangle \ldots for\ \Psi \rightarrow \rho_0 \tag{1.22}$$

where, the Levy's constrained-search approach requires a search to be done over all the antisymmetric wavefunctions that give the electron density, $\rho_0$, for $F_{HK}[\rho_0]$ to give a minimum. Thus, Levy's method not only proves the first HK theorem, but also, gets rid of its initial limitation that, the density should correspond to a non-degenerate ground state. With this constrained-search, only the wave function corresponding to the $\rho_0$ would be selected out of the set of degenerate wavefunctions. Here, the variational search is over the space of trial wavefunctions, which give the density $\rho_0$ as against the search for a minimum of the energy functional, where, the only constraint is on the normalization of the wavefunction.

Levy's method, thus, saves the task of scanning the entire N-particle Hilbert space for searching the ground state wavefunction. As the set of trial wavefunctions chosen are antisymmetric, it adheres to the N-representability criterion, and, as long as the $\rho_0$ is obtained from an antisymmetric wavefunction, we need not bother about the v-representability of the electron density on the domain of variation in the HK variational principle. The method thus, gives us freedom from explicitly searching for a v-representable density and we can simply take into account the N-representability, which requires nothing more than the non-negativity, proper normalization, and continuity of the trial electron densities.

### 1.3.4 Kohn-Sham Method

The true practical applicability of the DFT for rigourous calculations came after Kohn and Sham proposed a clever indirect approach to the KE functional, $T[\rho]$ in 1965 [50]. The energy functional has the form as in Eq. 1.16 and the $F_{HK}[\rho]$ in Eq. 1.17 would be referred to as $F[\rho]$ hereon. The ground state density minimizes the $E[\rho]$ and thus, satisfies the Euler-Lagrange equation.

$$\left[\frac{\partial E[\rho]}{\partial \rho}\right] = \ \mu = \ \nu(r) + \frac{\partial F[\rho]}{\partial \rho(r)} \tag{1.23}$$

where, $\mu$ is the Lagrange multiplier associated with the constraint of Eq. 1.11 $\mu$ is a measure of the escaping tendency of the electronic cloud and is called the chemical potential. It is a constant, through all space for the ground state of a system.

We now discuss the general idea of the Kohn-Sham (KS) method. The exact form of the KE functional and the electron density in terms of the natural spin orbitals, $\phi_i$, and their occupation numbers, $n_i$, are,

$$T[\rho] = \sum_{i=1}^{N} n_i \langle \phi_i | -\frac{1}{2}\nabla^2 | \phi_i \rangle \tag{1.24}$$

$$\rho(r) = \sum_{i=1}^{N} n_i \sum_{s} |\phi_i(r,s)|^2 \tag{1.25}$$

The $\phi_i$ and $n_i$, are the eigenfunctions and eigenvalues of the first order reduced density matrix, $\gamma_1$ of Eq. 1.14, respectively. Here, the $n_i$'s require to be $0 \leq n_i \leq 1$, by the Pauli's principle. However, there are infinite possibilities for the above two expressions, of the KE functional and the electron density, of an interacting N-electron system. Kohn and Sham proposed to put $n_i = 1$ for N orbitals and $n_i = 0$ for the rest of them, thus, simplifying the expressions of KE functional and the electron density to,

$$T_s[\rho] = \sum_{i=1}^{N} \langle \phi_i | -\frac{1}{2}\nabla^2 | \phi_i \rangle \tag{1.26}$$

$$\rho(r) = \sum_{i=1}^{N} \sum_{s} |\phi_i(r,s)|^2 \tag{1.27}$$

where, $T_s[\rho]$ constitutes the major part of the exact KE. It corresponds to a non-interacting system, whereas, the $\rho(r)$ corresponds to an interacting system. The above description of $T_s[\rho]$ and $\rho(r)$ fits exactly with the determinantal form of the wavefunction for a noninteracting system of N-electrons. However, a similar problem of a unique decomposition of $\rho(r)$, which we touched upon earlier, but here, in terms of the orbitals to give a unique value of $T_s[\rho]$ comes up. To address this, KS invoked a corresponding reference noninteracting system with the Hamiltonian,

$$\hat{H}_s = \sum_{i}^{N} \left( -\frac{1}{2}\nabla_i^2 \right) + \sum_{i}^{N} \nu_s(r_i) \tag{1.28}$$

where, $\nu_s(r_i)$ does not contain the electron-electron repulsion term and the ground state electron density is $\rho(r)$ of Eq. 1.27. This $\rho(r)$ requires to be noninteracting v-representable; which means there needs to exist a noninteracting ground state with this $\rho(r)$. It turns out, however, that the $T_s[\rho]$ of Eq. 1.26, can be defined for any density obtained from an antisymmetric wavefunction. Although, $T_s[\rho]$ is uniquely defined for any density, it is not the exact KE, $T[\rho]$, but an exact component of it. The theory thus is of independent- particle form and yet exact. The F$[\rho]$ can now be separated into the following components as,

$$F[\rho] = T_s[\rho] + J[\rho] + E_{xc}[\rho] \tag{1.29}$$

where, the exchange-correlation energy, $E_{xc}[\rho]$ contains the non-classical part of the electron-electron repulsion energy and the remaining smaller part of the KE, i.e., $T[\rho] - T_s[\rho]$. The $T[\rho]$ is the exact KE.

The KS potential is defined as,

$$\begin{aligned} \nu_{eff}(r) &= \nu(r) + \frac{\partial J(\rho)}{\partial \rho(r)} + \frac{\partial E_{xc}[\rho]}{\partial \rho(r)} \\ &= \nu(r) + \int \frac{\rho(r')}{|r - r'|} dr' + \nu_{xc}(r) \end{aligned} \tag{1.30}$$

where, $\nu_{xc}$ is the exchange-correlation potential,

$$\nu_{xc} = \frac{\partial E_{xc}[\rho]}{\partial \rho(r)} \tag{1.31}$$

Rearranging the Eq. 1.23, the Euler equation now becomes,

$$\mu = \nu_{eff}(r) + \frac{\partial T_s[\rho]}{\partial \rho(r)} \tag{1.32}$$

$\rho(r)$ that satisfies Eq. 1.32, can be obtained from a given $\nu_{eff}(r)$ by solving N single-particle equations of the form,

$$\left[ -\frac{1}{2}\nabla^2 + \nu_{eff}(r) \right] \phi_i = \varepsilon_i \phi_i \tag{1.33}$$

where, the $\rho(r)$ is constructed using Eq. 1.27. Since, $\nu_{eff}(r)$ depends on $\rho(r)$, Eq. 1.33 needs to be solved self-consistently.

Eq. 1.30, 1.31 and 1.33 along with the expression for $\rho(r)$, i.e., Eq. 1.27 constitute the KS equations. However, for molecules an introduction of a basis is required, where, the molecular orbitals, $\phi_i$'s, are written as linear combination of the atomic orbitals (LCAO) in terms of contracted Gaussian functions, $\chi$'s, centered on atoms.

$$\phi_i(r) = \sum_{\mu}^{N} C_{\mu i}\chi_\mu(r) \tag{1.34}$$

The electron density can now be written as,

$$\rho(r) = \sum_{\mu}^{N}\sum_{\nu}^{N} P_{\mu\nu}\chi_\mu(r)\chi_\nu^*(r) \tag{1.35}$$

where, $P_{\mu\nu}$ is the density matrix. The single particle KS-DFT equations in Eq. 1.33 now gets transformed to the Kohn-Sham (KS) matrix equation.

$$HC = SCE \tag{1.36}$$

where, H is KS operator matrix in the AO basis, C is the coefficient matrix, the S is the overlap matrix and E is the energy matrix.

The total energy can be obtained by substituting the Eq. 1.29 for F[$\rho$] in that for E[$\rho$] below,

$$E[\rho] = \int \nu(r)\rho(r)dr + F[\rho] \tag{1.37}$$

The review articles on DFT are informative and make for an interesting reading [46, 47, 48, 49].

## 1.4 Exchange-Correlation Functional

The exchange-correlation functional, $E_{xc}[\rho]$, as mentioned earlier constitutes the non-classical part of the electron-electron repulsion term and a small part of the kinetic energy. The exchange-correlation term in the energy expression decides the accuracy of the DFT calculations. However, its exact form is unknown and a number of approximations are available and this makes an interesting topic of research in itself, which is being pursued by many researches.

The simplest approximation for the $E_{xc}[\rho]$ is, the local density approximation, LDA, first proposed by Kohn and Sham [50], which approximates the electron density of the system as a homogeneous electron gas, where, the energy per particle is estimated separately for the exchange and the correlation terms and the exchange-correlation energy functional for the LDA is,

$$E_{xc}^{LDA}[\rho] = \int \rho(r)(\varepsilon_x(\rho) + \varepsilon_c(\rho))dr \tag{1.38}$$

The exchange part, $\varepsilon_x(\rho)$, is given by the Dirac exchange [17] term and the correlation term by the analytic form put forth by Vosko, Wilk and Nusair [51] in 1980. There is also the spin density analog of the LDA called the local spin-density (LSD) approximation.

Although, it is well known that the LDA suits best for cases with slowly varying density, there are hundreds of application of the LDA to the atoms and molecules [52] which show inhomogeneity in their electronic distribution. In spite of the fact, that, the binding energies from the LDA are overestimated by about 10%, the quantities that involve difference of energies tend to come out quite good. The LDA thus, has a tendency to over bind. This is mainly due to the mutual cancellation of errors between the exchange and correlation terms. However, LDA is not accurate for chemical applications, which require the determination of energy differences with considerable precision. To improve the LDA approximation, one needs to have a functional that includes the gradients of the electron density. The gradient-corrected functional are of the form,

$$E_{xc}^{GGA} = \int f(\rho(r), \nabla\rho(r))dr \tag{1.39}$$

These functionals reduce the errors considerably in comparison to the LDA. However, there are too many such functionals in use in the literature, each of them yielding different energies for the same system, which, unlike in the *ab initio* methods, make benchmarking in DFT difficult. These functionals could in general be classified as, the functionals constructed holding LDA as a precursor, i.e., whose construction is based on the uniform electron gas [53, 54, 55, 56, 57, 58, 59, 60, 61, 62],

and the semi-empirical functional [63, 64, 65, 66, 67, 68, 69], which contains one or more parameters fitted to a particular finite system or class of systems. Such functionals are called generalized gradient approximations (GGAs) in the literature, even though it originally meant only the functionals constructed from LDA [57]. Among the earlier developed functionals, the PW91 [60] derived from the LDA contains no empirical input, and the Becke [70] exchange and the Lee-Yand-Parr [71] correlation functional (BLYP) constructed from the Colle-Salvetti correlation energy formula [72] belong to the category of semi-empirical functionals, and are still popular. The GGAs provide significant improvements upon the results obtained from the local schemes and their introduction have led to development of a large number of exchange-correlation functionals. However, for describing many of the chemical aspects of molecules the accuracy of the GGAs are not sufficient, which means that, the functionals need to be improved further. The GGAs could be further improved by mixing different functionals together along with the HF exchange to obtain a new functional. This is the basic idea of the hybrid exchange-correlation functionals and B3LYP is an example of one such commonly used hybrid functional. Unlike in the HF theory, the electron-electron repulsion term in the DFT has the self-interaction which is basically the interaction of an electron with itself. This term is zero in case of HF and other *ab initio* methods. There are therefore, self-interactions corrected (SIC) exchange-correlation functionals. An example is the SIC-method of Perdew et al. [74], which determines the self-interaction corrected exchange-correlation energy. Then, there are the class of meta-GGAs, which have a dependence on the higher order derivatives of the electron density and/or the kinetic energy density in addition to the electron density and its gradient.

## 1.5 Gaussian basis sets

In modern quantum chemistry programs for electronic structure and property calculations, Gaussian type functions (GTFs) [75] centered on atoms are used in the

LCAO framework given in Eq. 1.34 to describe the AOs in a molecule. The actual orbitals are more correctly described by the Slater type orbitals (STOs), however use of GTOs offers simplification in the calculations, which makes it the obvious choice for quantum chemical calculations. This can be justified by the fact that, the product of two Gaussians is a Gaussian. However, the loss in accuracy decreases, as more number of primitive Gaussian functions are added to obtain a contracted Gaussian function for describing the orbitals. The GTO has the form,

$$\phi_{GTO}(x, y, z) = N x^l y^m z^n e^{-\zeta r^2} \tag{1.40}$$

where, N is the normalization constant, x, y, z are the atom-centered cartesian coordinates, l, m, n are positive integers which more or less describes the angular momentum of the orbital, r is the radial distance to the atomic center, and $\zeta$ is a positive orbital exponent. A large exponent gives a more dense and compact description, whereas a small exponent gives a diffuse description for the orbital. The coefficients of expansion are used in the Eq. 1.34 to obtain the contracted Gaussian orbital. Spherical orbitals are usually given by, l=m=n=0, a $p_x$ orbital is given by, l=1, m=n=0, a $d_{xy}$ orbital is given by l=m=1, n=0, etc. Alternatively, the description can be improved by having more primitive Gaussians in the linear combination. Also, polarization and diffuse functions are added to the basis set to improve the performance of the basis set. For a more detailed reading about the basis sets one could refer to the chapter 3, section 3.6 of Ref. [3] and Ref. [76].

## 1.6 Response Properties

Response properties of molecules have been a topic of extensive research and a lot of literature is available for different kinds of properties both static and dynamic using different theoretical approaches. A change in the environment of a molecule has an effect on the structural and electronic property of the molecule. Especially, in case of a weak external perturbation the effects on the electronic distribution of the molecule, is manifest in the response property of the molecule. The response

property is basically the derivative of energy with respect to the perturbation concerned. The properties can, in general, be classified as electric, magnetic, etc. depending on the perturbation. In principle, to obtain the response properties of a particular order one would require to evaluate explicitly the corresponding order derivative of energy with respect to the perturbation concerned. This may, however, be too complicated and time consuming depending of the nature of the theory being used. Calculation of the energy derivatives can be done in two ways. The preferred method is the finite difference formulae. An alternative method consists of calculating a number of energy values close to the point, where, the derivative is to be evaluated, and fitting an analytical approximation, usually a polynomial to the points. However, the method has a lot of numerical instabilities, unless the number of points greatly exceeds the order of derivatives sought. The analytical calculation of energy derivatives has two advantages over the numerical procedure. It is usually more efficient and more accurate numerically. However, the main disadvantage of analytical derivative methods is the significant amount of programming involved to implement them. There have been lot of approaches to obtain the response properties reported in literature. In the following section, we describe the general response approach for the response electric properties, before we review other approaches reported in literature.

## 1.7 Response Approach

In presence of a weak external electric field perturbation, molecular Hamiltonian tends to have a explicit dependence on the perturbation. The Hamiltonian, in general, could be written as,

$$H(F) = H^{(0)} - \mu_i F_i - \frac{1}{3}\theta_{ij} F_{ij} - \dots \tag{1.41}$$

where $H^{(0)}$ is that for the unperturbed molecule and $\mu_i = \sum_a e_a r_{ai}$ and $\theta_{ij} = \theta_{ji} = \frac{1}{2}\sum_a e_a(3r_{ai}r_{aj} - r_i^2\delta_{ij})$ are the dipole and quadrupole moment operators; i and j span the x, y, z directions, $F_i$ is the electric field component and $F_{ij}$ is the electric

field gradient, which denotes the non-homogeneous nature of the electric field and so on. The energy of such a system would also have a dependence on the field, F and can be expanded in a Taylor series as,

$$E(F) = E^{(0)} - \mu_i^{(0)} F_i - \frac{1}{2}\alpha_{ij} F_i F_j - \frac{1}{6}\beta_{ijk} F_i F_j F_k - \frac{1}{3}\theta_{ij}^{(0)} F_{ij} - \frac{1}{3} A_{i,jk} F_i F_{jk} - \frac{1}{6} B_{ij,kl} F_i F_j F_{kl} - \ldots \quad (1.42)$$

where, $\mu_i^{(0)}$ is the permanent dipole moment, $\alpha_{ij}$ is the dipole-dipole polarizability (referred to as polarizability), $\beta_{ijk}$ is the dipole-dipole-dipole hyperpolarizability (referred to as dipole first hyperpolarizability)and so on. Similarly, $\theta_{ij}^{(0)}$ is the quadrupole moment, $A_{i,jk}$ is the dipole-quadrupole polarizability and $B_{ij,kl}$ is the quadrupole-quadrupole polarizability and so on ... Thus, the above expansion of energy demonstrates different orders of the molecular polarizabilities describing the distortion in the molecule by the external electric field and field gradient. Some details on theory and experiments for determining these quantities could be found in Buckingham [77].

### 1.7.1 Linear Response Approach

When the external electric field perturbation is uniform and homogeneous, the Hamiltonian retains only the linear response term and can be given as,

$$H(F) = H^{(0)} - \mu_i F_i \quad (1.43)$$

This involves the dipole moment operator which was described earlier in this section. Now, the induced dipole moment $\mu_i(F)$ could be expanded to obtain the dipole-based response properties namely, the polarizability, $\alpha_{ij}$, dipole first hyperpolarizability, $\beta_{ijk}$, and so on.

$$\mu_i(F) = \mu_i^{(0)} + \sum_j \alpha_{ij} F_j + \frac{1}{2}\sum_{j,k} \beta_{ijk} F_i F_j F_k + \ldots \quad (1.44)$$

The dipole moment of the molecule is the first derivative of ground state energy of the molecule with respect to the electric field perturbation at the zero field, the

polarizability is the second derivative of energy and the first hyperpolarizability is the third derivative of energy with respect to the electric field at zero field. These all can be expressed as,

$$\mu_i = -\left(\frac{\partial E}{\partial F_i}\right)_{F=0} \tag{1.45}$$

$$\alpha_{ij} = -\left(\frac{\partial^2 E}{\partial F_i \partial F_j}\right)_{F=0} \tag{1.46}$$

$$\beta_{ijk} = -\left(\frac{\partial^3 E}{\partial F_i \partial F_j \partial F_k}\right)_{F=0} \tag{1.47}$$

Alternatively, the first derivative of energy could also be obtained as the expectation value of the dipole moment operator as,

$$< \mu_i >= \sum_{ab} \frac{P_{ab}\langle\phi_a|\hat{\mu_i}|\phi_b\rangle}{\langle\phi_a|\phi_b\rangle} \tag{1.48}$$

The indices a and b run over the atomic orbitals, $\hat{\mu_i}$ is the dipole moment operator for direction i, where i spans the x, y and z directions and $\mu_i$ is the $i^{th}$ component of the electronic dipole moment and $P_{ab}$ is the orbital density matrix. For the exact wavefunction, the Hellmann-Feynman theorem holds [78, 79],

$$\frac{\partial E(F)}{\partial F} = \langle\psi|\frac{\partial H(F)}{\partial F}|\psi\rangle \tag{1.49}$$

The first derivative of energy with respect to the electric field is equal to the expectation value of the derivative of the Hamiltonian. This also shows the equivalence of the first derivative of energy to the expectation value of the dipole moment in case of electric properties.

Further, explicit evaluation of the subsequent derivatives of the energy with respect to the electric field for obtaining the response properties is not a simple task. Wigner's (2n+1) rule states that the $2n^{th}$ and/or $(2n+1)^{th}$ order perturbation contributions to a non-degenerate energy can be evaluated from a knowledge of the wavefunction through $n^{th}$ order [80]. This means that we can evaluate upto third order properties if the first-order response could be obtained. This is true when the first-order response is obtained in a variational manner.

To obtain properties up to third order, there are techniques based on *perturbative schemes*, in which, the calculations are done independent of the electric field perturbation and the response involves the coupling of the excited states. The *field dependent methods* include the finite-field and the coupled schemes. The first order-response of the wavefunction can be obtained through a coupled Hartree-Fock scheme, which is equivalent to, the derivative of the equation of stationarity, with respect to the external perturbation, written in an orbital basis. Here, the Hamiltonian has a field dependence and the coupled equations have an implicit dependence on the first-order response, and, as a result, they need to be solved iteratively for self consistency. The solution is the first order response of the wavefunction in terms of the derivative of the coefficients of the orbitals. Although, the coupled-perturbed Hartree-Fock (CPHF) equations dates back to more than 25 years ago [81], the implementation was done nearly 10 years later by Pople *et. al* [82] for closed shell SCF wavefunctions. In 1983, Pulay presented the second and third derivatives of variational energy expressions for the multiconfigurational SCF (MCSCF) wavefunctions [83]. Explicit expression for the second and third order derivatives have been worked out by Pulay in the 1983 paper. Semi-empirical models have also been used for calculation of the response electric properties. These models have been described extensively in literature [84, 85, 86, 76]. The derivatives were computed using different techniques for numerical differentiation [87, 88, 89]. And, the development of the electronic structure codes that evaluate such energy derivatives analytically, was possible only after the original work of Pulay concerning analytic gradient techniques [90]. A number of other articles on this subject appeared later [91, 92, 93]. The CPHF method is equivalent to the random phase approximation (RPA) [94] or the Time-dependent Hartree-Fock (TDHF) [95, 96] for static calculations within a given basis. Note that the Eq. 1.46 and Eq. 1.47 are defined for a static field limit, whereas, formally the hyperpolarizability has a frequency dependence and incorporating field dependence in the CPHF is a non-trivial extension of the methodology. Therefore, majority of the derivative-based

NLO calculations were reported at zero frequency. The review on second order optical nonlinearities by Kanis *et. al* (Ref. [97] and references therein) makes for an interesting reading. Implementations include the coupled-cluster (CC) and TDSCF procedures of Sekino and Bartlett [98, 99], the popular CPHF approach of Karna and Dupuis in HONDO program [100], and the TDHF based perturbative scheme of Rice, Handy and co-workers [101]. The correlation effects in these methods are of variable rigour. Rice and Handy also developed a time-dependent MP2 theory [102]. Multiconfiguration RPA and second order polarisation propagator methods were introduced by Yeager *et. al* [103] and by Oddershede *et. al* [104]. The theory has been extended to the CC by Koch and Jørgensen [105]. Calculations of dipole polarizabilities of rare gas and other closed shell atoms by Stott and Zaremba [106] and Mahan [107] are often cited as the first implementation of the static density functional response theory. Most earlier density functional calculations of molecular response properties have been for atoms of spherical symmetry. Both the above DFT implementations were developed for systems with spherical symmetry and neither are suitable for the Density Functional calculations of response properties. Colwell *et. al* have implemented the calculation of static molecular dipole polarizability and hyperpolarizability in the CADPAC package [108]. A lot of studies are reported on the molecular dipole polarizabilities and hyperpolarizabilities, and it may not be possible to refer to all of them here. Some of the studies for molecules [119, 120, 121, 122, 123, 124, 125, 108, 126] and a previous study for atoms and solids [127] have found DFT to give properties that are often significantly better than HF. Some other papers concerning the CPKS have also appeared [128, 129, 130, 131, 132, 133, 134, 135, 136]. The dynamic response properties can be obtained using the framework of TDDFT, a formal foundation for which has been laid Ghosh and Deb [109, 110], Bartlotti [111, 112], and Runge, Gross, Kohn and others [113, 114, 115, 116, 117, 118]. However, the correlated frequency-dependent programs are algebraically complicated and expensive and require large basis sets. It is unlikely that these theories are going to be practical for

studying the NLO properties of large systems. This makes us go back to alternative methodology involving the time-independent framework of DFT. In this thesis we would be mainly concerned with the static dipole polarizability and the dipole first- hyperpolarizability of closed shell molecules. The method for obtaining the dipole-quadrupole polarizability would also be presented (in chapter 4) in addition to the one for dipole polarizabilities (in chapter 2).

## 1.8 Motivation and Objective

There has been tremendous advancement in the field of NLO materials and the experimental techniques available to study them. Further, progress in the development of many such technologically important processes in areas like, optical information processing, telecommunications, integrated optics, optical computers, laser technology, etc. is based on the understanding of molecular properties of the constituent materials. DFT among other theoretical methods has been used to study molecular properties of such materials leading to designing of new NLO materials with potential for NLO applications. Determination of the first and second order polarizabilities, in particular, play an important role in understanding the response of the molecule to an external weak electric perturbation. Materials with high second order responses are considered important for NLO applications. The study of dipole-quadrupole polarizability could also prove useful. This all, motivated us to put forth a linear response approach to the DFT, for obtaining the linear and nonlinear electric polarizabilities of molecules.

In the KS-DFT formalism the complete analytic approach, to obtain the first order response of the electron density for molecules, requires the solution of the CPKS equations. The CPKS equation involves, the complex evaluation of the functional derivative of the exchange-correlation term in the construction of the derivative KS operator matrix. Since, there is an implicit dependence of the KS operator matrix on the derivative coefficient matrix, the CPKS equations need

to be solved in an iterative manner. However, this could take a long time and involves complicated algebra for obtaining the functional derivatives. The analytic CPKS formalism could be useful, in obtaining highly accurate values of response properties of small or reasonable sized molecules. Nevertheless, for large molecules, the computational time and effort shoots up drastically. As a result, this approach is not feasible for large scale applications. This, motivated us to put forth a formalism, which would not only simplify the procedure, but also, make the entire process of obtaining the solution of the CPKS equations faster. Our method, as well as, its implementation and some interesting results obtained are presented in this thesis. The implementation would now make it easy to harness the benefit of our single-step method for the response electric property calculations of large molecules using large basis sets, which is a bottleneck in case of complete analytic CPKS for larger systems.

## 1.9 Organization of the Thesis

**Chapter 2:** In chapter 2, we present the details of a new formalism proposed by us, towards developing a simplified linear response approach to DFT for calculating the response electric properties, namely, dipole polarizability and dipole first-hyperpolarizability of molecules. The formalism is an approximation to the fully analytic coupled-perturbed Kohn-Sham (CPKS) method for obtaining the response of the electron density for molecules in the KS-framework of DFT, using the deMon DFT package. The algorithm for our earlier implementation of our method in the deMon-KS; the older version of the deMon software would be discussed in this chapter. We tested our method using small prototype molecules, namely, HF, BH, CO and $H_2O$, which would be discussed in the following chapter. The implementation of our method in the new version of deMon2k, as the old version (deMon-KS) is no longer used extensively by the scientific community, would also be presented in this chapter. The motivation as well as the advantages of our implementation in

the new version of deMon will also be highlighted.

**Chapter 3:** In this chapter, we present the polarizability and hyperpolarizability results for the HF, BH, CO and $H_2O$ molecules using different exchange-correlation functionals and basis sets. We discuss our results in comparison with those available from experiments and other DFT as well as *ab initio* methods. The calculations for HF and BH have also been done at different internuclear separations around the equilibrium bond distance. In this chapter we will discuss the effect of basis sets and the functionals on the polarizability and the hyperpolarizability of the molecules. The feasibility of our method using DFT for bond distances away from equilibrium will also be focused upon.

**Chapter 4:** In this chapter, we present the extension of our formalism for the calculation of dipole-quadrupole polarizability of molecules. The algorithm and the implementation for this property in deMon2k will be discussed. We will also present a comparison of results of polarizability and hyperpolarizability using our earlier implementation in deMon2k with the analytic CPKS method developed by a research group in Mexico. However, the hyperpolarizability module has been added to their program by us. Here we would also discuss about the analytic implementation as against our simplified approach. We would also emphasize on the future scope of our method in general, for obtaining the response properties of molecules.

**Chapter 5:** The possibility of large scale applications using our formalism discussed in Chapter 2 motivated us to implement it in the new version of the deMon2k software. The technical details of our implementation in the deMon2k for faster and more efficient calculations of the electric properties of molecules has been discussed in the earlier chapter. Two sets of calculations are presented in this chapter. We present the calculations for even number alkali metal atom clusters. We study the polarizability and first-hyperpolarizability results of $Na_2$, $Na_4$, $Na_6$, and $Na_8$, Sodium atom clusters using our method. We also analyze the mean polarizability per atom values graphically for each of the clusters and try

to understand the structure property relationship. We have carried out HF and MP2 benchmark calculations for comparison. We also study the NLO properties of the para-nitroaniline molecule (PNA) and its substituted derivatives using our method. We study how the methyl substitutions at various position and sites in the PNA molecules affects the polarizability and the first-hyperpolarizability values of the molecule. We compare our results with available MP2 results. In addition to studying the subtitution effect we attempt to understand the performance of our method for these prototype organic molecules.

Chapter 2

# The Non-Iterative Approximate CPKS Formalism


## *Abstract:*

In this chapter we present the non-iterative approximation of the coupled-perturbed Kohn-Sham (NIA-CPKS) procedure proposed by us for obtaining the response of the electron density. This density response is further used for obtaining the response electric properties up to the third-order. In this chapter, we describe the theory involved and present the technical details of the implementation of our method in the deMon density functional software. This initial implementation in the old version of deMon will be described. We recently implemented the NIA-CPKS method in the new version of deMon. We will discuss the advantages of the implementation of the NIA-CPKS. The overall merit of the method will also be highlighted in this chapter.


## 2.1 The NIA-CPKS method

In the presence of a finite external perturbation, the molecule experiences a change in its electronic distribution, which, in turn is reflected in its properties. In this thesis, we would be dealing with electric field perturbation for closed shell cases only. Introduction of Gaussian basis centered on atom, for molecules, transforms the DFT equations into the Kohn-Sham (KS) matrix equation. This allows the evaluation of the coefficients of expansion of the KS orbitals in terms of the contracted Gaussian orbitals (atomic orbitals). These orbitals can directly give the

electron density. Thus, to study the response molecular electric properties, the response of the molecule to the electric field perturbation in terms of the electron density can be obtained through the derivative of the density with respect to the electric field. This derivative electron density or the density response could be obtained variationally. The variational equations when transcribed in a basis involves the derivative of the KS matrix, and can be shown to be equivalent to the CPKS equations. The CPKS equations are the derivative of the KS matrix equations with respect to the electric field. The unperturbed KS matrix equation is,

$$HC = SCE \tag{2.1}$$

where, H is the KS operator matrix, C the coefficient matrix, S the overlap matrix and E is the energy matrix. In the presence of a static uniform external electric field the Hamiltonian would have a explicit dependence on the field. We have considered only the linear response term in the Hamiltonian for this thesis. The perturbed Hamiltonian would then be,

$$H(F) = H^{(0)} + \mu F \tag{2.2}$$

where, F is the electric field perturbation, $H^{(0)}$ is the ground state Hamiltonian operator, and $\mu$ is the dipole moment operator. The second term in the above equation is the linear response term. The energy in turn would have a dependence on the field and can be expressed as a Taylor series expansion,

$$\begin{aligned} E(F) = E^{(0)} - \sum_i \mu_i F_i - \frac{1}{2}\sum_{i,j} \alpha_{ij} F_i F_j \\ -\frac{1}{6}\sum_{i,j,k} \beta_{ijk} F_i F_j F_k \ldots \end{aligned} \tag{2.3}$$

where, $E^{(0)}$ is the unperturbed energy, $\mu_i$ are the dipole moment components, $\alpha_{ij}$ and $\beta_{ijk}$ are the dipole polarizability, and first- hyperpolarizability tensor components respectively. Each of the i, j and k corresponds to the x, y and z directions. Similarly, the induced dipole moment component can be given as,

$$\mu_i(F) = \mu_i + \sum_j \alpha_{ij} F_j + \frac{1}{2}\sum_{j,k} \beta_{ijk} F_i F_j F_k + \ldots \tag{2.4}$$

where, $\mu_i$ is the permanent dipole moment and the other quantities are similar to those in the expansion for the perturbed energy above. The electron density can also be given as a Taylor series expansion,

$$\rho(r) = \rho^{(0)} + \sum_i \left(\frac{\partial \rho(r)}{\partial F_i}\right)_0 F_i + \frac{1}{2}\sum_{ij}\left(\frac{\partial^2 \rho(r)}{\partial F_i \partial F_j}\right)_0 F_i F_j + \ldots \tag{2.5}$$

To obtain the linear response of the energy functional with respect to the external perturbation, we employ a variational principle. This allows us the use of the (2n+1) rule [137]. The $n^{th}$ order explicit derivative of the functional, $E^{(n)}$, contains the unperturbed and all $m^{th}$ order derivatives of density (m≤n). For example, the explicit first derivative of the functional, $E^{(1)}$, contains $\rho^{(0)}$ and $\rho^{(1)}$. The stationarity of the functional with respect to the unperturbed density can be given by,

$$\frac{\partial E^{(1)}}{\partial \rho^{(0)}} = 0 \tag{2.6}$$

The above condition yields an equation for the first derivative of $\rho$ with respect to the unperturbed density, $\rho^{(0)}$ obtained from the unperturbed DFT equations. Progressive use of the stationarity of $E^{(n)}$ with respect to $\rho^{(0)}$ for (m≤n) yields up to $n^{th}$ order density. These variational conditions allow us to evaluate up to the desired $(2n+1)^{th}$ order of energy. For example, the $\rho^{(0)}$, $\rho^{(1)}$ determines the energy derivatives $E^{(2)}$ and $E^{(3)}$ obtained by the use of the stationary condition.

$$\frac{\partial}{\partial F}\frac{\partial E^{(0)}}{\partial \rho^{(0)}} = 0 \tag{2.7}$$

The derivative of the stationary equation with respect to the field when written in a basis is equivalent to the CPKS matrix equation which gives the response density or the first derivative of density. The CPKS matrix equation can be given as,

$$H'C^{(0)} = S'C^{(0)}E + SC'E + SC^{(0)}E' \tag{2.8}$$

where, the primes denote the first derivatives with respect to the electric field. The $C'$ in the CPKS equation can be written in terms of a new matrix $U'$ as,

$$C' = C^{(0)}U' \tag{2.9}$$

Pre-multiplying the Eq. 2.8 by $C^{(0)\dagger}$ and substituting for $C'$ we get a simplified form of the equation for the $U'$ matrix and the element of the occupied-virtual block of the $U'$ matrix is given as,

$$U'_{ia} = \sum_{\mu\nu} C^{\dagger}_{\mu i} H'_{\mu\nu} C_{\nu a} / (\varepsilon_i - \varepsilon_a) \tag{2.10}$$

where, the suffix i spans the occupied molecular orbitals (MO), suffix a spans the virtual MOs and $\mu$, $\nu$ are the indices for the atomic orbitals (AO), the C and the $\varepsilon$ are the coefficient matrix and the eigenvalues respectively, of the unperturbed DFT calculation, $H'$ is the derivative KS-operator matrix in the AO basis. The virtual-occupied block of the $U'$ matrix is put negative of the occupied-virtual block and the remaining elements of the matrix are zero. This is similar to the CPHF procedure [92], for the closed shell cases using the Hartree-Fock (HF) theory, except that, DFT involves the exchange-correlation term in the CPKS equations in place of the exchange term in the HF theory. The derivative coefficient matrix $C'$ is obtained from Eq. 2.9. Using this, the derivative density matrix, $P'$, which is the first order response of the electron density is obtained using the expression below.

$$P'_{\mu\nu} = \sum_{i} (C'_{\mu i} C_{\nu i} + C'_{\nu i} C_{\mu i}) \tag{2.11}$$

The derivative KS-operator matrix, $H'$, in case of electric field perturbation consists of the two-electron and the response term. The $H'$ has an explicit dependence on the $C'$ and as a result the CPKS equations need to be solved in an iterative manner, i.e. for every iteration the derivative KS-operator matrix in the AO basis has to be reconstructed using the $C'$ of the earlier iteration. The two-electron term in the $H'$ constitutes the complicated functional derivative of coulomb as well as the exchange-correlation term with respect to the electric field perturbation, which is an algebraically complicated and time consuming step in the completely analytic CPKS method. Also, this needs to be done till the self-consistency is attained.

We have proposed a simplified approach to the completely analytic CPKS method for the closed shell cases which yields a single step solution of the CPKS

equations [145, 146, 147, 148]. We construct the first derivative of the KS-operator matrix, $H'$ with respect to the electric field in a numerical manner, using the finite field approximation. This is done by evaluating the KS-operator matrix at different field values around zero field and plugging in these matrices in the finite-field expression for the first derivative to obtain the approximated derivative KS-operator matrix. This numerically obtained derivative KS-operator matrix, $H'$, the coefficient matrix, $C^{(0)}$ and the eigenvalues, $\varepsilon$ of the unperturbed DFT calculation when put in Eq. 2.10 leads to a single step solution of the CPKS matrix equation.

The $U'$ matrix is the solution of the CPKS matrix equation and carries the information of the response of the electron density to the external perturbation which would be passed on to the derivative density matrix via the $C'$. The Eq. 2.9 could now be used to obtain the $C'$ matrix or the derivative coefficient matrix. The $C'$ along with the $C^{(0)}$ matrix from the unperturbed DFT calculation when put in Eq. 2.11 gives the derivative density matrix, $P'$. This derivative density is obtained for the x, y and z directions by constructing the $H'$ matrices for the respective directions using the finite-field method mentioned above and solving the single-step CPKS equation. DFT uses a variational principle for obtaining the energy and also the analytic CPKS method gives the response of the density in a variational manner. The first-order response properties obtained by taking explicit derivatives of the energy with respect to the perturbation or an expectation value for the corresponding property turn out to be equivalent when the theory is exact or variational in nature, as deduced from the Hellman-Feynman theorem [78, 79]. Also, as described above we make use of the (2n+1) rule [83] for higher energy derivatives. Thus, the first order response in the form of derivative density matrix obtained from the solution of the CPKS matrix equation can be used to obtain the second order as well as third order response properties, namely, dipole polarizability and the first hyperpolarizability. The dipole polarizability is obtained as,

$$\alpha = Trace(\mu P') \tag{2.12}$$

The third derivative of energy, i.e. the dipole first- hyperpolarizability is obtained

as,

$$\beta = Trace(H'P'P') \tag{2.13}$$

where, $H'$ is the derivative KS-operator matrix in the MO basis. We have thus described the NIA-CPKS formalism in this section of the chapter. The implementation of our method in the deMon would be discussed in the following sections of this chapter.

## 2.2 About the deMon software

The software package for density functional theory (DFT), by the name 'deMon', has been used for implementing the work presented in this thesis. The name deMon, stands for, densité de Montréal. The earliest version of deMon was described in Alain St-Amant's thesis [138] from which evolved the deMon-KS set of programs [138, 139, 140] that is used in this thesis. The transformation and modification of the deMon-KS further led to the new version of the deMon called the deMon2k [141]. The deMon2k software has a variety of features and can be used for a range of calculations, namely, geometry optimization, transition state search, single-point energy calculations, molecular dynamic simulations (MD), Time-dependent DFT (TDDFT), calculation of properties like polarizabilities, hyperpolarizabilities, NMR, IR and Raman spectra and intensities, and thermodynamic data of atoms, molecules and solids. It has interfaces for visualization packages like Molden, Molekel and Vu and is portable to various computer platforms and operating systems. Several developments and implementations in deMon ranging from analytical to numerical schemes for properties and a variety of applications are available.

The deMon set of programs is a modern density functional theory (DFT) package based on the Kohn-Sham (KS) method and uses the linear combination of atomic orbitals (LCAO) framework with Gaussian type orbital (GTO) basis sets centered on atoms. Although both deMon-KS and deMon2k are based on the KS method the structure of the two programs is quite different from each other.

The KS self-consistent field (SCF) energy expression using the KS orbitals and the electronic density can be given as,

$$E_{SCF} = \sum_{\mu,\nu} P_{\mu\nu} H_{\mu\nu} + \frac{1}{2} \sum_{\mu,\nu} \sum_{\sigma,\tau} P_{\mu\nu} P_{\sigma\tau} \langle \mu\nu || \sigma\tau \rangle + E_{xc}[\rho] \tag{2.14}$$

where, P is the density matrix, H is the core Hamiltonian operator matrix, the second term involves the electron repulsion integrals and the last term is the exchange-correlation energy.

The deMon set of programs is different from various other DFT packages as it uses an auxiliary basis and follows the variational fitting procedure of Dunlap *et. al* [142, 143] for estimation of the coulomb energy. The auxiliary basis are used for fitting of the charge density, where the approximate density, $\tilde{\rho}(r)$ is expanded in primitive Hermite Gaussians $\overline{k}(r)$ centered on atoms as,

$$\tilde{\rho}(r) = \sum_{k} x_k \overline{k}(r) \tag{2.15}$$

The calculation of the coulomb repulsion integrals which scales as $N^4$ is avoided in deMon by using the auxiliary function density as described above. Hence, only three-center electron repulsion integrals (ERIs) are required for the SCF and energy calculation. Using the LCAO in the Gaussian orbital framework for expansion of the $\rho(r)$ and the $\tilde{\rho}(r)$ the SCF energy expression is approximated as,

$$\begin{aligned} E_{SCF} = \sum_{\mu,\nu} P_{\mu\nu} H_{\mu\nu} + \sum_{k} x_k \sum_{\mu,\nu} P_{\mu\nu} \langle \mu\nu || k \rangle \\ - \frac{1}{2} \sum_{k,l} x_k x_l \langle k || l \rangle + E_{xc}[\tilde{\rho}] \end{aligned} \tag{2.16}$$

The exchange-correlation energy as well as potential can be obtained from the approximated density, $\tilde{\rho}$ by using an auxiliary basis. However, for high accuracy, especially, in case of calculation of sensitive properties like frequencies and polarizabilities the use of density in the orbital basis is recommended for calculation of the exchange-correlation energy and potential. Additionally, deMon uses a grid for the numerical integration of the exchange-correlation energy and potential. The tolerance of the grid indicates the accuracy of the numerical integration of the diagonal elements of the exchange-correlation potential matrix. The tolerances for

the grid can be chosen from, $10^{-4}$, $10^{-5}$ and $10^{-6}$ a.u. respectively. Alternatively, the tolerance of the grid can be specified in the input. There are also separate options for the electrostatic moments calculations, which gives the dipole, quadrupole and octupole moments of the system. The finite-field $\alpha$, $\beta$ and $\gamma$ calculations are also available in deMon2k. In the deMon-KS the dipole and quadrupole moments are available, however, the polarizability calculations are absent. For more details of the keywords and their purpose one could refer to the deMon2k manual and the references therein [144]. The use of the auxiliary basis and the grid options are similar in both deMon2k and deMon-KS. However, the deMon2k being an improved version of the deMon-KS is more accurate and efficient implementation of the program. Other than the minor improvements and new keywords introduced in the deMon2k, it also includes few other implementations, namely, TDDFT, MD, etc., which were missing in the deMon-KS.

## 2.3 Implementation of the NIA-CPKS method in deMon

Initially we implemented the NIA-CPKS in the old version of deMon Software, deMon-KS Module, Release 3.5, Copyright 1998 by the University of Montreal and the authors [138, 139, 140]. We implemented it in the following way. Here, we carried out perturbed DFT calculation at symmetrically placed field values around zero field for the x, y and z directions for obtaining the perturbed KS-operator matrices at the different field values in the three directions. The derivative KS-operator matrix was constructed numerically for each of the directions by plugging in the perturbed KS-operator matrices in the finite-field 5-point approximation for the first derivative. We used the following expression for construction of the derivative KS-operator matrix, $H'$.

$$H' = \frac{(H(-2) - 8 * H(-1) + 8 * H(+1) - H(+2))}{12 * f} \tag{2.17}$$

where the values in parenthesis after H are the placement of the field values around zero field, and the f is the field interval. We introduced a CPKS module to the deMon-KS program for obtaining the density response. The $H'$ matrix, the eigenvalues and eigenvectors of the unperturbed calculations are required as input.

Our recent implementation in the deMon2k (deMon 2004, Version 1.07) [141], has been done for the use of cartesian orbitals and the density could be obtained either using an auxiliary basis (through fitting) or orbital basis for obtaining the exchange-correlation functional. However, the density in the orbital basis is the preferred choice for the response property calculation [144]. An keyword for finite-field polarizability calculation in the deMon2k turns on the self-consistent perturbation (SCP) calculations after the unperturbed DFT calculations. Thus, the induced dipole moment are calculated for each of the SCP calculations. The finite-field step value can be chosen in the input. The SCP calculations are done for the x, y and z directions. deMon2k gives the finite-field polarizability tensor components using the induced dipole moment values evaluated at the end of each of the SCP calculations. The perturbed KS-operator matrices from these SCP calculations are plugged into the finite-field three-point expression for the first derivative to obtain the derivative KS-operator matrix for the x, y and z directions. The three point formula used is,

$$H' = \frac{H(+1) - H(-1)}{F(+1) - F(-1)} \tag{2.18}$$

where, $H'$, is the derivative KS-operator matrix and the values +1 and -1 in parenthesis, denote the symmetrically chosen field values and F is the magnitude of the the electric field. This numerically constructed derivative KS-operator matrix is put into the CPKS equation, which has been introduced as a separate module. It includes expressions for Eq. 2.10, Eq. 2.11, and for the calculations of the polarizability tensor elements. CPKS matrix equations are solved for the x, y and z directions and the solution is the derivative density matrix, $P'_x$, $P'_y$ and $P'_z$ for the three directions respectively. The trace of the product of the density matrices with the dipole moment integrals give the polarizability tensor components. The first

hyperpolarizability is calculated using the $P'$ and $H'$ matrices. That completes the description of the implementation of NIA-CPKS method in the deMon2k [148].

## 2.4 Advantages of the NIA-CPKS implementation

The key advantage of the method is the simplification from the iterative scheme to the single step procedure. The analytic construction of the derivative KS-operator matrix is a tedious and time consuming step in the complete analytic procedure. It also involves working out as well as programming of the algebraically complicated functional derivatives of the exchange-correlation term in the KS operator matrix. This has been successfully and cleverly avoided in our method.

Additionally, the exchange-correlation part of the KS-operator matrix can be evaluated using, either, the auxiliary basis or the orbital basis, for fitting the density. Since, the derivative KS operator matrix is constructed numerically, both alternatives for obtaining the density now becomes available for the response property calculation.

The implementation of the NIA-CPKS would now make it easy to harness the benefit of our single-step method for response property calculations of large molecules using large basis sets, which is even now a bottleneck in case of complete analytic CPKS. The NIA-CPKS method thus expands the possibility of using the simplification for large molecules, clusters and systems of the like.

Chapter 3

# Some test calculations from our approximate CPKS method


## *Abstract:*

In this chapter, we present linear and nonlinear electric properties of HF, BH, CO and $H_2O$ using a density functional response approach, which is a combination of numerical and analytical technique and is thus a simplification of fully analytic method. The implementation of the method in deMon-KS is described in the earlier chapter. Our method is tested using molecules HF, BH, CO and $H_2O$, which are marked by high degree of electron correlation and for which extensive *ab initio* benchmark results are available. Further, we have made a study of possible incorporation of non-dynamical electron correlation by studying HF and BH at several internuclear distances. The polarizability and first hyperpolarizability values have been obtained using different exchange-correlation functionals and Gaussian basis sets. The permanent dipole moment values are also reported.


## 3.1 Introduction

Molecular properties [149] are basically the response of the molecular system under study to the corresponding perturbation in electric or magnetic fields. These properties can be calculated either by numerical differentiation (i.e. the finite field approach) or, preferably, by analytic approach. When the perturbation is an electric field the corresponding molecular property is the electric property. Electric

properties [98, 150, 151, 152, 153, 154, 155, 156] have been of interest in the recent past as a result of the development of lasers and new experimental techniques and the fact that these properties give information about the system under study. The fully analytic response approach for calculating the electric properties of molecules has been developed for the Hartree-Fock method [92, 157] and the highly correlated methods like the coupled-cluster (CC) [158, 159, 160, 161] in the recent past.

The implementation of the linear response approach to the Kohn-Sham (KS) density functional theory (DFT) would be highly useful for studying the effects of a static homogeneous electric field perturbation on the electronic distribution in the molecule in the ground state. There have been efforts in the field of DFT to develop such analytic approaches for obtaining the response atomic [162] and molecular properties, however, those are complicated and computationally expensive. For the DFT the implementations of the complete analytic approach are available for the LDA using auxiliary basis for fitting the density, also, the TDDFT dynamic response implementations could be used for obtaining frequency dependent polarizabilities. In the time-dependent framework, this would give the static dipole polarizability in the ground state at zero frequency. Most of these calculations have been restricted only to the use of numerical finite field approach. Our method described in the earlier chapter is relatively simple and yet retains the accuracy of the response properties obtained due to its numerical-analytical implementation. In addition, owing to the variational nature of DFT, there exists an inherent (2n+1) rule for the energy derivatives [137], and thus, the Hellmann-Feynman [78, 79] theorem holds true, as a result, the first order response of the electron density is used to evaluate the second and third order response properties, namely, dipole polarizability and first hyperpolarizability using fully analytic expressions.

Our method, as described in chapter 2, is a step towards the fully analytic method for calculation of static molecular electric properties (namely, polarizability and first hyperpolarizability) for the closed-shell molecules. Using Gaussian basis

sets centered on atoms, the DFT equations can be transformed into the Kohn-Sham matrix equation, which allows evaluation of the coefficients of expansion of Kohn-Sham orbitals in terms of the contracted Gaussian orbitals (atomic orbitals (AO)). These orbitals directly provide us the electron density of the system. The first derivative of the density with respect to the external perturbation is derived variationally. This variational equation, when transcribed in a basis involves the derivative of the Kohn-Sham matrix, and can be shown to be equivalent to the coupled-perturbed Kohn-Sham (CPKS) equation. The density derivative can be obtained from the derivative of the coefficients of the Kohn-Sham orbitals in this basis. In our procedure described in chapter 2, we used the finite field approximation for construction of the derivative Kohn-Sham matrix and subsequently solve the analytic CPKS equations for obtaining the coefficient derivatives. We obtain up to third order energy derivatives from the knowledge of the first order density.

To explore the efficacy of the implementation of our method for different cases, we have chosen different molecules. HF is a prototype test molecule for which full configuration (FCI) and coupled-cluster (CC) results are available for comparison. We present the results for the HF at various internuclear distances. BH is known to have strong effects of quasi-degeneracy around the equilibrium distance. Properties of BH have been studied at different internuclear distances of B-H. We have also carried out calculations for CO, which is known to have prominent effects of electron-correlation. Calculations for the equilibrium geometry of water molecule are also presented. Our results using different exchange-correlation functionals employing relatively good basis sets are benchmarked against extensive coupled-cluster (CC) level and the experimental results wherever available. We now give the method used and the computational details of the calculation followed by results and discussion.

## 3.2 Method

The general analytic variational approach to calculate properties is now discussed. The application of an arbitrary uniform electric field to a molecule results in distortion of the molecule in response to the field. The energy of the molecule can then be expanded as a power series in the field, F, if the field is small.

$$E(F) = E(0) - \sum_i \mu_i F_i - \frac{1}{2}\sum_{i,j} \alpha_{ij} F_i F_j - \frac{1}{6}\sum_{i,j,k} \beta_{ijk} F_i F_j F_k \tag{3.1}$$

In the above equation i, j and k span the x, y and z directions, the first term is the energy of the molecule in the absence of the electric field perturbation, $\mu_i$, is the static dipole moment, $\alpha_{ij}$ is the dipole polarizability, $\beta_{ijk}$ is the first hyperpolarizability and so on ... Alternatively, the above static response properties can also be defined by expanding the field-dependent dipole moment as,

$$\mu_i(F) = \mu_i + \sum_j \alpha_{ij} F_j + \frac{1}{2}\sum_{j,k} \beta_{ijk} F_i F_j F_k + \ldots \tag{3.2}$$

where the first term on the right hand side is the permanent dipole moment, and the rest of the terms are as described above. Both the above definitions of the properties are equivalent since the Hellmann-Feynman theorem stands true for the exact solution of the Schrodinger equation and even for the approximate solutions depending on the nature of approximations used. To obtain the higher derivative of the energy functional with respect to the external perturbation (electric field), we use the variational principle to calculate the first-order derivative of density. As described in chapter 2, this is obtained by making the variational DFT equations stationary with respect to the electric field, F.

$$\frac{\partial}{\partial F}\frac{\partial E}{\partial \rho} = 0 \tag{3.3}$$

The above stationary equation can be transcribed in the Kohn-Sham framework using orbital derivatives with respect to the electric field. The first derivative of

density can be written in terms of the KS orbital derivatives. On introduction of the atomic orbital basis, the above equation transforms into the CPKS matrix equation and provides us with the first derivative of the coefficients of KS orbital in the AO basis. This, in turn, provides us with the first- order derivative of density. The CPKS equations are equivalent to the derivative of the Kohn-Sham matrix equation with respect to external perturbation. Further, the use of the (2n+1) rule simplifies the formula for second and third energy derivatives. The second and third energy derivatives with respect to external fields can be written in terms of only the unperturbed density and its first derivative with respect to field, which are obtained by the first derivatives of the coefficients of the Kohn Sham orbital in the basis.

## 3.3 Computational details

The exchange correlation part of the KS operator has been obtained by fitting it in terms of Gaussian functions, as already available in the deMon-KS [140] system of programs. Following this approach, the complete analytic approach would involve fitting the derivative of the KS matrix as well. The step of fitting the derivative of exchange-correlation part of KS operator is a difficult as well as computationally extensive. As a first step toward this analytic approach, we have devised a method, which is a mixture of numerical and analytical procedure. In this, the step of fitting the derivative of exchange-correlation part is by-passed by constructing the derivative of the Kohn-Sham matrix using a finite field approximation. The elements of the derivative Kohn-Sham matrix are computed as a difference between the elements of the Kohn-Sham matrices calculated at suitably chosen electric field values around zero field, namely, +0.002 a.u., +0.001 a.u., -0.001 a.u. and -0.002 a.u. through the deMon-KS [140] system of programs. Using this derivative Kohn-Sham matrix, the derivative of the molecular orbital coefficients in terms of the atomic basis is obtained analytically by solving the CPKS equation in a single-

step. The coefficient derivatives lead to the first-order density. We can then obtain up to the third-order property through the knowledge of the first-order density. The dipole moment, which is a first-order property, can be simply calculated through the ground state density. The CPKS code for obtaining the response of the density was written and integrated with the deMon-KS code. Using the first-order density the formulas for the second-order and third-order properties were coded.

We present calculation of properties of molecules, namely, HF, BH, CO and $H_2O$ in this chapter, for which high quality *ab initio* results are available. The selection of molecules would also serve as a test of the method. In addition, we have used the method to examine the properties of HF and BH at different internuclear distances, where non-dynamic electron correlation will be important.

Hydrogen fluoride is a prototype molecule for which coupled-cluster (CC) and full CI results are available for comparison. We carried out calculations for $R_e$, $0.75R_e$, $1.5R_e$ and $2.0R_e$ bond distances. Four different exchange-correlation functionals and three different basis sets were used for the calculations. The functionals chosen were PW91 [60] exchange and correlation, PW86 [56, 57] exchange and correlation, B88 [70] exchange with PW91 correlation and B88 [70] exchange with P86 for correlation. The basis sets used were i) double zeta DZ basis set of Dunning, ii) double zeta with p and d polarization functions DZP basis set of Dunning and iii) Sadlej. We have employed (5,1; 5,1) auxiliary basis for the hydrogen atom and (5,2; 5,2) auxiliary basis for the fluorine atom for the HF calculations. The calculations at different bond distances, $0.75R_e$, $1.0R_e$, $1.5R_e$ and $2.0R_e$, are also presented.

Boron mono-hydride is an ideal small system for study and assessment of the method in critical quasi-degenerate situations. Thus our study involving calculation of dipole moment, polarizability and first hyperpolarizability has been presented for BH at $R_e$, $0.75R_e$, $1.5R_e$ and $2.0R_e$ BH distances. We have chosen a contracted Gaussian basis of triple-zeta with two polarization functions, TZ2P quality, in which different *ab initio* results are available for comparison. The full basis consists of 10 primitive s and 6 primitive p functions contracted to 5s and 3p type functions

for boron, augmented by two contracted d functions out of 4 primitive functions (with two primitives in each) [163]. For hydrogen, 6s and 4p functions have been contracted to 3s and 2p functions. In addition, we have employed auxiliary basis (5,1; 5,1) for hydrogen and (5,2; 5,2) for boron for fitting exchange-correlation part.

Similarly CO represents an interesting system, where electron correlation plays an important role in determining the sign of the dipole moment. In this case, however, the molecule has been studied only at the equilibrium geometry. Three different basis sets have been used for the study. One of them is an extensive basis consisting of 12 primitive s and 8 primitive p functions contracted to 8s and 6p functions augmented by 3 uncontracted d functions (12s 8p 3d)/ [8s 6p 3d] for each of C and O atom [163]. An auxiliary basis (4,4; 4,4) has been employed for DFT exchange correlation fitting throughout our calculation for CO. Standard *ab initio* results from CCSD, Brueckner orbital-based CCD, CCSD (T), and BCCD (T) have been presented in the above orbital basis for comparison. Calculations on CO molecule have been performed with a second basis which is of valence triple-zeta with polarization (TZVP) quality for both C and O, primitive 10s, 6p set contracted to 4s and 3p functions with one d function left uncontracted and denoted as VTZP [123]. This basis set, optimized for DFT methods by Godbout *et al.* [164] has been taken from the deMon-KS basis set library. The third set of calculations on CO has been performed with the VTZP basis of Godbout *et al.* with one uncontracted s and d field induced polarization (FIP) functions added to it for both carbon and oxygen atoms, the exponents of which have been taken from Ref. [123]. We denote this basis set as VTZP+. In these two bases, available finite field DFT results through deMon using (4,4; 4,4) auxiliary basis for both carbon and oxygen atoms with LDA functional and analytic CPHF results from HONDO7 [165] have been presented for comparison [123].

Two sets of calculations have been carried out for the $H_2O$ molecule. In the one using Sadlej basis set of Ref. [166] we have used auxiliary bases (5,1; 5,1) and (5,3; 5,3) for the hydrogen and the oxygen atoms respectively for fitting the

exchange-correlation. The geometry used in this calculation for water molecule was an O-H bond distance of 0.957 Åand an H-O-H bond angle of 104.5 degrees. In the second set of calculations we have used the VTZP and VTZP+ basis sets mentioned earlier. The VTZP+ basis was obtained by augmenting the VTZP basis with one uncontracted p FIP function for hydrogen atom and two uncontracted s and d FIP functions for oxygen atom. The exponent of the functions added was taken from Ref. [123]. The auxiliary basis sets used were (3,1; 3,1) and (4,4; 4,4) for the hydrogen and oxygen atoms respectively. The geometry of the water molecule used for the second set of calculation was taken from Ref. [123]; an O-H bond distance of 0.9576 Åand an H-O-H bond angle of 104.48 degrees were used.

The equilibrium distance of BH and CO used in the calculation was 2.329 a.u. and 2.1323 a.u. respectively. The nonlocal exchange-correlation functionals used were B88 exchange [70] with PW91 correlation [60], PW86 exchange [56] with PW91 correlation, PW86 exchange with P86 correlation [57], B88 exchange with P86 correlation and PW91 exchange with PW91 correlation. Out of the above, functionals BPW91 and PW86PW91 were used for the calculations of BH as well as CO and functionals PW86, BP86 and PW91 were used for the calculations of $H_2O$.

## 3.4 Results and Discussion

We first discuss the results for the Hydrogen Fluoride (HF) molecule as presented in tables. We present the calculation of dipole moment, polarizability and first hyperpolarizability of HF molecule at different H-F distances. The details of the basis sets used and the exchange-correlation functionals are given in Computational details section. The equilibrium bond distance, $R_e$ was taken to be 1.7328 a.u. The calculations for $0.75R_e$, $1.0R_e$, $1.5R_e$ and $2.0R_e$ are tabulated in Tables. 3.1, 3.2, 3.3, 3.4, respectively. The RHF calculations are also presented. All values are given in atomic units. We have compared our values with the experimental and

benchmark Full CI (FCI) values, wherever possible for the HF molecule.

**Dipole moment**

In Table. 3.2, we present the results for the $1.0R_e$. The experimental dipole moment [98] value reported is 0.707 a.u. The FCI results for DZ [150] and DZP [152] bases are 0.898 and 0.762 a.u., respectively. The available CCSD-LR [150] calculations give 0.896 and 0.699 a.u. for DZ and Sadlej basis, respectively, whereas a value of 0.707 a.u. has been reported from the CCSD [151] calculations for the Sadlej basis. Our calculations predict the value of dipole moment between 0.854 and 0.868 a.u. for DZ basis, 0.728 and 0.743 a.u. for DZP basis, and 0.673 and 0.685 a.u. for the Sadlej basis using the four different exchange-correlation functionals. Although there is no variational principle for the energy derivatives, we see that the dipole moment values progressively decrease with increasing basis sets. DFT method systematically improves the values compared to FCI results in both DZ and DZP basis and we expect the same behavior for the Sadlej basis. Comparison with the CC results in Sadlej basis shows this improvement. The PW91 and BP86 functionals seem to give better results for dipole moment with respect to the benchmark FCI values for DZ and DZP basis. In the case of Sadlej basis, we do not have FCI value for comparison. We therefore consider the dipole moment value from the CCSD and CCSD-LR method as benchmark for comparison. It can be noted that the PW86 and BP86 give results closer to the CCSD and CCSD-LR values for the dipole moment in this basis. The dipole moment values from DFT are lower than the RHF, FCI, and the CC values, and overcorrect the effects of electron correlation. Table. 3.1 presents the dipole moment of HF at $0.75R_e$. There are no FCI results available for $0.75R_e$. However, we are able to compare our results with the values from the CCSD-LR method of Kondo, Piecuch, and Paldus [150]. The dipole moment values reported using the CCSD-LR method are 0.801 a.u. for DZ basis and 0.567 a.u. for Sadlej [150] basis. The DFT values systematically overcorrect the correlation effects in the dipole moments as seen before for the HF distance of $1.0R_e$ . The BP86 predicts dipole moment values in good agreement with

the benchmark CC values for the $0.75R_e$ bond distance. The results for $1.5R_e$ are presented in Table. 3.3. In this case we observe larger variation in values with basis sets. The results from the CCSD-LR [150] calculations for DZ and Sadlej basis and the FCI values for DZ and DZP basis are presented as benchmarks. Comparison with these benchmarks reflects better performance of the BPW91 functional in case of $1.5R_e$. At $2.0R_e$ Table. 3.4, dipole moments are observed to be exaggerated in relation to the benchmark FCI and CCSD-LR values in different basis. None of the functionals perform well in such a case. Study of the dipole moment trends in the paper by Kondo, Piecuch, and Paldus [150] and Ghose *et al.*[152] show a maximum in the dipole moment values between $1.5R_e$ and $2.0R_e$ depending on the basis set. Such a trend is missing in the DFT results. It appears that the DFT description is unable to account for the significant multireference effects present at $2.0R_e$ and hence may not lead to size-consistent values.

**Polarizability**

The $\alpha_{xx}$ and $\alpha_{zz}$ components of polarizability for each bond distance are given in the respective tables. The experimental values[98] for polarizability of HF molecules are 5.08 a.u. for the $\alpha_{xx}$ and 6.04 a.u. for the $\alpha_{zz}$ component. In Table. 3.2 for 1.0Re, the polarizability values calculated using the Sadlej basis set are quite close to the experimental values of polarizability. The FCI values for the $\alpha_{zz}$ component are 4.14 a.u.[150] and 4.50 a.u.[152] for DZ and DZP basis sets, respectively. Kondo, Piecuch, and Paldus [150] have predicted the $\alpha_{zz}$ component of polarizability from their CCSD-LR method to be 4.179 a.u. using DZ basis and 6.521 a.u. using the Sadlej basis. In comparison with the FCI values for the DZ and DZP basis sets and the CCSD-LR values for the Sadlej basis, our values remain overcorrected due to correlation effects. However, the BPW91 and BP86 functional calculate the $\alpha_{zz}$ component of the polarizability to a reasonable accuracy. For the $0.75R_e$ bond distance in Table. 3.1, the $\alpha_{xx}$ component varies from 0.883 to 1.017 a.u. for DZ basis and is $\sim$2.0 a.u. for DZP basis. The Sadlej basis, however, gives a value nearly 2.5 times greater than the value obtained from the DZP basis.

There is no benchmark comparison available for this. The $\alpha_{zz}$ component from the CCSD-LR method is predicted to be 1.899 a.u. for DZ basis and 4.547 a.u. for the Sadlej basis. There is no benchmark available for the DZP basis. Comparing with the CCSD-LR values in DZ and Sadlej basis, we observe that the DFT values are generally in good agreement and the BP86 functional provides the best agreement. We also observe that the DFT method overcorrects the effects of electron correlation.

In Table. 3.3 for $1.5R_e$, the values for the $\alpha_{xx}$ components vary within 0.02 a.u. and lie between 0.5 and 0.6 a.u. for the DZ basis and around 2.0 a.u. for DZP basis. For the Sadlej basis, the values for the $\alpha_{xx}$ component range from 6.971 to 7.801 a.u. for the four functionals. In this case, no benchmark values are present. For the $\alpha_{zz}$ component of polarizability, FCI or CCSD-LR values are available for comparison. We again observe a general tendency of the DFT method to overcorrect the effect of electron correlation. In this case the deviation of all the functionals from FCI or CCSD-LR values is generally higher. The values of perpendicular and parallel components of polarizability for $2.0R_e$ are presented in Table. 3.4. For the perpendicular component there is no benchmark value available. In the case of parallel component, we observe that our results are in very good agreement with the benchmark FCI or CCSD-LR values. This is in contrast to the dipole moment values at this distance. In the case of the Sadlej basis, there is somewhat larger variation with CCSD-LR values. However, for this basis no FCI results are available. Compared with CCSD-LR, the electron correlation is overcorrected in the DFT method. On the other hand, such effects are nonexistent for the DZ basis, where our results agree very well with FCI values. All the functionals provide very reliable results. In general, we observe an increasing trend of polarizability for the important parallel component as the HF bond is stretched. This is in agreement with the FCI or CCSD-LR trend. The values generally tend to increase as we progress to higher basis. This trend is expected until they saturate with the experimental value.

**Hyperpolarizability**

The $\beta_{zzz}$ component of the first hyperpolarizability for the HF molecule has been calculated at various bond distances. FCI, CCSD, and CCSD-LR values for $1.0R_e$ are available for comparison for the DZ basis, whereas there are CCSD and CCSD-LR values for comparison with Sadlej basis results. The results from the DZ and Sadlej bases do not show any trend. Moreover, the values seem to be overcorrected and are higher than the FCI values, except for the PW91 functional, which gives lower value than the FCI one. However, general agreement of the values is quite satisfactory. There are no benchmark results for comparison with the hyperpolarizability values from the DZP basis. The CCSD-LR values for the zzz component of hyperpolarizability for $0.75R_e$ in Table. 3.1 have been predicted to be 24.929 a.u. for DZ basis and 22.225 a.u. for the Sadlej basis. There are no FCI results available for comparison for the $0.75R_e$ bond distance. The hyperpolarizability values for the DZ and Sadlej bases are overestimated. There is a huge difference between the benchmark CCSD-LR or FCI values and our values of hyperpolarizability for the $1.5R_e$ and $2.0R_e$ bond distance. None of the functional recovers the results at the stretched distance with any accuracy. This may be due to the inability of the DFT method to account for the multireference effects and the size-inconsistency of the functionals used.

Table. 3.5 presents the results of BH at $0.75R_e$, $R_e$, $1.5R_e$ and $2.0R_e$. Results of our calculation using the present numerical finite field method using both BPW91 and PW86PW91 functionals are presented for dipole moment, perpendicular and parallel components of polarizability and parallel components of first hyperpolarizability. The properties using completely numerical method are also presented with other *ab initio* results. We have presented results from ECC response method [167, 168] as benchmark for the $0.75R_e$, $1.5R_e$ and $2.0R_e$ for comparison as no other benchmark results are available. Further at the DFT level, fully finite field results using the same functionals along with analytic CPHF values from HONDO7 program are also presented to show the efficacy of the numerical-analytical method.

At $0.75R_e$, we observe that our method provides dipole moment results close to ECC results compared to the finite field ones. The same trend is observed for at all distances, except at $2.0R_e$. At $2.0R_e$ the dipole moment value of BH predicted by our method is better than the CPHF value, although it is quite overestimated as compared to the ECC result. For $R_e$, we observe that, for $\mu_z$ the *ab initio* calculations provide near FCI results [163]. It is seen that our numerical finite field results are also substantial improvements over the CPHF results and are, in fact, much improved over the complete finite field results. This shows that the utility of analytic evaluation of dipole moment improves the value significantly. We now discuss the trends in the polarizability of the BH molecule at the different bond distances studied. However, we are unable to discuss the perpendicular component of polarizability for all the bond distances, except $R_e$ due to non-availability of any benchmark results for comparison. The $\alpha_{xx}$ component of polarizability for BH at $R_e$ using our method was observed to be $\sim$4 a.u. less than the values from CC-based methods and FCI values [163], whereas the parallel component of polarizability, $\alpha_{zz}$, are overestimated by the DFT by $\sim$ 1 a.u. for both the BPW91 and PW86PW91 exchange-correlation functionals at $0.75R_e$ and for the PW86PW91 functional at $R_e$. It is seen that the BPW91 functional overestimates the component by slightly more than 4 a.u. as compared to the CC results and the FCI values. The $\alpha_{zz}$ component of polarizability for the BH molecule at $1.5R_e$ and $2.0R_e$ are less than the CPHF value but are very much separated from the values predicted by the ECC. This may be possibly due to the dominance of multi-reference effects at stretched geometries that are not incorporated in DFT calculations. There is a general instability in the $\beta_{zzz}$ values obtained by the DFT response. We hope that a fully analytic method, in which, the derivative of the Fock operator will be obtained by complete analytic procedure, may improve the results of $\beta$.

Table. 3.6 presents the property results of CO in the more extensive [8s6p3d] contracted basis of C and O at $R_e$. Though CCSD (relaxed) and BCCD provide near experimental results of dipole moment [163], it can be seen that the present DFT

results are nearly as accurate and have comparable values to some of the CC-based results. It is, however, important to note that the DFT results provide correct sign of the dipole moment, which is indeed extremely gratifying. Both the BPW91 and PW86PW91 functionals of DFT provide quite satisfactory results for perpendicular as well as parallel components of polarizability for CO molecule. Parallel component of polarizability is obtained, in particular, as accurate as, extensive CC results as well as experimental results. What is even more gratifying is the agreement of $\beta$ along the internuclear axis. Although no experimental results are available the agreement with various CC calculations is remarkable. We have also calculated $\beta_{xxz}$ values through our DFT response method for which no other results are available.

We have also presented the results of CO in a lower basis of TZVP quality, which we denote as VTZP, and VTZP+ basis using BPW91 and PW86PW91 functionals in Table. 3.6. The VTZP+ basis is augmented by s and d FIP functions for both carbon and oxygen atoms. In this case extensive *ab initio* results were not available. Only LDA results obtained through deMon-KS with a completely finite field procedure are reported [123]. In both VTZP and VTZP+ basis, we observe the correct sign of the dipole moment and significantly the correct trend of values of our numerical-analytic procedure compared to the LDA results [123]. A closer study shows that the dipole moment values from the TZVP basis set are closer to the experimental dipole moment value than the TZVP+ results. Comparing the results of the above two basis sets, one observes the stability of $\alpha$ values and in general the values of $\beta$. However, the change of $\beta$ values even with this marginal change in basis can be noted.

Table. 3.7 presents the property results for $H_2O$ molecule. We have carried out two sets of calculations for $H_2O$. In the first set of calculation we have used Sadlej's polarized electric property orbital basis set [151] with (5,1; 5,1) and (5,3; 5,3) auxiliary basis sets for the hydrogen and the oxygen atoms respectively using BP86, PW86P86 and PW91PW91 exchange-correlation functionals. We have compared our results with the available TDHF, MBPT (2), CCSD and experimen-

tal results of Sekino and Bartlett [151]. In this the $\mu_z$ results from our method are reasonably good in comparison with CCSD and experimental values. The one from the BP86 functional is closer to the experimental value as compared that from PW86P86 and PW91PW91. The components of polarizability and the $\beta_{zzz}$ as well as $\beta_{yyz}$ component of first hyperpolarizability are slightly overestimated over the CCSD and experimental values wherever applicable. The hyperpolarizability values are however stable as compared to the $\beta$ values for BH, which were highly unstable. However, we expect the complete analytic picture to take care of these small discrepancies in the response property values.

The second set of calculation for $H_2O$, which was carried out using VTZP and VTZP+ orbital basis employing (3,1; 3,1) and (4,4; 4,4) auxiliary basis for the hydrogen and oxygen atoms respectively are also presented in Table. 3.7 The VTZP+ basis set had an augmented p FIP function for the hydrogen atom and s and d FIP functions for the oxygen atom. The exponents for the augmented functions were taken from Ref. [123]. We have used BP86 and PW91PW91 exchange-correlation functionals for calculations involving both VTZP as well as VTZP+ basis set. Complete finite field LDA results from DEMON was available for comparison. In addition, we have also presented the CPHF results for comparison. The dipole moment values from our method are observed to be better than the available LDA as well as the CPHF values. The dipole moment values from the VTZP+ basis are in fact closest to the experimental values as compared to the values from VTZP basis. The values of dipole moment and the components of polarizability using the VTZP basis set are highly underestimated and are away from the experimental values, but remain nearly close to each other for CPHF, LDA and our method. An overall study shows that the VTZP+ basis set gives relatively good results of dipole moment as well as polarizability for the $H_2O$ molecule as compared to the experimental values. The values for the VTZP and VTZP+ basis have no comparison available and are relatively stable.

## 3.5 Conclusion and Scope

We have performed a detailed calculation of the molecular electric response properties to test our implementation of the numerical-analytical linear response approach in the deMon-KS for HF, BH, CO and $H_2O$ molecules. The chosen molecules are marked by high degree of electron correlation. While we have studied CO only at equilibrium, HF and BH has been studied at different internuclear distances. In case of water molecule, although we have carried out the study at equilibrium geometry, two slightly varying geometries have been used in the calculations. For CO as well as $H_2O$ molecule we find that the DFT procedure, as developed by us, produces quite good results. Results of the B-H molecule show that the DFT method proposed by us for produces reasonably correct values of $\alpha$ even at stretched geometry. However there is instability in the $\beta$ values of BH, which should be investigated later. Whereas, in case of HF molecule, we observe errors at large distances more prominently in the $\beta$ values, while polarizability values are more well behaved until the distances we studied. The errors are observed even for the dipole moment values for the stretched bond distances of the HF molecule. In general, DFT does not seem to give correct values for the stretched geometries of molecules as in such cases the multireference character in the system makes a strong appearance, whereas KS-DFT has a single determinant picture for studying the ground states.

**Table** 3.1: Coupled−perturbed Kohn−Sham dipole moment, polarizability, and first hyperpolarizability values of HF molecule[a] at $0.75R_e$ (in atomic units)

| DFT | $\mu_z$ | | | $\alpha_{xx}$ | | | $\alpha_{zz}$ | | | $\beta_{zzz}$ | | |
|---|---|---|---|---|---|---|---|---|---|---|---|---|
| | DZ | DZP | Sadlej | DZ | DZP | Sadlej | DZ | DZP | Sadlej | DZ | DZP | Sadlej |
| PW91 | 0.798 | 0.624 | [b] | 0.908 | 1.964 | [b] | 1.989 | 2.799 | [b] | -6.79 | -6.19 | [b] |
| PW86 | 0.794 | 0.607 | 0.555 | 1.017 | 2.078 | 5.539 | 1.989 | 2.673 | 4.994 | -5.99 | -6.24 | -3.62 |
| BPW91 | 0.787 | 0.606 | 0.564 | 0.964 | 2.046 | 5.002 | 1.934 | 2.685 | 4.718 | -5.54 | -5.36 | -4.32 |
| BP86 | 0.795 | 0.607 | 0.563 | 1.010 | 2.086 | 5.286 | 1.939 | 2.681 | 4.655 | -5.62 | -5.47 | -9.15 |
| RHF | 0.803 | 0.631 | 0.590 | 0.883 | 1.956 | 3.982 | 1.187 | 2.484 | 3.981 | -4.31 | -3.82 | -1.41 |
| CC[c] | 0.801 | | 0.567 | | | | 1.899 | | 4.547 | -4.93 | | -2.23 |

[a]The molecule in the z direction; F and H atom on the negative and positive side of the z axis, respectively.
[b]For the functional PW91 in Sadlej basis the DFT equations did not converge to the correct ground state.
[c]From CCSD-LR method Ref. [150].

**Table** 3.2: Coupled−perturbed Kohn−Sham dipole moment, polarizability, and first hyperpolarizability values of HF molecule[a] at 1.0$R_e$ (in atomic units)

| DFT | $\mu_z$ | | | $\alpha_{xx}$ | | | $\alpha_{zz}$ | | | $\beta_{zzz}$ | | |
|---|---|---|---|---|---|---|---|---|---|---|---|---|
| | DZ | DZP | Sadlej | DZ | DZP | Sadlej | DZ | DZP | Sadlej | DZ | DZP | Sadlej |
| PW91 | 0.868 | 0.743 | 0.673 | 0.798 | 2.015 | 5.792 | 4.280 | 4.827 | 6.961 | -16.61 | -15.12 | -6.09 |
| PW86 | 0.860 | 0.729 | 0.682 | 0.846 | 2.070 | 6.317 | 4.263 | 4.728 | 7.017 | -19.12 | -17.73 | -12.23 |
| BPW91 | 0.854 | 0.728 | 0.677 | 0.805 | 2.042 | 5.823 | 4.177 | 4.668 | 6.719 | -18.06 | -16.71 | -10.88 |
| BP86 | 0.868 | 0.734 | 0.685 | 0.837 | 2.074 | 6.170 | 4.165 | 4.647 | 6.892 | -18.67 | -17.18 | -11.09 |
| RHF | 0.936 | 0.805 | 0.757 | 0.739 | 1.983 | 4.457 | 4.002 | 4.359 | 5.742 | -17.59 | -14.58 | -8.14 |
| FCI | 0.898[b] | 0.762[c] | | | | | 4.14[b] | 4.50[c] | | -17.32[b] | | |
| CC[b] | 0.896 | | 0.699 | | | | 4.179 | | 6.521 | -17.513 | | -9.869 |
| CCSD[d] | | | 0.707 | | | 5.164 | | | 6.327 | | | -8.91 |
| Expt.[e] | | 0.707 | | | 5.08 | | | 6.40 | | | | |

[a]The molecule in the z direction; F and H atom on the negative and positive side of the z axis, respectively.

[b]From CCSD-LR method Ref. [150].

[c]From Ref. [152].

[d]From Ref. [151].

[e]From Ref. [98].

**Table** 3.3: Coupled−perturbed Kohn−Sham dipole moment, polarizability, and first hyperpolarizability values of HF molecule[a] at $1.5R_e$ (in atomic units)

| DFT | $\mu_z$ | | | $\alpha_{xx}$ | | | $\alpha_{zz}$ | | | $\beta_{zzz}$ | | |
|---|---|---|---|---|---|---|---|---|---|---|---|---|
| | DZ | DZP | Sadlej | DZ | DZP | Sadlej | DZ | DZP | Sadlej | DZ | DZP | Sadlej |
| PW91 | 0.971 | 0.941 | 0.928 | 0.572 | 2.007 | 6.971 | 11.023 | 11.267 | 13.379 | -33.13 | -35.03 | -19.51 |
| PW86 | 0.955 | 0.920 | 0.940 | 0.587 | 2.020 | 7.801 | 11.061 | 11.209 | 13.895 | -38.85 | -38.82 | -39.94 |
| BPW91 | 0.935 | 0.902 | 0.908 | 0.567 | 2.000 | 7.201 | 10.983 | 11.210 | 13.366 | -39.49 | -40.81 | -36.56 |
| BP86 | 0.973 | 0.935 | 0.945 | 0.583 | 2.021 | 7.779 | 10.974 | 11.142 | 13.573 | -40.27 | -40.63 | -40.33 |
| RHF | 1.198 | 1.150 | 1.142 | 0.564 | 2.008 | 5.559 | 12.634 | 12.317 | 13.488 | -76.81 | -70.82 | -68.67 |
| FCI | 0.923[b] | 0.896[c] | | | | | 12.47[b] | 12.30[c] | | -2.39[b] | | |
| CC[b] | 0.926 | | 0.912 | | | | 12.383 | | 14.348 | -1.012 | | -24.302 |

[a]The molecule in the z direction; F and H atom on the negative and positive side of the z axis, respectively.
[b]From CCSD-LR method Ref. [150].
[c]From Ref. [152].

**Table** 3.4: Coupled-perturbed Kohn−Sham dipole moment, polarizability, and first hyperpolarizability values of HF molecule[a] at 2.0$R_e$ (in atomic units)

| DFT | $\mu_z$ | | | $\alpha_{xx}$ | | | $\alpha_{zz}$ | | | $\beta_{zzz}$ | | |
|---|---|---|---|---|---|---|---|---|---|---|---|---|
| | DZ | DZP | Sadlej | DZ | DZP | Sadlej | DZ | DZP | Sadlej | DZ | DZP | Sadlej |
| PW91 | 1.081 | 1.079 | 1.167 | 0.488 | 1.928 | 7.977 | 19.122 | 19.452 | 23.334 | -33.48 | -34.49 | -28.24 |
| PW86 | 1.068 | 1.068 | 1.166 | 0.499 | 1.942 | 9.324 | 18.688 | 19.195 | 23.308 | -38.57 | -35.48 | -39.09 |
| BPW91 | 1.013 | 1.010 | 1.084 | 0.487 | 1.926 | 8.233 | 18.785 | 19.159 | 22.676 | -39.31 | -40.05 | -58.15 |
| BP86 | 1.092 | 1.090 | 1.175 | 0.497 | 1.941 | 9.107 | 18.925 | 19.281 | 23.179 | -37.77 | -38.09 | -65.93 |
| RHF | 1.510 | 1.501 | 1.570 | 0.500 | 1.945 | 6.838 | 26.541 | 26.283 | 28.746 | | | |
| FCI | 0.605[b] | 0.621[c] | | | | | 18.42[b] | 19.20[c] | | 367[b] | | |
| CC[b] | 0.640 | | 0.820 | | | | 18.531 | | 26.189 | 352.68 | | 279.80 |

[a]The molecule in the z direction; F and H atom on the negative and positive side of the z axis, respectively.
[b]From CCSD-LR method Ref. [150].
[c]From Ref. [152].

**Table** 3.5: Coupled−perturbed Kohn−Sham dipole moment, polarizability and first hyperpolarizability values of BH molecule (in atomic units)

| Bond length | $\mu_z$ | $\alpha_{xx=yy}$ | $\alpha_{zz}$ | $\beta_{zzz}$ | $\beta_{xxz=yyz}$ |
|---|---|---|---|---|---|
| $0.75R_e$ | | | | | |
| CPHF | 0.966 | 25.25 | 15.53 | 71.5 | 0.2 |
| FF (BPW91) | 0.910 | | 17.95 | | |
| FF (PW86PW91) | 0.905 | | 16.40 | | |
| BPW91 | 0.890 | 17.54 | 17.98 | -12.1 | 11.1 |
| PW86PW91 | 0.896 | 18.02 | 16.40 | -10.0 | 36.1 |
| ECC | 0.799 | | 16.93 | -55.8 | |
| $R_e$ | | | | | |
| CPHF | 0.686 | 22.76 | 22.58 | -20.9 | 52.5 |
| FF (BPW91) | 0.638 | | 27.69 | | |
| FF (PW86PW91) | 0.621 | | 24.11 | | |
| BPW91 | 0.574 | 16.57 | 27.79 | 406.4 | 689.2 |
| PW86PW91 | 0.580 | 16.49 | 24.11 | -137.2 | 51.6 |
| ECC | 0.514 | | 23.66 | -51.9 | |
| CCSD (non-rel)[a] | 0.5298 | 20.433 | 23.044 | -29.04 | |
| CCSD (rel)[a] | 0.5256 | 20.308 | 23.145 | -27.70 | |
| BCCD[a] | 0.5257 | 20.311 | 23.143 | -27.53 | |
| CCSD (T)[a] | 0.5190 | 20.298 | 23.270 | -29.35 | |
| BCCD (T)[a] | 0.5190 | 20.295 | 23.270 | -29.20 | |
| Full-CI[a] | 0.5171 | 20.289 | 23.306 | -29.25 | |
| Expt.[a] | 0.4997 | | | | |
| $1.5R_e$ | | | | | |
| CPHF | -0.244 | 22.32 | 47.51 | -118.2 | 19.6 |
| FF (BPW91) | -0.184 | | 42.42 | | |
| FF (PW86PW91) | -0.179 | | 43.40 | | |
| BPW91 | -0.278 | 16.30 | 42.42 | -129.8 | 9.6 |
| PW86PW91 | -0.279 | 16.73 | 43.40 | -128.5 | 9.7 |
| ECC | -0.344 | | 62.97 | -57.4 | |
| $2.0R_e$ | | | | | |
| CPHF | -1.261 | 26.94 | 83.34 | 56.8 | -78.7 |
| FF (BPW91) | -0.826 | | 64.13 | | |
| FF (PW86PW91) | -0.816 | | 64.23 | | |
| BPW91 | -0.934 | 18.25 | 64.13 | -150.5 | -33.3 |
| PW86PW91 | -0.946 | 18.75 | 64.24 | 33.5 | -33.5 |
| ECC | -0.262 | | 30.16 | -246.6 | |

The molecule in the z direction; B and H atom on the negative and the positive side of the z axis, respectively.

[a] From Ref. [163].

**Table** 3.6: Coupled−perturbed Kohn−Sham dipole moment, polarizability and first hyperpolarizability values of CO molecule at $R_e$(in atomic units)

| Basis set | $\mu_z$ | $\alpha_{xx=yy}$ | $\alpha_{zz}$ | $\beta_{zzz}$ | $\beta_{xxz=yyz}$ |
|---|---|---|---|---|---|
| [8s 6p 3d] | | | | | |
| BPW91 | 0.075 | 10.21 | 15.52 | 34.7 | 6.0 |
| PW86PW91 | 0.073 | 10.58 | 15.66 | 27.5 | 5.7 |
| CCSD (non-rel)[a] | 0.070 | 11.85 | 15.79 | 29.4 | |
| CCSD (rel)[a] | 0.040 | 11.76 | 15.50 | 30.3 | |
| BCCD[a] | 0.038 | 11.74 | 15.52 | 30.6 | |
| CCSD(T)[a] | 0.061 | 11.91 | 15.61 | 30.2 | |
| BCCD(T)[a] | 0.058 | 11.90 | 15.62 | 30.4 | |
| Expt.[a] | 0.043 | 11.86 | 15.51 | | |
| VTZP | | | | | |
| CPHF | -0.120 | 8.79 | 13.79 | 23.0 | 1.05 |
| BPW91 | 0.060 | 7.97 | 14.69 | 19.9 | 3.1 |
| PW86PW91 | 0.052 | 8.18 | 14.85 | 20.3 | 3.3 |
| LDA[b] | 0.074 | 9.63 | 14.87 | 17.6 | 2.6 |
| VTZP+ | | | | | |
| CPHF | -0.102 | 10.93 | 14.36 | 30.9 | 3.9 |
| BPW91 | 0.074 | 9.98 | 15.39 | 31.6 | 4.8 |
| PW86PW91 | 0.073 | 10.35 | 15.50 | 39.8 | 6.7 |
| LDA[b] | 0.095 | 12.32 | 15.75 | 31.3 | 6.6 |
| Expt.[b] | 0.048 | 12.1 | 15.7 | | |

The molecule in the z direction; C and O atom on the negative and the positive side of the z axis, respectively.

[a] From Ref. [163].

[b] From Ref. [123].

**Table** 3.7: Coupled−perturbed Kohn−Sham dipole moment, polarizability and first hyperpolarizability values of $H_2O$ molecule (in atomic units)

| Basis set | $\mu_z$ | $\alpha_{xx}$ | $\alpha_{yy}$ | $\alpha_{zz}$ | $\beta_{zzz}$ | $\beta_{xxz}$ | $\beta_{yyz}$ |
|---|---|---|---|---|---|---|---|
| Sadlej[a] | | | | | | | |
| BP86 | 0.712 | 10.43 | 10.64 | 10.35 | -10.9 | -2.4 | -15.8 |
| PW86 | 0.707 | 10.72 | 10.88 | 10.66 | -12.6 | -3.7 | -17.3 |
| PW91 | 0.689 | 10.53 | 10.66 | 10.40 | -6.1 | -6.3 | -10.3 |
| SCF/TDHF[b] | 0.780 | 7.84 | 9.17 | 8.50 | -4.6 | -0.6 | -9.7 |
| MBPT (2)[b] | 0.730 | | 10.05 | 9.75 | -8.7 | -2.4 | -10.6 |
| CCSD[b] | 0.729 | | 9.89 | 9.49 | -7.3 | -2.0 | -10.8 |
| Expt.[b] | 0.721 | | | | | | |
| VTZP[c] | | | | | | | |
| CPHF | 0.864 | 7.55 | 3.85 | 6.03 | -6.6 | -0.8 | -15.3 |
| BP86 | 0.827 | 7.95 | 4.34 | 6.62 | -10.0 | -2.5 | -17.9 |
| PW91 | 0.826 | 7.98 | 4.33 | 6.65 | -7.3 | -2.1 | -14.5 |
| LDA[d] | 0.852 | 7.93 | 4.02 | 6.65 | -9.8 | -2.3 | -16.6 |
| VTZP+[c] | | | | | | | |
| CPHF | 0.793 | 9.03 | 7.64 | 8.28 | -6.8 | -0.4 | -9.8 |
| BP86 | 0.726 | 10.22 | 9.76 | 9.99 | -20.7 | -8.1 | -14.6 |
| PW91 | 0.722 | 10.38 | 10.29 | 10.11 | -6.6 | 1.7 | -12.0 |
| LDA[d] | 0.743 | 10.32 | 9.96 | 10.12 | -17.1 | -6.3 | -12.9 |
| Expt.[d] | 0.727 | 10.31±0.09 | 9.55±0.09 | 9.91±0.02 | | | |

[a]The molecule in the positive z-direction; O atom is placed at the origin and the two H atoms are in the yz plane. The equilibrium geometry used was $R_{OH}$= 0.957 Åand $\theta_{HOH}$= 104.58 degrees. The auxiliary basis used for the hydrogen and oxygen atoms were (5,1; 5,1) and (5,3; 5,3), respectively.

[b] From Ref. [151].

[c] The molecule in the positive z-direction; O atom is placed at the origin and the two H atoms are in the xz plane. The equilibrium geometry used was $R_{OH}$= 0.9576 Åand $\theta_{HOH}$= 104.488 degrees. The auxiliary basis used for the hydrogen and oxygen atoms were (3,1; 3,1) and (4,4; 4,4), respectively.

[d]From Ref. [123].

Chapter 4

# Static Polarizabilities from CPKS methods and extension of NIA-CPKS to dipole-quadrupole polarizability


## *Abstract:*

In this chapter, we present the extension of the non-iterative approximation to the CPKS (NIA-CPKS) for the calculation of the dipole-quadrupole polarizability, $A$, of molecules. Details of the formalism for calculation of $A_{x,yz}$ components will be discussed. Additionally, we compare the polarizabilities, and first hyperpolarizabilities of molecules obtained from our NIA-CPKS formalism, with those obtained from a recent implementation of another approximate CPKS implementation in which, auxiliary derivative density is used. This has been implemented in the deMon2k, by a Mexican group. The hyperpolarizability module to this program has been added by us. We will compare the results from the NIA-CPKS with the ones from this implementation.


## 4.1 Introduction

A lot of attention has been focused on obtaining properties like the dipole polarizability, $\alpha$, and first hyperpolarizability, $\beta$, which are the fundamental characteristics of atoms and molecules. However, the amount of literature available for higher order

polarizabilities, namely, the dipole-quadrupole polarizability, $A$, is comparatively smaller in number. Accurate values are reported for a few molecules only [169, 170]. Recently, Quinet *et. al.* have given an analytic procedure based on the time-dependent Hartree-Fock (TDHF) scheme for evaluating the frequency dependent electric dipole-quadrupole polarizability, $A$ [171]. The higher order polarizabilities are important in the understanding of intermolecular interactions, scattering of electromagnetic waves, etc. [77, 172]. Maroulis has reported best/recommended $A$ values using a combination of Møller-Plesset scheme [169], whereas the gradient of the dipole-quadrupole polarizability are estimated and shown to be in good agreement with experiment [173]. Amos has presented a coupled-perturbed Hartree-Fock (CPHF) scheme to evaluate the static $A$ values. Quinet *et. al* also describes a method for evaluating dynamic $A$ values. The quantities $A$ and $\partial A/\partial Q$, i.e. its derivative with respect to cartesian coordinates and vibrational normal coordinates are determined within collision-induced light-scattering and high-resolution infrared absorption spectroscopies [172, 175, 176, 177]. $A$, is also relevant to the description of intermolecular interactions and dielectric properties [77, 172]. Few other work involving the dipole-quadrupole polarizability are available in literature [178, 179, 180, 181, 182, 183, 184, 185, 186, 187]. Hohm and Maroulis, have used finite-field method to obtain the polarizabilities of $TiCl_4$, $ZrCl_4$ and $HfCl_4$ [185]. The convergence of the Taylor series expansion of the field dependent energy, induced dipole moment and the induced quadrupole moment, is faster, when weak electric fields are used. This allows a reliable determination of the electric properties. This was shown by Hohm and Maroulis [186]. Effects of electron correlation on the molecular properties have been obtained at the MP2 level by Helgaker *et. al* [188]. Wiberg *et. al* have extracted induced multipole moments via MP2 density [189].

However, most of these reported calculations are, using the *ab initio* theories, and, dipole-quadrupole polarizability calculations using the DFT are scarce. We, therefore, put forth a method which will simplify the scenario for these calculation

in the KS-DFT framework.

## 4.2 Theory

As discussed, in the section 1.7, the Hamiltonian has a dependence on the electric field in the presence of a weak static electric field. The induced dipole moment, and quadrupole moment, can then be expanded as [77],

$$\mu_i(F) = \mu_i^{(0)} + \alpha_{ij}F_j + \frac{1}{3}A_{i,jk}F_{ij} + \dots \tag{4.1}$$

$$\theta_{ij}(F) = \theta_{ij}^{(0)} + A_{i,jk}F_j + \dots \tag{4.2}$$

where, the $F_i$ and $F_{ij}$ are the electric field and the electric field gradient, respectively, and the i, j and k span the x, y and z directions. The $\theta_{ij}$, in the above equation, is given as a traceless quantity; $\theta_{ij} = 3/2[e_a(r_{ai}r_{aj} - r_a^2/3\delta_{ij})]$. The $A_{ij}$, are tensor elements of the electric dipole-electric quadrupole polarizability, and $\mu^{(0)}$ and $\theta^{(0)}$ are the permanent dipole and quadrupole moments in the absence of the external electric field. The quantity $A$, describes the dipole moment induced by the electric field gradient. This quantity can be obtained if the response of the electron density to the external weak static electric perturbation is obtained.

## 4.3 Methodology

The quantity, $A$, could be obtained as a trace of the product of the response density matrix and quadrupole moment integrals. The quadrupole moment operator has been given in the earlier section. For obtaining the derivative density matrix, we go back to the non-iterative approximation to the coupled-perturbed Kohn-Sham (NIA-CPKS), described in chapter 2. Using exactly the identical formalism, where, the Hamiltonian has a $\mu.F$ term, and, solving the single-step CPKS matrix equation by plugging in the derivative of the Kohn-Sham (KS) operator matrix, the derivative coefficient matrix is obtained. This derivative coefficient matrix, along

with the coefficient matrix of the unperturbed calculation, gives the derivative density matrix. The trace of the product of the derivative density matrix of the x, y and z directions with the quadrupole moment integrals of xx, xy, xz, yy, yz and zz, gives the corresponding tensor component of the dipole-quadrupole polarizability, $A$ as,

$$A_{i,jk} \; = \; Tr(P'_i.\theta_{jk}) \tag{4.3}$$

where, i, j and k span the x, y and z directions, $P'$, is the derivative density matrix and $\theta$, is the quadrupole moment integrals. We thus, obtain the tensor components of the dipole-quadrupole polarizability using the NIA-CPKS procedure.

## 4.4 Polarizability and Hyperpolarizability Calculations using Approximate CPKS Methods

We, now, present a comparison between two approximate CPKS implementations. The one described in chapter 2, and referred to as NIA-CPKS, is a single-step solution of the CPKS matrix equations in a orbital basis [145, 146, 147, 148]. The newly implemented approximate CPKS, proposed by the deMon developers group in Mexico, is also a non-iterative approximation of the CPKS, and uses the auxiliary density response (ADR) [190]. Hereon, we refer to their implementation by the abbreviation CPKS-ADR. Both the implementations have been done in deMon2k program.

Both the above mentioned implementations have been done to the KS-DFT and use Gaussian basis centered on atoms. In both implementations, an auxiliary basis is required for fitting of the coulomb integrals. The coulomb energy is evaluated using a variational fitting procedure proposed by Dunlap, Connolly and Sabin [142, 143]. There is a fitting using auxiliary basis functions of the charge density for obtaining the exchange-correlation potential in deMon2k. The single-step NIA-CPKS method, could be used for the fitting using the auxiliary basis, as well as orbital basis, for evaluation of the exchange-correlation functional. Also, it is well

known that, for sensitive response property calculations, use of the orbital density is recommended. However, the CPKS-ADR implementation available for the analytic polarizability tensor calculation, can be used only when an auxiliary basis is used, for obtaining the exchange-correlation potential. Also, the CPKS-ADR has been implemented only for the VWN functional in the deMon2k program, as against, our NIA-CPKS implementation, which can be used for both local as well as non-local exchange-correlation functionals. In the NIA-CPKS method the derivative Kohn-Sham operator matrix is obtained using a finite-field approximation, whereas, in the CPKS-ADR method, the iterative procedure is avoided by obtaining a density matrix response, $P'$, using an auxiliary density response, $x'$, The auxiliary density response is obtained through the solution of the matrix linear equation system (LES) [191]. Thus, using this density matrix response, the derivative KS-operator matrix is constructed and solved in a single step, to obtain the final density matrix response used for the polarizability calculations. The general idea of the CPKS for both implementations remains the same, except, for the manner in which, the KS derivative matrix is obtained. Calculations of polarizability and first hyperpolarizability from both implementations are presented in this chapter.

## 4.5 Computational Details

We, present polarizability and first hyperpolarizability calculations from the NIA-CPKS and CPKS-ADR methods. The calculations were carried out using the VWN [51] exchange-correlation functional. The A2 auxiliary basis as available in the deMon2k auxiliary basis set library has been used, for fitting of the density used for evaluation of the exchange-correlation term in the Kohn-Sham (KS) operator. We have carried out the calculations using NIA-CPKS method for the VWN functional. We present the results of the polarizabilities from the NIA-CPKS, for density fitted using the orbital basis (referred to as BASIS in the tables) as well as the auxiliary basis (referred to as AUXIS in the tables). The calculations are reported for

$Na_2$, $Na_4$, $Na_6$ and $Na_8$ clusters, using Sadlej [192] and TZVP-FIP1 [193] basis sets. The xx, yy and zz components of $\alpha$, and all the tensor components of $\beta$ are tabulated. The Na cluster geometries are optimized at the DZVP/A2 level using the exchange-correlation functional of Perdew and Wang (PW86) [56, 57]. The details of the optimization could be found in section 5.4. The restricted Kohn-Sham (RKS) scheme has been used for the response property calculations. The tolerance on the density was set to $10^{-9}$ a.u. The grid accuracy of $10^{-6}$ a.u. and a finite-field value of 0.001 a.u. has been used for the CPKS calculations. The hyperpolarizability module was added to the CPKS-ADR program for obtaining the $\beta$ tensor components.

## 4.6 Results and Discussion

We present the dipole polarizability and first hyperpolarizability calculations for the Na clusters, namely, $Na_2$, $Na_4$, $Na_6$ and $Na_8$ using the NIA-CPKS and CPKS-ADR methods. The calculations from the NIA-CPKS method are presented using the orbital, as well as, auxiliary basis in the tables, whereas, the CPKS-ADR values are calculated using the auxiliary basis only. A2 auxiliary basis was used. The calculations have been carried out for the Sadlej and TZVP-FIP1 basis sets. The $\alpha_{xx}$, $\alpha_{yy}$ and $\alpha_{zz}$ components of polarizability along with mean polarizability values, $\overline{\alpha}$, are presented in Table. 4.1. The experimental values, given in the Table. 4.1 were calculated from the measurement of relative polarizabilities of Knight *et al.* [194] and the absolute measurement of the atomic polarizability by Molof *et al.* [195]. Tables. 4.2 - table. 4.5 present the

In general, there is a decrease in the polarizability values from both methods for each cluster, as we go from the Sadlej to the TZVP-FIP1 basis set, except, in case of $\alpha_{zz}$ component for the $Na_2$ and $Na_8$ clusters, which shows a slight increase. This trend is also reflected in the mean polarizability values. It can be noted that, for Sadlej basis, values obtained using the AUXIS option for the NIA-CPKS, are

closer to the CPKS-ADR results, as compared to, the NIA-CPKS values obtained using the BASIS option. This trend is more or less repeated for the TZVP-FIP1 basis, except, in case of $Na_4$ cluster, where, the values from the BASIS option are closer to the ones from CPKS-ADR. However, the BASIS option is recommended for sensitive properties like polarizability calculations, where the electron correlation as well as basis sets play an important role. $\overline{\alpha}$ values seem to be underestimated in comparison to the experimental values. The difference between the calculated values and experiments goes on increasing as we go from the $Na_2$ to $Na_8$ cluster. This is mainly, due to the temperature effects prevalent in experiments that are missing in both the methods. Also, local density approximated VWN functional is well known for its over-binding nature, which could be another reason for the underestimation of the polarizability values. However, we observe, NIA-CPKS gives, $\overline{\alpha}$ values closer to the experiments. This trend is apparent for mean polarizability values as we go to larger clusters. Another observation is, that, the $\overline{\alpha}$ values using the BASIS option for the NIA-CPKS method gives values closer to the experiments as we move from $Na_2$ to $Na_8$ for Sadlej as well as TZVP-FIP1 basis. In general, the Sadlej basis gives values better than TZVP-FIP1 basis.

We, now discuss the hyperpolarizability results in Table. 4.2. $Na_2$ has zero first hyperpolarizability, however, as seen in the tables, both methods give a finite value for the $\beta$ components, which may be due to numerical errors in the implementations of both the methods. We see that, the error is more when the auxiliary basis are used for fitting of the charge density, whereas, it is less when the orbital basis is used. Also, the CPKS-ADR method shows a larger error in the $\beta_{zzz}$ values, in comparison to, the NIA-CPKS method for both basis sets. However, the error is more in case of Sadlej basis for both methods. The TZVP-FIP1 basis gives a relatively smaller error in the $\beta$ values for the $Na_2$ cluster in comparison to all the other values. In Table. 4.3, the NIA-CPKS gives negligible values for the $\beta$ components for both the basis sets using AUXIS as well as BASIS option. This trend is similar for the values for the TZVP-FIP1 basis using CPKS-ADR method, except, for the high value of

-20.4 a.u. for the $\beta_{yyy}$ component. The values from Sadlej basis for CPKS-ADR method, however, show a different trend, and, are higher than the other values for the $Na_4$ cluster. The effect of the basis set can be clearly noted here for the CPKS-ADR method, however, we are unable to explain them due to lack of availability of experimental values. A general trend, that can be observed in Tables. 4.4 and Table. 4.5 for the $\beta$ values from the NIA-CPKS method is that, the values using AUXIS approach is larger than those using BASIS approach, except, for $\beta_{yxx}$ and $\beta_{zxx}$ components in Table. 4.4 for the $Na_6$ cluster, and, for $\beta_{yyy}$ and $\beta_{zzz}$ components in Table. 4.5 for $Na_8$ cluster. Although, certain $\beta$ components in Table. 4.4 and Table. 4.5 from the CPKS-ADR and NIA-CPKS methods are close to each other, a clear correlation between the two cannot be established due to inconsistency in the values for the other components of $\beta$. Additionally, the values from the ADR-CPKS method, for Sadlej and TZVP-FIP1 basis, also vary widely. However, the $\beta$ values for the Sadlej and TZVP-FIP1 basis of the $Na_6$ and $Na_8$ clusters are more stable using both AUXIS and BASIS options in the NIA-CPKS method.

## 4.7 Conclusion and Scope

We observed that the polarizability values were underestimated by both methods, however, for larger clusters the BASIS option of the NIA-CPKS gave better values of $\overline{\alpha}$, in comparison to AUXIS approach and the CPKS-ADR values. In case of hyperpolarizabilities, we found a numerical error in the values for the $Na_2$ cluster. The error was less in case of the values from NIA-CPKS method, especially, using the BASIS option. We found, the CPKS-ADR values for $\beta$ highly inconsistent for the two basis sets, whereas, there was a relative stability in the values obtained using the BASIS option of the NIA-CPKS method for all the sodium atom clusters. Despite, the complicated nature of the CPKS-ADR, that is closer to the analytic CPKS, the results for the polarizabilities and hyperpolarizabilities do not show much improvement from the NIA-CPKS which is a much simpler implemen-

tation and proves to be stable in terms of the $\beta$ results. Also, the values would improve further when a better exchange-correlation functional is chosen, which is not possible in case of the CPKS-ADR method as this is implemented for the VWN functional only. We found the results for $\beta$ obtained from the density obtained using orbital basis for evaluating the exchange-correlation term in the KS operator using the NIA-CPKS, led to more stable values than the ones obtained using the auxiliary basis. The NIA-CPKS can be used for both the local as well as non-local functionals. This is possible because the derivative KS-operator matrix is obtained in a finite-field manner. As a result, the NIA-CPKS method is viable for large molecules and larger basis sets.

The scope of our method lies in the single-step solution as well as the numerical approximation used for obtaining the derivative KS-operator matrix, which can be exploited for extending our formalism for other properties, namely, the magnetic response properties. A similar implementation could also be done for the time-dependent dynamic response for excited state properties. The central idea of obtaining the derivative KS-operator matrix in the NIA-CPKS makes it highly useful for applications to large molecules.

**Table** 4.1: Dipole polarizability and first hyperpolarizability from NIA-CPKS and CPKS-ADR methods in deMon2k(in Atomic Units)

| Basis | System | $\alpha$ values | CPKS-ADR | NIA-CPKS AUXIS(BASIS) | Expt. |
|---|---|---|---|---|---|
| Sadlej | $Na_2$ | $\alpha_{xx}$ | 179.54 | 184.04(183.95) | |
| | | $\alpha_{yy}$ | 179.54 | 183.63(183.96) | |
| | | $\alpha_{zz}$ | 312.66 | 315.28(316.02) | |
| | | $\overline{\alpha}$ | 223.91 | 227.65(227.97) | 251.90 |
| | $Na_4$ | $\alpha_{xx}$ | 781.15 | 781.53(775.62) | |
| | | $\alpha_{yy}$ | 283.57 | 284.20(282.23) | |
| | | $\alpha_{zz}$ | 362.80 | 364.63(361.34) | |
| | | $\overline{\alpha}$ | 475.84 | 476.79(473.06) | 538.62 |
| | $Na_6$ | $\alpha_{xx}$ | 554.99 | 559.23(562.44) | |
| | | $\alpha_{yy}$ | 636.59 | 640.46(644.61) | |
| | | $\alpha_{zz}$ | 682.71 | 687.20(692.45) | |
| | | $\overline{\alpha}$ | 624.76 | 628.96(633.16) | 816.62 |
| | $Na_8$ | $\alpha_{xx}$ | 675.25 | 677.57(689.12) | |
| | | $\alpha_{yy}$ | 676.39 | 677.26(688.91) | |
| | | $\alpha_{zz}$ | 782.91 | 783.21(777.76) | |
| | | $\overline{\alpha}$ | 711.52 | 712.68(718.60) | 868.75 |
| TZVP-FIP1 | $Na_2$ | $\alpha_{xx}$ | 155.95 | 158.63(157.09) | |
| | | $\alpha_{yy}$ | 155.95 | 158.61(157.09) | |
| | | $\alpha_{zz}$ | 313.40 | 317.17(314.27) | |
| | | $\overline{\alpha}$ | 208.43 | 211.47(209.48) | 251.90 |
| | $Na_4$ | $\alpha_{xx}$ | 765.29 | 772.69(767.82) | |
| | | $\alpha_{yy}$ | 269.78 | 271.40(268.91) | |
| | | $\alpha_{zz}$ | 354.85 | 357.34(353.57) | |
| | | $\overline{\alpha}$ | 463.31 | 467.14(463.43) | 538.62 |
| | $Na_6$ | $\alpha_{xx}$ | 548.02 | 552.47(553.60) | |
| | | $\alpha_{yy}$ | 629.12 | 632.78(635.12) | |
| | | $\alpha_{zz}$ | 676.78 | 679.00(682.10) | |
| | | $\overline{\alpha}$ | 617.97 | 621.42(623.61) | 816.62 |
| | $Na_8$ | $\alpha_{xx}$ | 671.05 | 674.63(683.30) | |
| | | $\alpha_{yy}$ | 670.82 | 674.83(680.63) | |
| | | $\alpha_{zz}$ | 784.28 | 782.92(781.70) | |
| | | $\overline{\alpha}$ | 675.38 | 710.79(715.21) | 868.75 |

[a]Experimental values calculated from the measurement of relative polarizabilities of Knight *et al.* [194] and the absolute measurement of the atomic polarizability by Molof *et al.* [195]

**Table** 4.2: Dipole polarizability and first hyperpolarizability of $Na_2$ cluster from NIA-CPKS and CPKS-ADR methods in deMon2k using Sadlej and TZVP basis (in Atomic Units)

| | Sadlej | | TZVP-FIP1 | |
|---|---|---|---|---|
| $\beta$-component | CPKS-ADR | NIA-CPKS AUXIS(BASIS) | CPKS-ADR | NIA-CPKS AUXIS(BASIS) |
| $\beta_{zxx}$ | -1.7 | -2.5(0.8) | 1.3 | 0.5(0.5) |
| $\beta_{zyy}$ | -1.7 | -2.0(0.8) | 1.3 | 0.5(0.5) |
| $\beta_{zzz}$ | -11.4 | -4.8(3.2) | 9.0 | 1.6(2.1) |

**Table** 4.3: Dipole polarizability and first hyperpolarizability of $Na_4$ cluster from NIA-CPKS and CPKS-ADR methods in deMon2k using Sadlej and TZVP basis (in Atomic Units)

| | Sadlej | | TZVP-FIP1 | |
|---|---|---|---|---|
| $\beta$-component | CPKS-ADR | NIA-CPKS AUXIS(BASIS) | CPKS-ADR | NIA-CPKS AUXIS(BASIS) |
| $\beta_{xxx}$ | -42.6 | -0.8(0.0) | 3.5 | 0.6(0.0) |
| $\beta_{xyy}$ | 77.3 | -0.9(-4.2) | 1.8 | 1.1(0.0) |
| $\beta_{xzz}$ | 25.9 | 0.0(-0.5) | 0.7 | 0.0(0.0) |
| $\beta_{yxx}$ | -109.3 | -1.4(-4.3) | -5.1 | -2.9(-2.5) |
| $\beta_{yyy}$ | -596.5 | 0.2(-5.0) | -20.4 | -2.3(-0.6) |
| $\beta_{yzz}$ | 36.9 | 1.2(-0.2) | 0.6 | -0.4(0.4) |
| $\beta_{zxx}$ | -14.2 | 0.2(0.5) | -0.3 | 0.3(0.0) |
| $\beta_{zyy}$ | 69.3 | 0.0(0.6) | -0.2 | 0.2(0.0) |
| $\beta_{zzz}$ | 12.4 | 0.4(0.5) | 0.0 | 0.0(0.1) |

**Table** 4.4: Dipole polarizability and first hyperpolarizability of $Na_6$ cluster from NIA-CPKS and CPKS-ADR methods in deMon2k using Sadlej and TZVP basis (in Atomic Units)

| | Sadlej | | TZVP-FIP1 | |
|---|---|---|---|---|
| $\beta$-component | CPKS-ADR | NIA-CPKS AUXIS(BASIS) | CPKS-ADR | NIA-CPKS AUXIS(BASIS) |
| $\beta_{xxx}$ | -3698.3 | -3796.0(-2794.4) | -4000.6 | -3991.8(-3390.7) |
| $\beta_{xyy}$ | -158.3 | -632.3(-290.3) | -872.2 | -636.0(-350.0) |
| $\beta_{xzz}$ | -1271.5 | -1229.0(-929.7) | -2021.2 | -1371.3(-1145.1) |
| $\beta_{yxx}$ | 320.3 | 386.6(532.6) | 631.8 | 290.4(654.8) |
| $\beta_{yyy}$ | -2916.8 | -3697.1(-2981.5) | -3213.3 | -3987.7(-3609.2) |
| $\beta_{yzz}$ | -756.4 | -898.4(-726.4) | -437.1 | -1027.2(-880.7) |
| $\beta_{zxx}$ | 384.8 | 227.4(509.6) | 1019.0 | 236.0(591.7) |
| $\beta_{zyy}$ | -333.0 | -439.8(-133.9) | 374.3 | -381.8(-144.0) |
| $\beta_{zzz}$ | -3243.2 | -3314.8(-2496.4) | -2261.9 | -3341.9(-2945.5) |

**Table** 4.5: Dipole polarizability and first hyperpolarizability of $Na_8$ cluster from NIA-CPKS and CPKS-ADR methods in deMon2k using Sadlej and TZVP basis (in Atomic Units)

| | Sadlej | | TZVP-FIP1 | |
|---|---|---|---|---|
| $\beta$-component | CPKS-ADR | NIA-CPKS AUXIS(BASIS) | CPKS-ADR | NIA-CPKS AUXIS(BASIS) |
| $\beta_{xxx}$ | -710.0 | -106.9(-171.5) | 275.2 | -195.1(-194.9) |
| $\beta_{xyy}$ | 894.8 | 804.7(609.1) | 1501.6 | 701.1(607.1) |
| $\beta_{xzz}$ | -799.7 | -629.8(-531.1) | 361.8 | -614.8(-542.4) |
| $\beta_{yxx}$ | 392.8 | 770.4(612.5) | 549.9 | 727.3(622.2) |
| $\beta_{yyy}$ | 388.1 | 202.1(217.4) | -836.6 | 20.0(177.6) |
| $\beta_{yzz}$ | -1588.0 | -963.2(-733.7) | -960.1 | -1069.2(-743.5) |
| $\beta_{zxx}$ | 385.4 | 496.8(446.2) | 856.9 | 507.5(447.7) |
| $\beta_{zyy}$ | -33.7 | -292.6(-284.2) | 351.4 | -318.4(-288.2) |
| $\beta_{zzz}$ | 750.2 | -166.3(-204.9) | -5032.6 | -206.9(-207.3) |

Chapter 5

# Nonlinear optical properties of some alkali metal clusters and derivatives of para-nitroaniline


## *Abstract:*

In this chapter we present the studies of static dipole polarizability and first-hyperpolarizability of two different class of systems using our implementation of the non-iterative approximation of the coupled-perturbed Kohn-Sham (CPKS) equations in the deMon2k. A detailed study of the even number sodium atom clusters has been carried out. We attempt to bring out the structure-property relationship as well as the correlation and basis set effects for the $Na_n$, n=2, 4, 6 and 8 sodium atom clusters by comparing our KS-DFT response calculations with the benchmark MP2 and HF calculations. Additionally, we investigate the effects of substitution, position of the substituent and the symmetry on the nonlinear optical properties of para-nitroaniline and its derivatives using our method. MP2 calculations are used as benchmark.


## 5.1 Metal Clusters

Linear and nonlinear response electric properties, namely, dipole-polarizability and dipole first-hyperpolarizabilities, of metal clusters have been of considerable interest over the past decade [196]. The size dependence of the optical properties [196, 197] makes the study of clusters even more interesting for understanding the

correlation between the two. Clusters [198] are aggregates of atoms or molecules, generally intermediate in size. Clusters of up to 40 atoms are considered to be small sized. The properties of small clusters vary so much with size and shape that, their correlation with number of component particles is not simple. For large clusters, the properties approach those of the corresponding bulk material. Molecules are characterized by having definite compositions, and, in most cases, definite structures. The properties of clusters, on the other hand, depend on the number of atoms in the cluster and so does the most stable structure. Clusters thus, differ from conventional molecules because of composition and structure. Clusters could be composed of any number of particles of the same or different kind, and can be further classified as homogeneous or heterogeneous clusters, respectively, and for most of them, as the number of atoms increases, the number of stable structures grows rapidly. Clusters have drawn interest for several reasons. There are powerful ways to study them, both experimentally and theoretically. Clusters may give way to make altogether new kinds of materials, to carry out chemical reactions in new ways, and to gain understanding of the intermediate matter, which exists as one goes from molecules to crystals to bulk. All these make cluster science a fascinating field, which offers possibilities for new materials and processes.

In general, metal clusters have been studied to a reasonable extent [199]. However, the presence of a single valence electron makes the alkali metal clusters the simplest metal cluster. Hence, it has been used as a prototype system for understanding the size effects in metal clusters. Here, we concentrate on sodium clusters of up to 8 atoms. Polarizabilities of the sodium clusters, have been reported using, theory [200, 201, 202, 203, 204, 205, 206, 124, 193, 207] as well as experiments [207, 194, 208, 195]. Guan *et al.* (Ref. [124] and references therein) have done all-electron density functional calculations for $Na_n$ (n=1-6) clusters using local and gradient-corrected functionals. They have discussed several popular models for studying polarizability of clusters spanning the simplest and oldest conducting sphere model for studying the clusters to the free electron model used for studying

the bulk alkali metals. Guan et al. have also mentioned about the quantum mechanical jellium sphere approximation differing from the classical sphere model due to the fact that, the quantum mechanical density extends beyond the radius of the classical sphere, thus the effective sphere being larger.

In the first part of this chapter, we study the correlation of response electric properties with size for the homonuclear alkali metal clusters of Sodium using an approximate formalism proposed by us and discussed in Chapter 2 [145, 146, 147]. We study the dipole polarizability and the first-hyperpolarizability of the even number of Na atom clusters using local density approximation (LDA) and generalized gradient approximation (GGA) based exchange-correlation functionals in the presence of an external homogeneous static electric field perturbation. We also discuss the effect of electron correlation on the polarizabilities. We have done an all-electron calculation for the optimizations as well as for the response properties. Calculations, that consider all the electrons in the cluster, are not very common. This is, especially, the case for *ab initio* calculations. There are some all-electron optimizations available using the DFT [124, 193]. We use atomic units throughout, unless otherwise stated.

## 5.2 Para-nitroaniline (PNA) and its methyl substituted derivatives

Organic molecules with delocalized $\pi$ electrons have attracted a lot of attention as they exhibit particularly large nonlinear responses [209]. The microscopic structure-property relationship for such molecules may lead to discovery of improved nonlinear optical (NLO) characteristics in materials, thus, facilitating the designing of new NLO molecules [97]. This all can be done through study of the polarizability and the hyperpolarizability using computational methods. Electron-correlation effects play a crucial role in the determination of these properties. NLO properties of a variety of push-pull phenylenes have been studied extensively [210, 211]. The sensitivity

of the NLO properties to the conjugation length, donor and acceptor substitutions and effects due to symmetry in the molecule are well known [212]. Over the period, para-nitroaniline (PNA) has been identified as a prototype system to understand the large nonlinear responses exhibited due to the presence of donor-acceptor moieties which lead to charge transfer in the PNA molecule. There are a number of studies available for the PNA molecule [213, 214, 215, 216, 217, 218, 219, 220]. The static response properties of the PNA and its methyl substituted derivatives have been studied in the second half of this chapter.

## 5.3 General Theory

DFT [40, 221] has been widely used for molecular response property calculations. Response property of molecule is the response of the molecule to some kind of perturbation. For an external perturbation the molecular energy has a dependence on the perturbation and can be expanded as a Taylor series expansion. In the presence of a static electric field perturbation, the energy expansion becomes,

$$E(F) = E(0) - \sum_i \mu_i F_i - \frac{1}{2}\sum_{i,j} \alpha_{ij} F_i F_j - \frac{1}{6}\sum_{i,j,k} \beta_{ijk} F_i F_j F_k \tag{5.1}$$

where, i, j and k are summation indices each spanning the x, y and z direction, the first term is the energy of the molecule in the absence of the electric field perturbation, F, the second term, gives the dipole moment, the third term gives the dipole polarizability, the fourth term gives the dipole first-hyperpolarizability and so on ...

Alternatively, the field dependent dipole moment in turn can be written as,

$$\mu_i(F) = \mu_i + \sum_j \alpha_{ij} F_j + \frac{1}{2}\sum_{j,k} \beta_{ijk} F_i F_j F_k + \ldots \tag{5.2}$$

where, i, j and k span the x, y and z directions, $\mu_i$, $\alpha_{ij}$ and $\beta_{ijk}$ is a component of the permanent dipole moment, dipole polarizability and the dipole first-

hyperpolarizability, respectively, and so on ... These molecular electric response properties can be obtained by explicitly obtaining the derivatives of energy with respect to the perturbation, i.e. analytically using the coupled Kohn-Sham method [108, 126, 128, 129, 130, 131] or by doing a least squares fit to a polynomial [123], or by using a numerical finite-field method. Choosing the finite field values symmetrically (eg. $\pm$ 0.001 a.u., like we have chosen in this work), the next highest contamination in the numerical procedure can be eliminated, thus ensuring more numerical stability of the results. However, the precision in the calculation of energies, limits the size of the field value. In the analytical response approach, the CPKS equations need to be solved to obtain the response of the electron density in terms of the derivative of the molecular orbital coefficients. The CPKS matrix equations are basically the derivatives of the perturbed KS operator matrix equations with respect to the electric field perturbation, where the Hamiltonian has a dependence on the electric field and can be written as,

$$H(F) = H_0 + \mu F \tag{5.3}$$

where, the first term is, the unperturbed Hamiltonian and the second term is, the perturbation that is linear in field, F. We thus, have a linear response term in the Hamiltonian. Solving the CPKS equations, we can obtain the perturbed density matrix. And, due to the variational nature of the DFT, we can make use of the $(2n + 1)$ rule for the energy derivative [83], which is a result of the Hellmann-Feynman theorem [78, 79]. As a consequence, the first order response of the electron density, which is the first-order change in the density, can be used to obtain response properties up to the third order. This means that, we can evaluate not only the dipole polarizability, but also the dipole first-hyperpolarizability using this response of the electron density.

## 5.4 Computational details of Na cluster calculations

The linear combination of Gaussian-type orbitals Kohn-Sham density functional theory (LCGTO-KS-DFT) method, as implemented in the program deMon2k [222], was used to carry out all geometry optimizations and harmonic vibrational frequency calculations. The program uses the formalism of the Kohn-Sham equations [50] and analytic energy gradients for the structure optimizations. The exchange-correlation potential was numerically integrated on an adaptive grid [223]. The grid accuracy was set to $10^{-5}$ in all calculations. The Coulomb energy was calculated by variational fitting procedure proposed by Dunlap, Connolly and Sabin [142, 143]. For the fitting of the density, the *AUXIS* option with the auxiliary function set A2 [164] was used in all the optimization calculations and the vibrational analysis calculation following the earlier work of Calaminici *et al.* [193], which was found sufficient for the purpose. In order to localize different minima on the potential energy surface (PES), the structures of the studied sodium clusters have been optimized considering as starting points, different initial geometries and multiplicities. In order to avoid spin contamination the calculations were performed with the restricted open shell Kohn-Sham (ROKS) method. The ROKS method in deMon2k is the DFT analog of the Roothaan's open shell equations for HF theory [224], it means that all coupled alpha and beta electrons occupy the same space orbital and that the corresponding close shell exchange-correlation potential is given as average of the alpha and beta exchange-correlation potential. The calculations were performed in the LDA using the exchange-correlation contributions proposed by Vosko, Wilk and Nusair [51] and employing all-electron basis sets [164]. The same functional was used for the frequency analysis in order to distinguish between minima and transition state on the potential energy surface (PES). Cluster optimizations were also carried out at the GGA using the same basis and auxiliary function set with the exchange-correlation functional of Perdew and Wang (PW86) [56, 57]. A

quasi-Newton method in internal redundant coordinates with analytic energy gradients was used for the structure optimization [225]. The convergence was based on the Cartesian gradient and displacement vectors with a threshold of $10^{-4}$ and $10^{-3}$ a.u., respectively. For the sodium tetramer, the GGA calculation required tougher convergence criteria of $10^{-7}$ and $10^{-6}$ due to the fact that, at this level of theory, the PES of this system is extremely flat. A vibrational analysis was performed in order to discriminate between minima and transition states. The second derivatives were calculated by numerical differentiation (two-point finite difference) of the analytic energy gradients using a displacement of 0.001 a.u. from the optimized geometry for all 3N coordinates. The harmonic frequencies were obtained by diagonalizing the mass-weighted Cartesian force constant matrix. The response property calculations were then freshly carried out for these ground state Na cluster geometries using our implementation of the single step approximate CPKS procedure in the 1.7 version [141] of the deMon2k. The choice of the field strengths at an interval of 0.001 a.u. could be justified by simply noting the difference between the calculated $\beta$ value and the theoretical value of zero for $Na_2$. We have used an electric field strength of 0.001 a.u. for our response calculations as the error in the $\beta$ value of $Na_2$ was minimum for this interval, the error increased for any value around 0.001 a.u. The details of the implementation of our method [145, 146, 147] in deMon2k can be found discussed in detail in Chapter 2. The derivative density matrices for the x, y and z directions obtained at the end of the calculation are used to obtain the polarizability tensor components. The polarizability is obtained as the trace of the product of the derivative density matrix for a direction a, with the dipole moment integrals in direction b, where a, and b span the x, y and z directions, thus giving the corresponding polarizability component. Thus all the components of the polarizability tensor can be obtained using the derivative density matrix. The first hyperpolarizability, which is the third derivative of energy with respect to the electric field, can also be obtained as per the (2n+1) rule [83]. The first-hyperpolarizability can be trivially obtained using the deriva-

tive KS-operator matrix in the MO basis and derivative coefficient matrix for all permutations thus obtaining each of the components of the hyperpolarizability tensor. The novelty of our method lies in the simple single-step solution to the CPKS equations which avoids the complicated algebra as well as expensive computational time that would be required to construct the analytic derivative KS-operator matrix involving the derivative of the exchange-correlation term. Also, the derivative KS-operator matrix needs to be evaluated for every iteration. Our method circumvents this complication, thus, saving time and computational efforts. It is highly advantageous for response property calculations involving large molecules or large basis sets or both. We report the mean and anisotropic polarizability, and mean first-hyperpolarizability values obtained using the respective tensor components. The mean polarizability was calculated from the polarizability components as:

$$\overline{\alpha} = \frac{1}{3}(\alpha_{xx} + \alpha_{yy} + \alpha_{zz}) \tag{5.4}$$

and the polarizability anisotropy as,

$$|\Delta\alpha|^2 = \frac{3tr\alpha^2 - (tr\alpha)^2}{2} \quad \text{(general axes)} \tag{5.5}$$

$$= \frac{1}{2}[(\alpha_{xx} - \alpha_{yy})^2 + \quad (\alpha_{xx} - \alpha_{zz})^2 + (\alpha_{yy} - \alpha_{zz})^2] \quad \text{(principle axes)} \tag{5.6}$$

The orientationally averaged first-hyperpolarizability were obtained as,

$$\beta_i = \frac{1}{3}\sum_k \beta_{ikk} \tag{5.7}$$

$$\beta = \sqrt{\beta_x^2 + \beta_y^2 + \beta_z^2} \tag{5.8}$$

It is well known that a general characteristic required for basis sets to perform well for polarizability calculation is that they should contain diffuse functions [226]. An economical strategy for constructing these kinds of basis sets is to augment valence basis sets of reasonable good quality with additional polarization functions [192, 227, 228, 229]. We have chosen as valence basis a newly developed triple zeta basis set (TZVP), which was optimized for gradient corrected DFT calculations [230]. The basis set was then augmented with three field-induced polarization

(FIP) functions, two p and one d, which were derived following the work of Zeiss *et al.* [227]. They derived the FIP function exponents from an analytic analysis of the field-induced charges in hydrogen orbitals. The exponents of the additional FIP functions have been already presented in Ref. [193]. In order to avoid the contamination of the valence basis set with the diffuse p- and d-type Gaussians of the FIP functions, spherical basis functions are used in all the calculations. The resulting basis set is named TZVP-FIP1 [193]. Our DFT response property calculations were done using the Sadlej [192] and TZVP-FIP1 basis sets with the *CARTESIAN* option for the orbitals. We did not employ the auxiliary basis for fitting the exchange-correlation functional in our response property calculations; i.e the *VXCTYPE BASIS* option was used. The calculations were done using the LDA based VWN [51] and GGA based BP86 [70, 57] functionals in the deMon2k for both the basis sets. This entire set of response calculations were repeated for both the sets of Na cluster geometries. In our calculations, we have chosen only closed shell Na clusters due to the fact that, we have implemented the linear response approach in a numerical-analytical manner in the deMon2k only for closed shell cases. We have therefore used the restricted Kohn-Sham (RKS) scheme of calculation, where, the grid accuracy of $10^{-6}$ a.u. was used for the property calculations. The density convergence was set to $10^{-10}$ a.u. in the HF, MP2 [231] as well as DFT calculations. The HF and MP2 benchmark calculations were carried out using the GAMESS [232] and the DFT calculations were done using deMon2k program. The DFT optimized structures were used for the MP2 and the HF calculations. These properties are evaluated using the finite field method available in GAMESS for a finite field value of 0.001 a.u. The results are discussed in the following section.

## 5.5 Results and Discussion

### 5.5.1 Equilibrium geometries

We report the ground state structures of the even number sodium atom clusters from dimer to octamer obtained using the VWN and PW86 (bond distances in parenthesis) functionals in Fig. 5.1. The equilibrium structures obtained from both functionals are similar and show a general topological agreement with the earlier theoretical reports [201, 202, 233]. All-electron type optimizations for the sodium clusters using GGA based functionals available but scarce [124, 193]. We have carried out all-electron type optimization for both VWN as well as PW86 functionals in the present work.

The dimer bond distance is equal to 3.017 Å with both the optimizations, whereas the experimental value is 3.078 Å [234]. The geometries for the remaining clusters differ very slightly for the two optimizations. The ground state structure of $Na_4$ is a $D_2h$ rhombic structure, whereas the one for the $Na_6$ is a $C_5v$ pentagonal pyramid. The equilibrium geometry for the $Na_8$ is a compact dicapped octahedral (DCO) structure.

### 5.5.2 Harmonic frequencies

We have tabulated the normal modes for both sets of optimized structure of the Na clusters in Table 5.1. The absence of imaginary frequency was used to confirm that all the optimized structure were minima on the PES. The reported experimental frequency for the dimer is 159 $cm^{-1}$ [235]. Our calculation for dimer using the VWN and PW86 functional gave 161 and 160 $cm^{-1}$ value, respectively, which are in good agreement with the experimental value. Earlier calculations of tetramer harmonic frequencies by Dahlseid *et al.* [236] at the configuration interaction-singles (CIS) level gave, 27, 43, 73, 98, 130 and 150 $cm^{-1}$ as the frequencies. The qualitative trend for our harmonic frequencies in Table 5.1 is similar, except for the first frequency

for the tetramer at the PW86 level which is small. It can be seen that, the first few frequencies of the clusters are smaller in magnitude. This could be attributed to the extremely flat PES of the clusters which further complicates the distinction between the global and the local minima. This could especially be a serious problem as we go to even larger clusters where the number of stable configurations increases drastically. In our calculations we had to tighten the convergence criterion for the tetramer due to its flat PES to obtain a minimum energy structure.

### 5.5.3 Static mean polarizability, polarizability anisotropy and first-hyperpolarizability

We have calculated the mean polarizability, $\overline{\alpha}$, and polarizability anisotropies, $|\delta\alpha|$ for the optimized minimum energy structures of $Na_2$, $Na_4$, $Na_6$ and $Na_8$, which are even numbered Sodium atom, clusters. We have also done the calculations for the dipole first-hyperpolarizability. Our calculations have been carried out at the DFT level. MP2 level calculations were done for benchmarking our results.

We also carried out calculations at the HF level to put correlation effects in clearer perspective. Additionally, we have also collected the dipole-based finite field polarizabilities as available in the deMon2k program to compare with our DFT polarizability values. The results are presented in graphical as well as tabular form. The graphs contain plots of mean polarizability per atom in atomic units against the number of atoms and compared with the available experimental values. The experimental values were calculated from the measurement of relative polarizabilities of Knight *et al.* [194] and the absolute measurement of the atomic polarizability by Molof *et al.* [195]. We will first discuss the polarizability results presented graphically.

The DFT response property calculations have been done using the VWN and BP86 functionals. The basis sets used for the calculations are Sadlej and TZVP-FIP1. There are two sets of Na cluster geometries used for the calculations, one

optimized using a VWN functional and the other optimized using the PW86 functional, and both sets optimized using DZVP/A2 basis set. Each figure has a plot showing mean polarizability per atom, values for all the four Na clusters obtained at VWN, BP86, MP2 and HF level of theory compared with the experimental values. The plots are presented in Fig. 5.2 - 5.5 corresponding to the combination of the exchange-correlation functional used for the optimization and the basis set used for the polarizability calculation. Comparison of the DFT values from the plots for the two sets of geometries shows that, for a given basis set and exchange-correlation functional the results do not show any change except for 1-2 a.u., which means that the level of optimization of the geometries do not affect the mean polarizability per atom for the DFT calculations. Since, the trends for the mean polarizability per atom are similar for both sets of optimized geometries of Na clusters, we will discuss only the general trend pointing out any difference wherever necessary.

A particular trend that can be seen for the mean polarizability per atom values for the VWN, BP86, MP2 and HF calculations in all the plots is that the values from the theoretical calculations for all the Na clusters are less than the experimental values of the mean polarizability per atom, except at two places for the calculations using the Sadlej basis set, one, in Fig. 5.5 for both the HF as well as MP2 values of the $Na_2$ cluster optimized at the PW86 level and second, in Fig. 5.3 for the MP2 value for the VWN optimized Na2 cluster. The value for the Na2 cluster in both cases is overestimated from that of the experiment by 8 a.u. which is about 6% as seen in both Fig. 5.3 and Fig. 5.5.

Also, the values from MP2 and the HF are closest to the experimental values followed by the ones using GGA BP86, the exception being in the case of calculations done using Sadlej basis for Na2 cluster optimized using VWN functional where, the BP86 values are closer to experiment as is evident from Fig. 5.3. The VWN values, in general, show the largest deviation from the experimental values. This is in line with the correlation effects being incorporated in the exchange-correlation functionals used for the DFT and the MP2 theory. For VWN, which

is a LDA based functional, the density is mapped locally to a homogeneous electron gas picture, which exhibits a strong overestimation of the correlation effects as is well known. However, for the mapping of the response of the density as a consequence of the external electric field perturbation, it is unable to show that strong correlation effects probably due to less non-local effects in the density redistribution. This can be clearly seen in the values of mean polarizability per atom which are farthest from the experimental ones in Fig. 5.2 - 5.5. The BP86 non-local functional and the *ab initio* methods on the other hand show the non locality in the density response although to different extents thus giving relatively higher values in comparison to VWN ones in all the plots. If we observe the trend in the experimental values of the Na clusters, we see that the polarizability per atom values increases from $Na_2$ to $Na_4$ to a reasonable extent, then there is a very slight increase from $Na_4$ to $Na_6$, whereas, from $Na_6$ to $Na_8$ there is a drastic drop in the value. Qualitatively, this trend is more correctly reflected by all four methods for the values from TZVP-FIP1 basis for both the sets of geometries. For the Sadlej basis, however, both the HF and MP2 values overshoot the experimental value of 126 a.u. as seen in Fig. 5.5 for the $Na_2$ cluster optimized at the PW86 level. Similarly, the Fig. 5.3 shows an overestimation of the HF polarizability value for the $Na_2$ cluster optimized at the VWN level. Also, slight increase in the experimental value from $Na_4$ to $Na_6$ is seen to be otherwise in all the calculations, independent of the optimization and level of calculation. The maximum deviation from the experimental values is for the $Na_6$ cluster results, irrespective of the level of theory used. This is the case for every calculation, the highest being 25% for the VWN method in Fig. 5.2. A comparison of the similarity in the plots for the TZVP-FIP1 basis set (i.e. Fig. 5.2 and 5.4) and the Sadlej basis set (i.e. Fig. 5.3 and 5.5) for the two sets of optimized geometries show that the level of optimization does not affect the polarizability calculations at the DFT level. This similarity in the plots can also be seen for the MP2 calculations using the TZVP-FIP1 basis set (i.e. Fig. 5.2 and 5.4), however, this is not the case for the Sadlej basis (Fig. 5.3 and

5.5). The behavior of the MP2 as well as HF calculations for the two basis sets could be assigned to the fact that the TZVP-FIP1 basis set has been optimized for the polarizability calculation using DFT, whereas, the Sadlej basis is an optimized basis for the polarizability calculation using *ab initio* methods.

In Table 5.2, we have compared the experimental and DFT mean polarizability per atom values obtained by Rayane *et al.* [207] in angstrom units with our DFT calculations for the Na cluster geometries optimized at the PW86-DZVP-A2 level. We have compared our results for the VWN and BP86 functionals obtained using the Sadlej and TZVP-FIP1 basis sets. The comparison has been done with the values reported by Rayane *et al.* [207] calculated at the PW91 level for the SU and 6-31G basis set and measured experimentally. Although, we have discussed our mean polarizability per atom values above earlier, we would like to have a comparison with other DFT results available. It can be clearly seen that, the values reported by Rayane *et al.* are closer to the experiment as compared to our results. They have argued that, the SU basis gives values closer to the experiment in comparison with the 6-31G basis as there is more polarization (d-orbitals) and diffuse functions in the SU basis which are expected to be important for polarizability calculation. On similar basis, we could assign the marginally better behavior of the Sadlej basis as compared to the TZVP-FIP1 basis, especially for the dimer, to the fact that there is a larger number of polarization functions in the Sadlej basis as compared to the TZVP-FIP1 whereas there are more diffuse functions in the TZVP-FIP1 basis set. Another reason for TZVP-FIP1 not performing better than the Sadlej basis despite being optimized for DFT could be the use of Cartesian basis functions in all our response property calculations. The use of spherical basis functions is advised to avoid contamination of the valence basis set with the diffuse p- and d-type Gaussians of the FIP functions. This could be explained by taking an example of s- and d-orbitals located on the same center. In the spherical representation of these two orbitals shells, i.e. the orbitals are constructed from a one dimensional radial function and real spherical harmonics, the overlap matrix elements vanish due

to the orthogonality of the spherical harmonics. Whereas, in the case of Cartesian representation, the d shell is overdetermined by a total symmetric component ($d_{xx}+d_{yy}+d_{zz}$) that can mix with the s-orbitals (a similar situation holds for the p- and f-shells). Rayane *et al.* [207] have also concluded that diffuse functions are less important for static response in the ground state calculations of clusters.

Calculated values of polarizability per atom using the PW91 functional reported by Rayane *et al.* are in better agreement with the experiments than our values calculated using VWN and BP86. In our calculation, we find that the values obtained from the BP86 are closer to the experiment than the VWN ones.

Table 5.3 - 5.6 gives our calculations done for each of the Na clusters, i.e. each cluster calculations are presented in separate tables. We have reported the polarizability anisotropy and the orientationally averaged first hyperpolarizability values obtained using the DFT, HF and MP2 calculations in these tables. The DFT finite field (FF) results of polarizability are also presented in the tables for comparison. We have already discussed the mean polarizability per atom values presented in Fig. 5.2 - 5.5. We now turn to the mean polarizability values and the polarizability anisotropy values given in the Tables 5.3 - 5.6. As we move across Tables 5.3 - 5.6 for the clusters $Na_2$ through $Na_8$, we observe that the DFT polarizability anisotropy value increases as we move from the dimer to the tetramer and decreases as we go to the hexamer and octamer. This trend in the values reflects the clear relation between the cluster structure and the polarizability anisotropy values. It is worth noting that, as the cluster structure becomes compact like in case of the octamer, the polarizability anisotropy value decreases. The value for the octamer is even less than the value for the dimer, which has an open structure. As we go from the tetramer to hexamer, we see that the hexamer being a closed structure as against the planar tetramer, it shows a decrease in the polarizability anisotropy value from that of the tetramer. A comparison of the polarizability anisotropy values for all the clusters among the two basis sets for each of the methods, show that the Sadlej basis gives values lesser than the TZVP-FIP1 basis, except for the case of the hex-

amer, where, the trend is reversed. A general trend of the BP86 functional giving slightly higher values for the polarizability anisotropy than the VWN functional can be seen in all the calculations. We could not compare our results with experiments as there is no experimental measurement of polarizability anisotropy available.

The implications from the values of the mean polarizability for the different methods, basis sets and functionals used would now be discussed. The TZVP-FIP1 basis used in the response property calculations is optimized for the gradient-corrected functions and is not correlation consistent. Although, it may be too small for *ab initio* MP2 calculations, we have carried out the MP2 calculations using the TZVP-FIP1 basis set for benchmarking our results. On the other hand, the Sadlej basis is optimized for ab initio polarizability calculations and is a medium-sized basis, as compared to the TZVP-FIP1. As the number of atoms in the cluster increases, the mean polarizability value increases. Our DFT mean polarizability values deviate from the corresponding finite-field DFT mean polarizabilities by less than 0.4 a.u. for the dimer, 0.6 a.u. for the tetramer, 1.6 a.u. for the hexamer and by less than 2.8 a.u. for the octamer. Also, the mean polarizability values from the GGA based BP86 functional are closer to the experimental values as compared to the ones using the VWN functional, for both sets of optimized sodium clusters. All this can be clearly observed from the mean polarizability values of the clusters in the Tables 5.3 - 5.6.

The following critical observations are made after comparison of the DFT mean polarizability values with the MP2 and HF values. In general, both the HF and the MP2 mean polarizability values are closer to the experimental values as compared to the DFT results. In fact, certain HF values are closer to the experimental results than the MP2 values which is unexpected, as MP2 is a correlated method, whereas, HF theory lacks correlation term in its energy expression. Also, usually DFT is believed to perform better than the HF theory due to incorporation of the correlation effects. We, however, see that as we go from the TZVP-FIP1 basis to the Sadlej in each of the Tables 5.3 - 5.6, the mean polarizability value

increases for the DFT, HF as well as MP2 method. But, what is worth noting is that, the HF overshoots the experimental value for the dimer in Table 5.3 for the Sadlej basis. This can be used to understand the basic problem in the HF theory that, as the basis set size increases further the mean polarizability value would go way beyond the experimental value. The results from MP2 theory do not show much improvement either, since MP2 energy does not contain contributions from singly excited determinant, which are important for dipole-based properties. The improvement may start appearing only at the MP4 level. However, MP4 calculations are computationally very expensive. It could be observed that, although, the DFT values are not closer to the experiments, there is a significant increase as we go from TZVP-FIP1 basis to the Sadlej and as we move from a local to a non-local functional. As a consequence, we could expect the mean polarizability values to approach the experimental values as the basis set size increases. The correlation effects due to a proper choice of the exchange-correlation functional may improve the results further. Thus it can be seen that for the response property calculation DFT provides a better choice than even the MP2 *ab initio* method. It may be noted that the temperature effects, which are present in the experiments are missing in the above theories, which makes the comparison of theory with experiment difficult.

We now discuss the hyperpolarizability results from our calculations. Due to absence of experimental data, we compare the DFT calculations with our HF and MP2 results. The $\beta$ value for the dimer should be zero. However, as seen in Table 5.3, there is a negligible value of at most 2.5 a.u. for the DFT calculations. This error shoots up for selections of the electric field strengths other than 0.001 a.u. that was chosen for these calculations. The error for the $\beta$ values of the dimer could be assigned to the percolation of the inaccuracies into the response density matrix due to the numerical approximation employed for obtaining the derivative KS-operator matrix in our method. For the tetramer in Table 5.4, the $\beta_x$ values for the VWN optimized structure varies between 14-20 a.u., which is reflected in the $\beta$ as the components along the other two directions are relatively lesser in

magnitude for the Sadlej and the TZVP-FIP1 basis, whereas the $\beta$ values for the PW86 optimized geometry are close to zero. The $\beta$ value for the TZVP basis from the BP86 method is closer to the MP2 value of 21.3 a.u., whereas for the Sadlej basis the $\beta$ value for the VWN is closer to the corresponding MP2 value of 14.1 a.u. and the value for the BP86 is overestimated for the VWN optimized structure. The HF $\beta$ values are less than the MP2 and corresponding DFT values. As we move to the PW86 optimized structure results in Table 5.4, the $\beta$ values from all methods are negligible. It can be seen that the tetramer has a rhombic planar structure that is symmetric due to which the $\beta$ values are not very high. The $\beta$ values are expected to increase as the asymmetry in the structure increases. The dimer and tetramer structures are nearly symmetric, which is also reflected from the $\beta$ values in the tables. As we move from tetramer to hexamer in Table 5.5, the $\beta$ values and its components show a dramatic increase in magnitude. The values from the MP2 and HF method are closer to each other. It is clear from the Table 5.5 that, both VWN and BP86 results are overestimated in comparison with the MP2 and HF values irrespective of the functional and basis set used for the calculation. This is true for both the optimized structures of the hexamer. All the component $\beta$ values for the hexamer in Table 5.5 are negative and the overestimation of the $\beta$ values is more for the BP86 functional as compared to the VWN. This could be due to the under binding of the electrons by the two DFT functionals. What is clearly noticeable in Table 5.6, is the sudden drop in the $\beta$ values for the octamer. This could be due to the compact structure of the octamer which is a result of the magic number of 8-electrons present in its valence shell. All the other calculations including MP2 and HF for both the geometries seem to be completely disordered. We could argue that, a small change in geometry can lead to a completely unexpected trend in the $\beta$ values, which are highly sensitive both to the correlation effects as well as structural instability. The MP2 and HF $\beta$ values are comparable for the TZVP-FIP1 and the Sadlej basis for the PW86 optimized structures of the octamer, whereas, the VWN and BP86 $\beta$ values are comparable for

the VWN optimized structures of the octamer. There are no experimental $\beta$ values available for comparison with our values, which could have helped to understand the behaviour of $\beta$ values of the sodium clusters better.

## 5.6 Computational details of calculations for PNA and its derivatives

We now give the computational details for the response property calculations of the PNA and its derivative organic molecules. We have used the geometries optimized at the MP2 level using the 6-31++G** basis reported in Ref. [215] for the sake of comparison of our response property results with those reported by Davis *et al.* [215] They report the dipole moments, dipole polarizability and first-hyperpolarizability calculation using the finite-field perturbation method (MP2) for the set of molecules chosen by us in this work. The structures of the molecules used in our work are given in Fig. 5.6. In our calculations the molecule is in the xy-plane with the x-axis being along the direction of the maximal extension with the amine group on the positive side of the x-axis and the z-axis perpendicular to the molecular plane. We have done the response property calculations at the DFT level of theory for different non-local exchange-correlation functionals using 6-31++G** basis. We have used our implementation of the approximate CPKS method in the deMon2k version 1.7 for our calculations [141]. The A2 auxiliary basis has been used for fitting the electron density, whereas the exchange-correlation potential has been evaluated using the orbital basis, which is the case for the *VXCTYPE BASIS* option in the input. The computational details section for the Na-cluster calculations in this chapter gives the working equations used for the $\alpha$ and $\beta$ calculations. It also includes a brief discussion of our method (the details could be found in chapter 2) used for the response property calculations. The dipole moment has been calculated as follows:

$$\mu = \sqrt{\mu_x^2 + \mu_y^2 + \mu_z^2} \tag{5.9}$$

We have carried out the calculations using the BP86 [70, 57], BPW91 [70, 60] and BLYP [70, 71] non-local DFT functionals. The calculations have been done using the electric field value intervals of 0.001 a.u. for the construction of the derivative KS-operator matrix used for the response property calculation. The *POLAR* keyword in the deMon2k program, which employs a finite field approximation to obtain dipole-based polarizabilities of molecules was used for obtaining the finite-field values of $\alpha$ and $\beta$ using 0.0032 a.u. field strength for comparison with our results. We used the *CARTESIAN* option for the orbitals with restricted Kohn-Sham (RKS) scheme of calculation, where, the grid accuracy of $10^{-6}$ a.u. was used for the property calculations. The density convergence was set to $10^{-10}$ a.u. for the DFT calculations. Our DFT calculations have been done using the deMon2k, whereas, the MP2 results [215] used for comparison are from GAMESS [232] and using a field strength of 0.001 a.u. The hyperpolarizability values reported by Davis *et al.* have been halved from those reported by the GAMESS program. We have, however, used the values from the Ref. [215] as reported by the program, i.e. we have doubled the reported values for comparison with our results. It can be noted that the calculated average static first-hyperpolarizability, $\beta$ values are comparable to the experimental quantity, $\beta(-2\omega;\omega,\omega)$, obtained from the solution-phase electric field induced second-harmonic generation (EFISH) experiments [214].

## 5.7 Results and Discussion

In this section, we discuss our response property results of polarizability and first-hyperpolarizability obtained using an approximate response approach proposed by us and the dipole moments for a set of organic molecules namely, para-nitroaniline (PNA) and its methyl substituted derivatives. The structures of all the molecules used for the calculations have been given in Fig. 5.6. A short label has been given for each of the molecules below their complete names in Fig. 5.6 for easy reference during the discussion of results. The DFT dipole moments, mean polarizability,

polarizability anisotropy and orientationally averaged polarizability and first- hyperpolarizabilities at the BP86, BPW91 and BLYP level using the deMon2k are presented for each of the molecules in a separate table. The results are presented in Tables 5.7 - 5.14. The finite-field dipole-based calculations of polarizability and the first- hyperpolarizability for the molecules using the different exchange-correlation functionals obtained using the deMon2k program are also given in each of the tables for comparison with the results from our method. Our results are also compared to the benchmark MP2 values of Davis *et al.* [215] obtained using the energy based finite-field method as available in the GAMESS [232] quantum chemistry program. The optical gap or the energy difference between the highest occupied molecular orbital(HOMO) and the lowest unoccupied molecular orbital (LUMO), are also given in each table along with the MP2 calculations reported by Davis *et al.* [215]. In this section, we would delve into the intricacies involved in the interpretation of our NLO property results. An important objective of the NLO property calculations of PNA and its methyl substituted derivatives, is that they provide an insight into the subtle variations reflected in the values due to change in the molecular architecture. Our results are in general agreement with those of Davis it et al. [215]

We begin with discussion of the dipole moments. The dipole moment, $\mu$, is obtained from the ground state response of the electron density and hence, does not require a density response calculation. The changes in the structure of the molecule in terms of the substituents is clearly shown by the changes in the dipole moment values in the tables, as we go from PNA to N-mtPNA-6 in Table 5.7, through Table 5.14. Due to the donor amino ($NH_2$) group substituted at the para position to the nitro ($NO_2$) group of the benzene ring and the orientation of the molecular skeleton, the major component of the dipole moment is along the x-axis. It can be noted that the MP2 values of the total dipole moment as well as its components are less than the corresponding values from the DFT in all the tables irrespective of the exchange-correlation functional used, except for the y-component of N-mtPNA-3 in Table 5.12 where the MP2 dipole moment value is higher by $\sim 0.02$ a.u. In case

of PNA in Table 5.7 the components along the y-axis is zero, however, it shows a noticeable increase in the value as we move to the other derivative molecules. This happens as the polarity in the molecules changes in the y-plane of the molecule due to substitution of the methyl group to the PNA skeleton. As a result, due to the substitution of the methyl group at the ring position, the symmetry of molecule in terms of the delocalized $\pi$ electron cloud is lost. This happens due to electron donating inductive effect of the methyl group which thus leads to a small polarity along the y-axis of the molecule. The inductive effects [237] arise due to the non-equal sharing of the bonding electrons in the $\sigma$ bond. All inductive effects are permanent polarizations in the ground state of molecules and are therefore reflected in the physical properties, like the dipole moment. In case of the polarizability or the linear response coefficients, $\alpha$, the MP2 values of mean polarizability as well as the components along the three directions given in the tables are, in general, less than the DFT values from our method as well as the finite-field DFT values. The values of the components of $\alpha$ in all the tables differ from the finite-field DFT values by not more than 1 a.u. The MP2 results for the components of the polarizability are, in general, less than the corresponding DFT values. This difference is more in case of the $\alpha_{xx}$ component in all the tables, which, in turn, is reflected by the mean polarizability values of all the molecules in Table. 5.7 - Table. 5.14. The MP2 values of $\overline{\alpha}$ differ from the DFT values by at most 10 a.u. Among the DFT functionals used, the BLYP shows a higher value for the dipole moment as well as the mean polarizability as compared to the other two functionals, whereas, the values from the BP86 and the BPW91 functionals are closer to each other. The polarizability anisotropy values in each of the tables are comparable to each other differing atmost by 1 a.u. The major contribution to the total $\beta$ for the molecules comes from the $\beta_x$ component. The DFT values of orientationally averaged $\beta$ and the total $\beta$ values in each table are, in general, comparable to each other as well as to the MP2 values for the respective molecule. When studying the connection of chemical structure with the second-order nonlinear response coefficients, $\beta$, we note the second-order

NLO effects in the organic molecules due to the strong donor-acceptor kind of intramolecular interaction. Also, the magnitude of the $\beta$ is relatively larger than the $\alpha$ values of PNA and its derivatives, which is due to the highly asymmetric charge distribution in the molecules. The $NH_2$ group is an electron donating (ortho and meta directing) group whereas the $NO_2$ group is an electron withdrawing (meta directing) group. This implies that the donor-acceptor kind of moieties at opposite ends in the PNA skeleton leads to intramolecular charge transfer. It is well known that molecules with $\pi$ conjugation and having this kind of donor-acceptor arrangement show higher nonlinear responses, which is a result of the delocalization of the $\pi$ electron cloud over the molecule. The donor $\pi$ conjugate-bridge-acceptor forms a typical SHG active molecule, if it lacks center of symmetry. However, the presence of the donor-acceptor in a molecule alone does not guarantee the NLO effects. Also, the molecule will not show NLO effects if the molecule possesses a center of symmetry. In PNA, the presence of a desirable resonance structure, in addition to the intramolecular charge transfer leads to the high value of $\beta$. However, the crystalline form of PNA has a centrosymmetric structure which does not show any macroscopic second-order NLO response. We have, therefore, considered the methyl substituted derivatives of PNA here, which eliminates the center of symmetry in the molecule thus leading to non-centrosymmetric crystal structure. The substitution of a methyl group to the benzene ring brings in asymmetry to a high degree in the electronic distribution which is reflected in the $\beta$ values of the derivatives. In case of PNA-2, where, the $CH_3$ group is at the ortho position to the $NH_2$, the *beta* values show an increase from the PNA, whereas the optical gap shows a decrease. Interestingly, for the PNA-3 with the $CH_3$ group at the meta position, there is an noticeable decrease in the $\beta$ value and increase in the optical gap from that of PNA. The behaviour of both $\Delta$E and $\beta$ for PNA-2 and PNA-3 can be explained as follows. Here, the molecular orbital picture also plays a crucial role in deciding the extent of charge transfer in terms of the HOMO-LUMO gap or the optical gap [97], which, in turn, can be used to understand its effect on the

$\beta$ values. $\Delta$E is directly proportional to the extent of charge transfer. For a small optical gap, the charge transfer occurs easily, thus, giving a higher value of $\beta$. The source of charge transfer is thus controlled by the energy of the HOMO, whereas, the acceptance of the charge is dominated by the LUMO energy. Although, quantitatively smaller, the methyl group shows a electron-donating inductive effect. In PNA-2, the methyl substitution is at the C closer to the electron-donating group, which leads to a higher HOMO energy and a lower LUMO energy, as compared to PNA-3. This leads to a smaller HOMO-LUMO energy gap for PNA-2 as compared to PNA-3. This small optical gap enhances further, the charge transfer, which, in turn, is reflected in the larger values of $\beta$ for PNA-2 than PNA-3. The trends in optical gap from our method matches with that shown by MP2 method. The decrease in the optical gap leading to increase in the NLO responses, both $\alpha$ and $\beta$ can be more clearly illustrated, when we substitute the amine H in PNA by a methyl group in N-mtPNA. This relation of the optical gap with $\beta$ and other higher order response coefficients could be used to tailor NLO materials, to obtain materials with increased optical responses, by manipulating the optical gap using variable molecular substituents. The optical gap values for the N-mtPNA and its derivatives can also be interpreted using a similar argument. On studying the N-mtPNA and its methyl substituted derivatives, we find that the 2- and 6-methyl substituted N-mtPNA derivatives show the above mentioned correlation of the HOMO-LUMO energy gap with the increase in $\beta$ values, distinctly. However, the change in the $\alpha$ values for the above molecules is not very clearly visible. Alternatively, the N-mtPNA-3 and N-mtPNA-5 with the methyl substitution at ortho position to the $NO_2$ meta directing group, shows a decrease in the $\beta$ values from N-mtPNA as the inductive effect of the methyl substituent is suppressed at this particular position. This, in turn, also quenches the polarization in the molecule, which is reflected in the dipole moment values of N-mtPNA-3 and N-mtPNA-5 which are less than the parent N-mtPNA. The N-mtPNA dipole moment shows an increase from the parent PNA on methyl substitution at the amine position. Also, the substitution at the N

position gives higher $\alpha$ and $\beta$ values in comparison to the isoelectronic counterparts of N-mtPNA, i.e., PNA-2 and PNA-3. The substitution of a second methyl to the N-mtPNA at different positions can, thus, give us insight into chemistry involved, which can be useful in designing materials with increased NLO responses.

## 5.8 Conclusion and Scope

We found that, the non-iterative approximation of CPKS method discussed in chapter 2, gave reasonably good values of polarizability as well as first hyperpolarizability for the Na-cluster calculations as well as for the $\pi$ conjugated donor-acceptor organic derivatives of PNA and its methyl substituted analogs. In case of MP2 and HF calculations for the Na-clusters, we found that, the HF values were comparable to the MP2 ones. This is mainly due to the cancellation of errors in the HF method and the basis set effect which even gave HF values closer to the experiment. The MP2 results do not improve the HF values of property for the Na-clusters. Although, the DFT results seem to converge towards the experimental values as the basis set is increased, improvement of the functional can lead to faster convergence of the results. However, it needs to be kept in mind that, the comparison of the polarizabilities from experiments with theory is not as simple, since, the temperature effects present in the experiments are missing in the theories used in our calculations. However, we were unable to evaluate the precision of our method for the first-hyperpolarizability calculations of the sodium clusters due to unavailability of experimental values. Measurements of these quantities experimentally, especially, for the smaller clusters would help us get more insight into the response electric properties of the Na clusters. Further, the basis set effects and correlation effects due to different exchange-correlation functionals, even meta-GGA for that matter could be the next step to try. The influence of using different auxiliary basis sets for fitting the coulomb potential, on these properties can be an interesting subject for future study. In case of PNA and its derivatives, our calculations could reproduce

the trends observed by Davis *et al.* [215] The effect of substitution on the NLO responses of the molecule and its effect on the optical gap were highlighted. The effect of position of substitution on $\beta$ and dipole moment values were also discussed. This study could be further extended to include substitutions using different organic fragments and the solvent effects, which are missing in the studies here; and could be another elaborate study. The results for both the sets of calculations were highly simplified due to our single step approximation to the CPKS, which could be exploited for enhancing the applicability of the DFT for calculation of the response properties for large systems employing large basis sets.

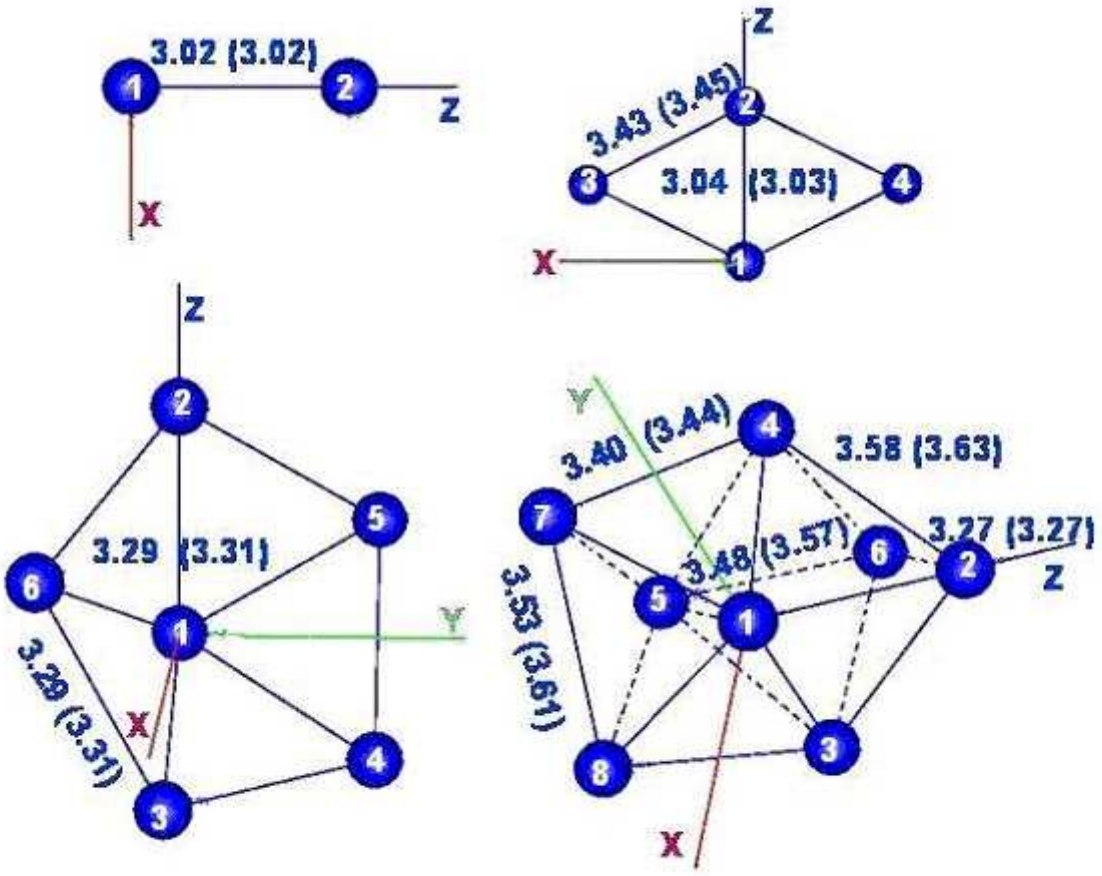


**Fig.** 5.1: Calculated equilibrium geometries and the orientations used for the calculations of $Na_n$ (n = 2, 4, 6, and 8) clusters using the VWN and PW86 (in parenthesis) functionals and A2/DZVP basis. Bond distances in Å.

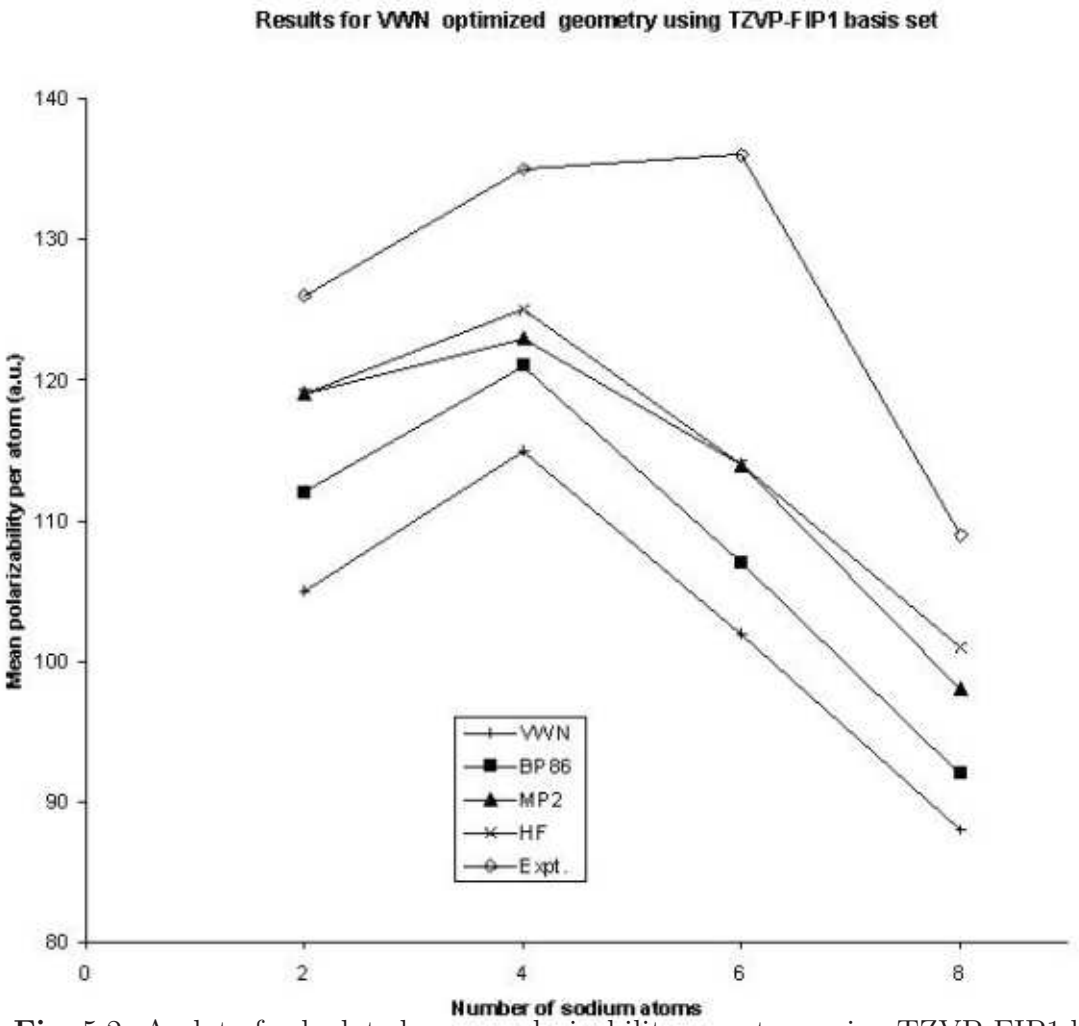


**Fig.** 5.2: A plot of calculated mean polarizability per atom using TZVP-FIP1 basis for $Na_n$ (n=2, 4, 6, and 8) clusters optimized using VWN/A2/DZVP versus number of atoms.

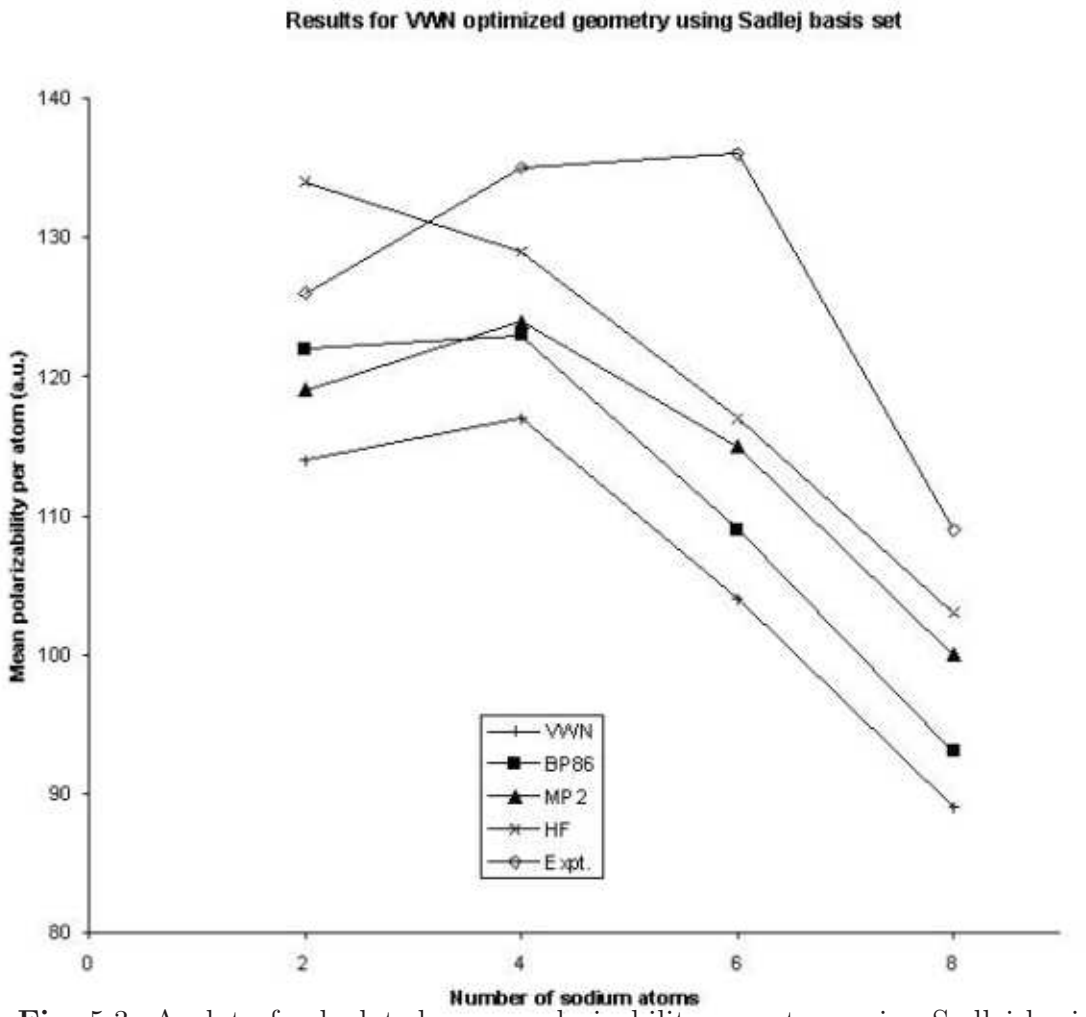


**Fig.** 5.3: A plot of calculated mean polarizability per atom using Sadlej basis for $Na_n$ (n=2, 4, 6, and 8) clusters optimized using VWN/A2/DZVP versus number of atoms.

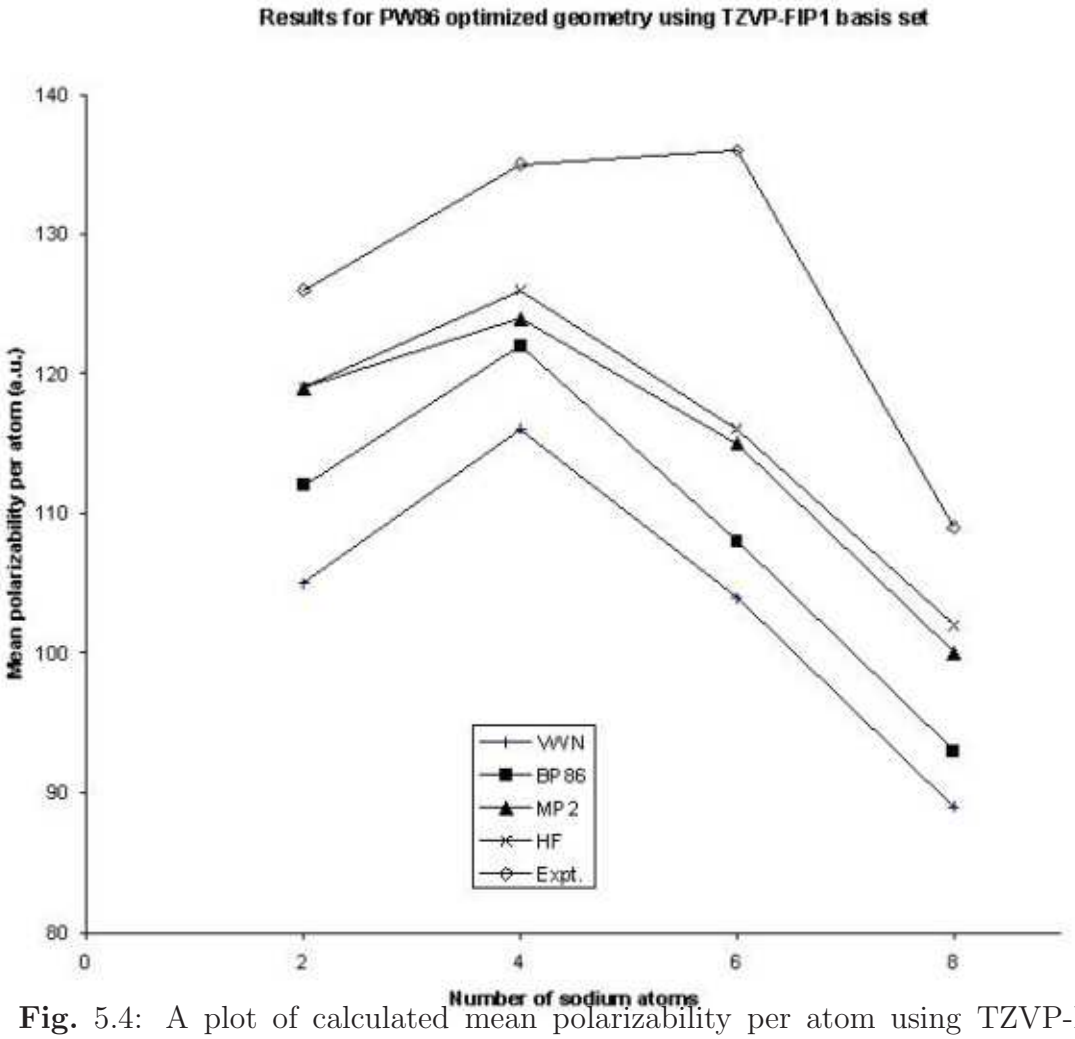


**Fig.** 5.4: A plot of calculated mean polarizability per atom using TZVP-FIP1 basis for $Na_n$ (n=2, 4, 6, and 8) clusters optimized using PW86/A2/DZVP versus number of atoms.

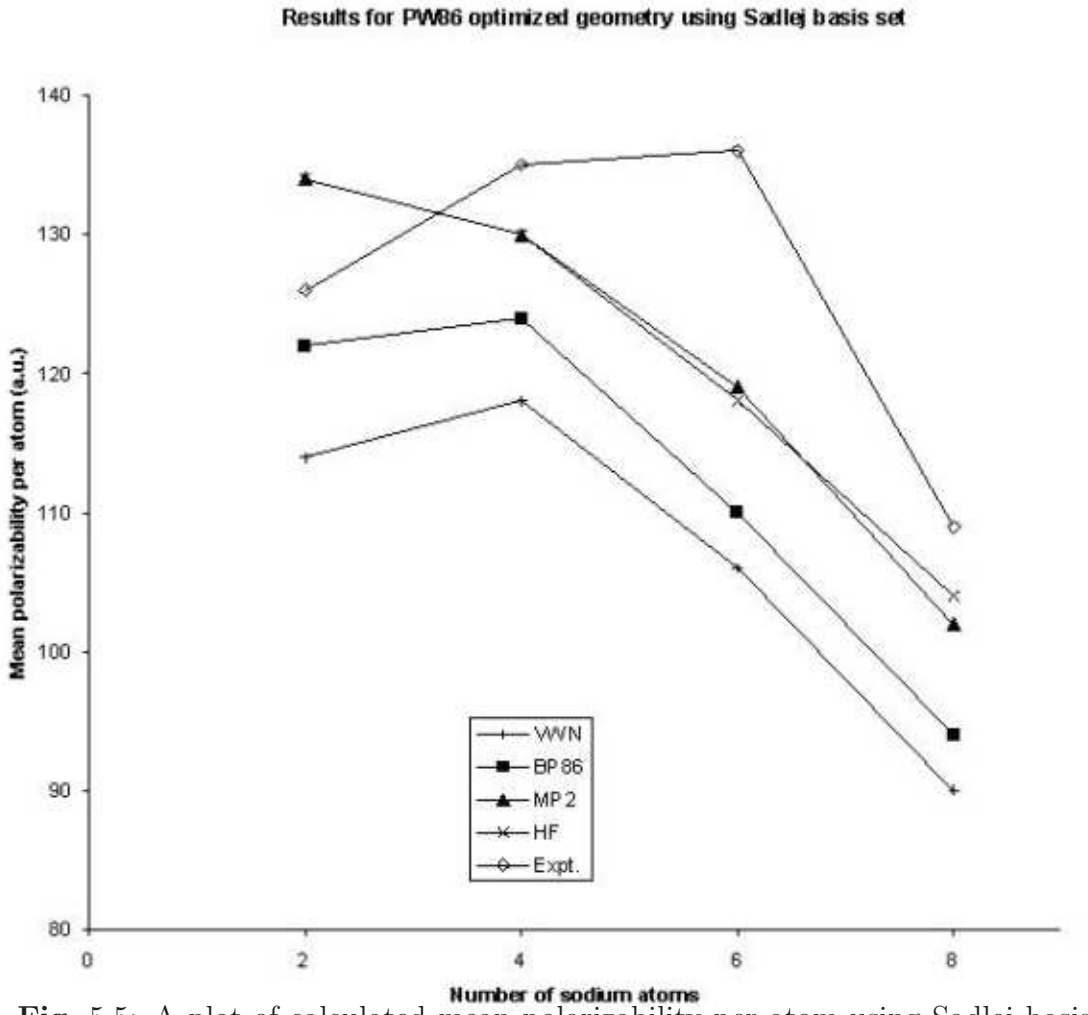


**Fig.** 5.5: A plot of calculated mean polarizability per atom using Sadlej basis for $Na_n$ (n=2, 4, 6, and 8) clusters optimized using PW86/A2/DZVP versus number of atoms.

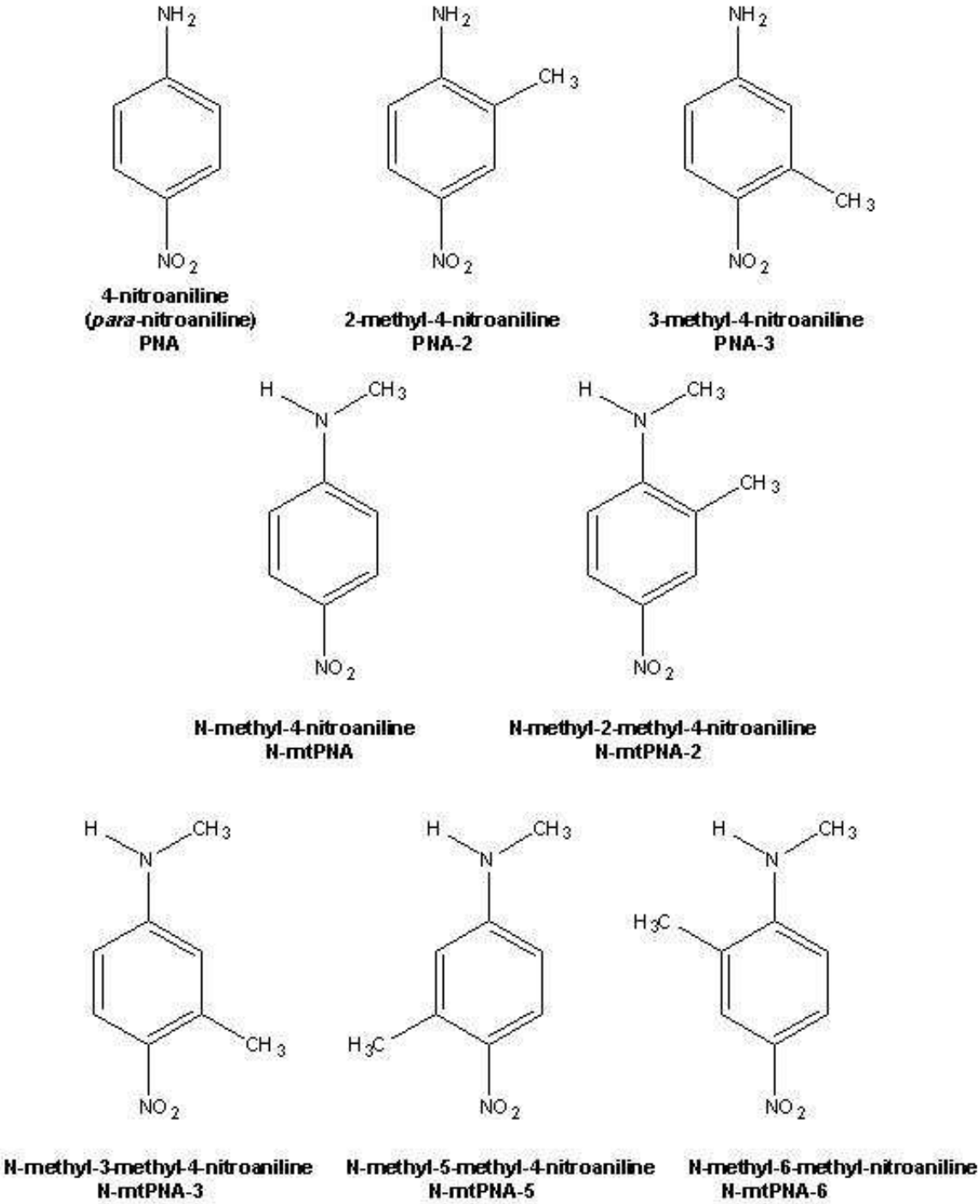


**Fig.** 5.6: Structures of para-nitroaniline and its methyl substituted derivatives used in our work

**Table** 5.1: Harmonic frequencies (in $cm^{-1}$) for the normal modes of $Na_n$ (n = 2, 4, 6, and 8) clusters in their calculated ground states using VWN functional and PW86 functional with DZVP basis set and A2 auxiliary basis.

| Cluster | VWN | PW86 | Expt. |
|---|---|---|---|
| $Na_2$ | 161 | 160 | 159[a] |
| $Na_4$ | 35, 37, 77 | 6, 43, 76 | |
| | 98, 144, 162 | 100, 141, 163 | |
| $Na_6$ | 31, 31, 55, | 36, 36, 46, | |
| | 75, 77, 91, | 70, 72, 89, | |
| | 91, 102, 102, | 89, 93, 94, | |
| | 142, 147, 147 | 140, 141, 142 | |
| $Na_8$ | 32, 49, 56, | 31, 49, 50, | |
| | 60, 65, 68, | 57, 60, 64, | |
| | 73, 77, 85, | 68, 69, 72, | |
| | 96, 108, 114, | 74, 101, 101, | |
| | 119, 129,134, | 106, 121, 127, | |
| | 137, 141, 180 | 130, 130, 131 | |

[a]From Verma *et al.* [227]

**Table** 5.2: Calculated values of static mean polarizabilities per atom (in Å$^3$) for $Na_n$ clusters (n = 2, 4, 6, and 8) optimized at the PW86/DZVP/A2 level in comparison with theory and experiment

| Clusters | XC | Basis | $\overline{\alpha}$ /n |
|---|---|---|---|
| $Na_2$ | PW91 | SU[a] | 19.1 |
| | PW91 | 6-31G[a] | 19.0 |
| | VWN | Sadlej(TZVP-FIP1) | 16.9(15.5) |
| | BP86 | Sadlej(TZVP-FIP1) | 18.0(16.6) |
| | | Expt.[a] | 19.65 |
| $Na_4$ | PW91 | SU[a] | 19.6 |
| (rhombus) | PW91 | 6-31G[a] | 19.3 |
| | VWN | Sadlej(TZVP-FIP1) | 17.5(17.2) |
| | BP86 | Sadlej(TZVP-FIP1) | 18.4(18.0) |
| | | Expt.[a] | 20.95 |
| $Na_6$ | PW91 | SU[a] | 17.4 |
| (pentagonal) | PW91 | 6-31G[a] | 17.3 |
| pyramid) | VWN | Sadlej(TZVP-FIP1) | 15.6(15.4) |
| | BP86 | Sadlej(TZVP-FIP1) | 16.3(16.1) |
| | | Expt.[a] | 18.63 |
| $Na_8$ | PW91 | SU[a] | 14.9 |
| (DCO) | PW91 | 6-31G[a] | 14.6 |
| | VWN | Sadlej(TZVP-FIP1) | 13.3(13.3) |
| | BP86 | Sadlej(TZVP-FIP1) | 13.9(13.8) |
| | | Expt.[a] | 16.69 |

[a]From Rayane *et al.* [207]

**Table** 5.3: Static mean polarizability, polarizability anisotropy and mean first-hyperpolarizability of $Na_2$ cluster optimized with DZVP/A2 (in atomic units)

| Optimized | Basis Set | Method | $\overline{\alpha}$ | $\lvert\Delta\alpha\rvert$ | $\beta_x = \beta_y$ | $\beta_z$ | $\beta$ |
|---|---|---|---|---|---|---|---|
| VWN | TZVP-FIP1 | MP2 | 237.08 | - | 0.0 | 0.0 | 0.0 |
| | | VWN | 209.48 | 157.17 | 0.0 | 1.0 | 1.0 |
| | | VWN-FF | 209.41 | 157.47 | | | |
| | | BP86 | 223.96 | 169.23 | 0.0 | 1.7 | 1.7 |
| | | BP86-FF | 223.63 | 170.17 | | | |
| | | HF | 237.37 | | 0.0 | 0.0 | 0.0 |
| | Sadlej | MP2 | 268.69 | - | 0.0 | 0.0 | 0.0 |
| | | VWN | 227.98 | 132.07 | 0.0 | 1.6 | 1.6 |
| | | VWN-FF | 227.89 | 132.60 | | | |
| | | BP86 | 243.02 | 140.96 | 0.0 | 2.5 | 2.5 |
| | | BP86-FF | 242.66 | 142.31 | | | |
| | | HF | 267.12 | | 0.0 | 0.0 | 0.0 |
| PW86 | TZVP-FIP1 | MP2 | 237.08 | - | 0.0 | 0.0 | 0.0 |
| | | VWN | 209.48 | 157.17 | 0.0 | 1.0 | 1.0 |
| | | VWN-FF | 209.41 | 157.47 | | | |
| | | BP86 | 223.96 | 169.23 | 0.0 | 1.7 | 1.7 |
| | | BP86-FF | 223.63 | 170.17 | | | |
| | | HF | 237.37 | | 0.0 | 0.0 | 0.0 |
| | Sadlej | MP2 | 268.69 | - | 0.0 | 0.0 | 0.0 |
| | | VWN | 227.98 | 132.07 | 0.0 | 1.6 | 1.6 |
| | | VWN-FF | 227.89 | 132.60 | | | |
| | | BP86 | 243.02 | 140.96 | 0.0 | 2.5 | 2.5 |
| | | BP86-FF | 242.66 | 142.31 | | | |
| | | HF | 267.12 | | 0.0 | 0.0 | 0.0 |
| Expt. | | | 251.90 | | | | |

[a]Experimental values calculated from the measurement of relative polarizabilities of Knight *et al.* [194] and the absolute measurement of the atomic polarizability by Molof *et al.* [195]

**Table** 5.4: Static mean polarizability, polarizability anisotropy and mean first-hyperpolarizability of $Na_4$ cluster optimized with DZVP/A2 (in atomic units)

| Optimized | Basis Set | Method | $\overline{\alpha}$ | $\lvert\Delta\alpha\rvert$ | $\beta_x$ | $\beta_y$ | $\beta_z$ | $\beta$ |
|---|---|---|---|---|---|---|---|---|
| VWN | TZVP[b] | MP2 | 490.55 | | 18.8 | -1.8 | -9.8 | 21.3 |
| | | VWN | 459.58 | 452.84 | 15.6 | -1.2 | -9.2 | 18.2 |
| | | VWN-FF | 459.42 | 454.36 | | | | |
| | | BP86 | 482.30 | 472.29 | 19.7 | 6.5 | -0.1 | 20.8 |
| | | BP86-FF | 481.74 | 474.52 | | | | |
| | | HF | 498.39 | | 6.9 | -2.0 | -7.3 | 10.2 |
| | Sadlej | MP2 | 513.92 | | 13.9 | -1.4 | 2.0 | 14.1 |
| | | VWN | 469.14 | 450.20 | 14.2 | 2.5 | -3.0 | 14.7 |
| | | VWN-FF | 469.18 | 452.38 | | | | |
| | | BP86 | 492.84 | 468.94 | 16.6 | 5.4 | -8.2 | 19.3 |
| | | BP86-FF | 492.49 | 472.34 | | | | |
| | | HF | 515.55 | | 0.3 | -1.7 | 6.4 | 6.6 |
| PW86 | TZVP[b] | MP2 | 494.73 | | 0.0 | 0.6 | 0.3 | 0.7 |
| | | VWN | 463.43 | 463.43 | 0.0 | -0.9 | 0.0 | 0.9 |
| | | VWN-FF | 463.33 | 463.94 | | | | |
| | | BP86 | 486.36 | 484.22 | 0.0 | -1.2 | 0.1 | 1.2 |
| | | BP86-FF | 485.81 | 484.48 | | | | |
| | | HF | 502.04 | | 0.0 | -0.6 | 0.0 | 0.6 |
| | Sadlej | MP2 | 518.00 | | 0.0 | -0.5 | 0.1 | 0.5 |
| | | VWN | 473.06 | 458.97 | -1.5 | -3.2 | 0.5 | 3.6 |
| | | VWN-FF | 473.14 | 461.23 | | | | |
| | | BP86 | 496.78 | 478.20 | 0.0 | -0.8 | 0.1 | 0.8 |
| | | BP86-FF | 496.52 | 481.58 | | | | |
| | | HF | 519.06 | | 0.0 | -0.4 | 0.0 | 0.4 |
| Expt. | | | 538.62 | | | | | |

[a]Experimental values calculated from the measurement of relative polarizabilities of Knight *et al.* [194] and the absolute measurement of the atomic polarizability by Molof *et al.* [195]

[b]TZVP-FIP1 basis set

**Table** 5.5: Static mean polarizability, polarizability anisotropy and mean first-hyperpolarizability of $Na_6$ cluster optimized with DZVP/A2 (in atomic units)

| Optimized | Basis | Method | $\overline{\alpha}$ | $\lvert\Delta\alpha\rvert$ | $\beta_x$ | $\beta_y$ | $\beta_z$ | $\beta$ |
|---|---|---|---|---|---|---|---|---|
| VWN | TZVP[b] | MP2 | 680.80 | | -1266.9 | -938.4 | -773.0 | 1755.9 |
| | | VWN | 614.16 | 374.13 | -1621.4 | -1200.5 | -929.3 | 2221.2 |
| | | VWN-FF | 613.87 | 374.35 | | | | |
| | | BP86 | 640.91 | 390.11 | -2046.4 | -1478.9 | -1207.3 | 2798.7 |
| | | BP86-FF | 639.81 | 391.03 | | | | |
| | | HF | 683.24 | | -1173.7 | -869.3 | -712.8 | 1625.2 |
| | Sadlej | MP2 | 704.06 | | -1147.9 | -854.0 | -705.9 | 1595.4 |
| | | VWN | 623.65 | 377.87 | -1332.2 | -995.6 | -819.1 | 1853.9 |
| | | VWN-FF | 623.16 | 377.56 | | | | |
| | | BP86 | 652.04 | 395.27 | -1527.2 | -1015.1 | -798.6 | 2000.1 |
| | | BP86-FF | 650.57 | 396.02 | | | | |
| | | HF | 701.13 | | -1172.3 | -873.9 | -719.3 | 1629.5 |
| PW86 | TZVP[b] | MP2 | 690.85 | | -1284.2 | -983.7 | -753.3 | 1784.5 |
| | | VWN | 623.61 | 384.59 | -1628.6 | -1278.4 | -832.6 | 2231.6 |
| | | VWN-FF | 623.20 | 385.70 | | | | |
| | | BP86 | 650.54 | 398.93 | -2095.9 | -1540.6 | -1186.7 | 2859.1 |
| | | BP86-FF | 649.66 | 401.80 | | | | |
| | | HF | 692.82 | | -1176.9 | -901.1 | -690.0 | 1635.0 |
| | Sadlej | MP2 | 714.07 | | -1157.4 | -888.9 | -683.6 | 1611.5 |
| | | VWN | 633.17 | 388.13 | -1338.1 | -1058.4 | -706.9 | 1846.7 |
| | | VWN-FF | 632.59 | 388.44 | | | | |
| | | BP86 | 661.88 | 405.03 | -1481.3 | -1091.5 | -751.9 | 1987.7 |
| | | BP86-FF | 660.27 | 406.75 | | | | |
| | | HF | 710.57 | | -1173.1 | -903.8 | -694.2 | 1635.5 |
| Expt. | | | 816.62 | | | | | |

[a]Experimental values calculated from the measurement of relative polarizabilities of Knight *et al.* [194] and the absolute measurement of the atomic polarizability by Molof *et al.* [195]

[b]TZVP-FIP1 basis set

**Table** 5.6: Static mean polarizability, polarizability anisotropy and mean first-hyperpolarizability of $Na_8$ cluster optimized with DZVP/A2 (in atomic units)

| Optimized | Basis | Method | $\overline{\alpha}$ | $\lvert\Delta\alpha\rvert$ | $\beta_x$ | $\beta_y$ | $\beta_z$ | $\beta$ |
|---|---|---|---|---|---|---|---|---|
| VWN | TZVP[b] | MP2 | 787.48 | | -90.6 | -2.8 | -4.1 | 90.7 |
| | | VWN | 706.50 | 107.28 | -44.5 | 12.2 | 20.7 | 50.6 |
| | | VWN-FF | 705.51 | 108.68 | | | | |
| | | BP86 | 736.18 | 109.78 | -10.6 | 51.4 | -9.5 | 53.3 |
| | | BP86-FF | 734.04 | 111.15 | | | | |
| | | HF | 805.62 | | -29.3 | 2.7 | 25.4 | 38.9 |
| | Sadlej | MP2 | 804.63 | | 1.6 | -7.0 | -4.4 | 8.2 |
| | | VWN | 711.19 | 97.80 | -35.4 | 43.0 | -17.7 | 58.4 |
| | | VWN-FF | 709.65 | 100.05 | | | | |
| | | BP86 | 744.20 | 105.40 | -55.3 | 36.6 | 9.3 | 67.0 |
| | | BP86-FF | 741.45 | 107.79 | | | | |
| | | HF | 819.90 | | -39.9 | 3.8 | 35.4 | 53.5 |
| PW86 | TZVP[b] | MP2 | 797.96 | | 10.2 | -25.7 | 3.9 | 27.9 |
| | | VWN | 715.21 | 104.11 | -43.4 | 18.8 | -15.9 | 49.9 |
| | | VWN-FF | 714.22 | 104.51 | | | | |
| | | BP86 | 743.64 | 100.91 | 13.3 | 18.8 | -0.6 | 23.0 |
| | | BP86-FF | 741.50 | 103.94 | | | | |
| | | HF | 815.15 | | -10.2 | -17.2 | -12.6 | 23.6 |
| | Sadlej | MP2 | 815.41 | | 10.7 | -26.2 | 3.5 | 28.5 |
| | | VWN | 718.60 | 93.59 | -31.2 | 32.1 | 122.3 | 130.2 |
| | | VWN-FF | 717.14 | 93.84 | | | | |
| | | BP86 | 750.63 | 93.55 | -76.9 | 81.5 | 208.7 | 236.9 |
| | | BP86-FF | 747.93 | 95.69 | | | | |
| | | HF | 829.78 | | -13.2 | -21.0 | -19.1 | 31.3 |
| Expt. | | | 868.75 | | | | | |

[a]Experimental values calculated from the measurement of relative polarizabilities of Knight *et al.* [194] and the absolute measurement of the atomic polarizability by Molof *et al.* [195]

[b]TZVP-FIP1 basis set

**Table** 5.7: Dipole moment, static polarizability, first hyperpolarizability and optical gap of para-nitroaniline (PNA)(in atomic units)

| | FF-BP86 | BP86 | FF-BPW91 | BPW91 | FF-BLYP | BLYP | FF-MP2[a] |
|---|---|---|---|---|---|---|---|
| $\mu_x$ | 3.138 | 3.138 | 3.134 | 3.134 | 3.147 | 3.147 | 2.754 |
| $\mu_y$ | 0.0 | 0.0 | 0.0 | 0.0 | 0.0 | 0.0 | 0.0 |
| $\mu_z$ | 0.0 | 0.0 | 0.0 | 0.0 | 0.0 | 0.0 | 0.0 |
| $\mu$ | 3.138 | 3.138 | 3.134 | 3.134 | 3.147 | 3.147 | 2.754 |
| $\alpha_{xx}$ | 166.93 | 166.79 | 166.11 | 165.98 | 168.75 | 168.68 | 148.40 |
| $\alpha_{yy}$ | 100.57 | 100.63 | 99.96 | 100.02 | 101.74 | 101.80 | 101.01 |
| $\alpha_{zz}$ | 51.07 | 50.97 | 50.41 | 50.31 | 52.24 | 52.20 | 50.95 |
| $\overline{\alpha}$ | 106.19 | 106.14 | 105.49 | 105.45 | 107.58 | 107.57 | 100.12 |
| $\lvert\Delta\alpha\rvert$ | 100.70 | 100.66 | 100.54 | 100.52 | 101.29 | 101.26 | |
| $\beta_{xxx}$ | 2142.4 | 2137.6 | 2133.9 | 2135.5 | 2207.0 | 2226.7 | 2129.2 |
| $\beta_{xyy}$ | -121.2 | -139.0 | -119.4 | -135.3 | -128.0 | -142.7 | -68.2 |
| $\beta_{xzz}$ | -59.4 | -95.3 | -85.4 | -89.4 | -96.2 | -99.7 | -56.9 |
| $\beta_x$ | 653.9 | 634.4 | 643.0 | 636.9 | 660.9 | 661.4 | 668.0 |
| $\beta_{yxx}$ | 2.3 | 0.0 | 1.0 | 0.0 | -21.1 | 0.0 | 0.1 |
| $\beta_{yyy}$ | 0.0 | 0.0 | 0.0 | 0.0 | 0.0 | 0.0 | 0.1 |
| $\beta_{yzz}$ | -10.7 | 0.0 | -18.5 | 0.0 | 17.4 | 0.0 | 0.1 |
| $\beta_y$ | -2.8 | 0.0 | -5.8 | 0.0 | -1.2 | 0.0 | 0.1 |
| $\beta_{zxx}$ | 0.0 | 0.0 | 0.0 | 0.0 | 0.0 | 0.0 | 0.0 |
| $\beta_{zyy}$ | 0.0 | 0.0 | 0.0 | 0.0 | 0.0 | 0.0 | -0.4 |
| $\beta_{zzz}$ | 0.0 | 0.0 | 0.0 | 0.0 | 0.0 | 0.0 | -0.1 |
| $\beta_z$ | 0.0 | 0.0 | 0.0 | 0.0 | 0.0 | 0.0 | -0.2 |
| $\beta$ | 653.9 | 634.4 | 643.0 | 636.9 | 660.9 | 661.4 | 668.0 |
| $\Delta$E | | 0.2152 | | 0.2146 | | 0.2100 | 0.3717 |

[a]Ref. [215]

**Table** 5.8: Dipole moment, static polarizability, first hyperpolarizability and optical gap of 2-methyl-4-nitroaniline (PNA-2)(in atomic units)

| | FF-BP86 | BP86 | FF-BPW91 | BPW91 | FF-BLYP | BLYP | FF-MP2[a] |
|---|---|---|---|---|---|---|---|
| $\mu_x$ | 3.160 | 3.160 | 3.157 | 3.157 | 3.171 | 3.172 | 2.771 |
| $\mu_y$ | -0.204 | -0.204 | -0.203 | -0.203 | -0.200 | -0.200 | -0.176 |
| $\mu_z$ | 0.0 | 0.0 | 0.0 | 0.0 | 0.0 | 0.0 | 0.0 |
| $\mu$ | 3.167 | 3.167 | 3.164 | 3.164 | 3.177 | 3.178 | 2.776 |
| $\alpha_{xx}$ | 176.74 | 176.76 | 175.85 | 175.89 | 178.32 | 178.38 | 156.44 |
| $\alpha_{yy}$ | 118.57 | 118.58 | 117.87 | 117.88 | 119.72 | 119.76 | 116.89 |
| $\alpha_{zz}$ | 59.78 | 59.72 | 59.04 | 58.97 | 60.90 | 60.92 | 59.31 |
| $\overline{\alpha}$ | 118.36 | 118.36 | 117.59 | 117.59 | 119.65 | 119.70 | 110.88 |
| $\lvert\Delta\alpha\rvert$ | 101.68 | 101.74 | 101.55 | 101.64 | 102.06 | 102.10 | |
| $\beta_{xxx}$ | 2165.4 | 2203.3 | 2163.1 | 2200.7 | 2250.5 | 2284.1 | 2102.8 |
| $\beta_{xyy}$ | -122.4 | -134.4 | -121.5 | -132.3 | -117.5 | -146.6 | -57.3 |
| $\beta_{xzz}$ | -30.8 | -94.2 | -18.7 | -88.2 | -91.8 | -102.7 | -54.4 |
| $\beta_x$ | 670.7 | 658.2 | 674.3 | 650.1 | 680.4 | 678.3 | 663.7 |
| $\beta_{yxx}$ | -74.1 | -65.4 | -68.1 | -63.0 | -64.0 | -62.5 | -41.9 |
| $\beta_{yyy}$ | -21.2 | -21.6 | -17.8 | -18.5 | 7.8 | -10.1 | -10.3 |
| $\beta_{yzz}$ | 8.1 | -9.9 | 10.6 | -7.8 | -25.3 | -12.9 | -15.3 |
| $\beta_y$ | -29.1 | -32.3 | -25.1 | -29.8 | -27.2 | -28.5 | -22.5 |
| $\beta_{zxx}$ | 0.0 | 0.0 | 0.0 | 0.0 | 0.0 | 0.0 | 0.3 |
| $\beta_{zyy}$ | 0.0 | 0.0 | 0.0 | 0.0 | 0.0 | 0.0 | 0.6 |
| $\beta_{zzz}$ | 0.0 | 0.0 | 0.0 | 0.0 | 0.1 | 0.0 | 0.1 |
| $\beta_z$ | 0.0 | 0.0 | 0.0 | 0.0 | 0.0 | 0.0 | 0.3 |
| $\beta$ | 671.3 | 659.0 | 674.8 | 650.8 | 680.9 | 678.9 | 664.1 |
| $\Delta$E | | 0.2081 | | 0.2077 | | 0.2032 | 0.3657 |

[a]Ref. [215]

**Table** 5.9: Dipole moment, static polarizability, first hyperpolarizability and optical gap of 3-methyl-4-nitroaniline (PNA-3)(in atomic units)

| | FF-BP86 | BP86 | FF-BPW91 | BPW91 | FF-BLYP | BLYP | FF-MP2[a] |
|---|---|---|---|---|---|---|---|
| $\mu_x$ | 2.956 | 2.955 | 2.952 | 2.952 | 2.968 | 2.968 | 2.630 |
| $\mu_y$ | -0.174 | -0.173 | -0.174 | -0.174 | -0.174 | -0.174 | -0.139 |
| $\mu_z$ | 0.0 | 0.0 | 0.0 | 0.0 | 0.0 | 0.0 | 0.0 |
| $\mu$ | 2.961 | 2.961 | 2.957 | 2.957 | 2.973 | 2.973 | 2.633 |
| $\alpha_{xx}$ | 175.77 | 175.80 | 174.87 | 174.73 | 177.34 | 177.34 | 159.71 |
| $\alpha_{yy}$ | 118.92 | 118.80 | 118.19 | 117.98 | 119.80 | 119.92 | 116.80 |
| $\alpha_{zz}$ | 59.80 | 59.93 | 59.06 | 58.96 | 60.90 | 60.95 | 59.27 |
| $\overline{\alpha}$ | 118.16 | 118.18 | 117.37 | 117.23 | 119.35 | 119.41 | 111.92 |
| $\lvert\Delta\alpha\rvert$ | 100.63 | 100.57 | 100.49 | 100.49 | 101.03 | 101.06 | |
| $\beta_{xxx}$ | 1873.4 | 1868.8 | 1862.6 | 1861.4 | 1917.8 | 1929.1 | 2014.5 |
| $\beta_{xyy}$ | -170.1 | -203.0 | -166.9 | -197.3 | -186.8 | -204.1 | -129.1 |
| $\beta_{xzz}$ | -76.0 | -85.6 | -60.1 | -79.9 | -90.7 | -93.7 | -55.5 |
| $\beta_x$ | 542.4 | 526.7 | 545.2 | 528.1 | 546.8 | 543.8 | 610.0 |
| $\beta_{yxx}$ | 56.2 | 31.9 | 46.9 | 32.0 | 36.7 | 36.6 | -8.3 |
| $\beta_{yyy}$ | -45.2 | -38.2 | -41.4 | -33.2 | -38.1 | -39.1 | -35.7 |
| $\beta_{yzz}$ | 0.2 | -21.8 | -6.9 | -19.2 | 0.7 | -25.6 | -31.0 |
| $\beta_y$ | 3.7 | -9.4 | -0.5 | -6.8 | -0.2 | -9.4 | 25.0 |
| $\beta_{zxx}$ | 0.0 | 0.0 | 0.0 | 0.0 | 0.0 | 0.0 | -1.8 |
| $\beta_{zyy}$ | 0.0 | 0.0 | 0.0 | 0.0 | 0.0 | 0.0 | -0.4 |
| $\beta_{zzz}$ | 0.0 | 0.0 | 0.0 | 0.0 | 0.0 | 0.0 | 0.0 |
| $\beta_z$ | 0.0 | 0.0 | 0.0 | 0.0 | 0.0 | 0.0 | -0.7 |
| $\beta$ | 542.4 | 526.8 | 545.2 | 528.1 | 546.8 | 543.9 | 610.5 |
| $\Delta$E | | 0.2209 | | 0.2202 | | 0.2155 | 0.3760 |

[a]Ref. [215]

**Table** 5.10: Dipole moment, static polarizability, first hyperpolarizability and optical gap of N-methyl-4-nitroaniline (N-mtPNA)(in atomic units)

| | FF-BP86 | BP86 | FF-BPW91 | BPW91 | FF-BLYP | BLYP | FF-MP2[a] |
|---|---|---|---|---|---|---|---|
| $\mu_x$ | 3.356 | 3.356 | 3.353 | 3.352 | 3.366 | 3.367 | 2.950 |
| $\mu_y$ | -0.284 | -0.284 | -0.282 | -0.282 | -0.288 | -0.288 | -0.272 |
| $\mu_z$ | 0.0 | 0.0 | 0.0 | 0.0 | 0.0 | 0.0 | 0.0 |
| $\mu$ | 3.368 | 3.368 | 3.365 | 3.364 | 3.378 | 3.379 | 2.963 |
| $\alpha_{xx}$ | 195.76 | 195.50 | 194.67 | 194.49 | 197.37 | 196.81 | 172.77 |
| $\alpha_{yy}$ | 111.18 | 110.91 | 110.52 | 110.17 | 112.42 | 112.02 | 110.93 |
| $\alpha_{zz}$ | 60.57 | 60.49 | 59.80 | 59.72 | 61.70 | 61.68 | 60.06 |
| $\overline{\alpha}$ | 122.50 | 122.32 | 121.66 | 121.48 | 123.83 | 123.52 | 114.59 |
| $\lvert\Delta\alpha\rvert$ | 118.31 | 118.21 | 117.99 | 117.98 | 118.73 | 118.36 | |
| $\beta_{xxx}$ | 2759.8 | 2755.9 | 2730.0 | 2747.5 | 2826.6 | 2812.8 | 2686.4 |
| $\beta_{xyy}$ | -157.0 | -162.2 | -155.5 | -156.7 | -157.1 | -165.9 | -88.4 |
| $\beta_{xzz}$ | -90.0 | -80.6 | -83.9 | -75.0 | -89.0 | -84.3 | -42.3 |
| $\beta_x$ | 837.6 | 837.7 | 830.2 | 838.6 | 860.2 | 854.2 | 851.9 |
| $\beta_{yxx}$ | -124.7 | -124.4 | -128.2 | -124.4 | -122.4 | -136.6 | -134.6 |
| $\beta_{yyy}$ | 12.1 | 20.0 | 15.0 | 20.6 | 32.7 | 22.2 | 6.3 |
| $\beta_{yzz}$ | -56.1 | -37.2 | -41.6 | -33.6 | -5.1 | -36.5 | -26.7 |
| $\beta_y$ | -56.2 | -47.2 | -51.6 | -45.8 | -31.6 | -50.3 | -51.7 |
| $\beta_{zxx}$ | 0.1 | 0.0 | 0.1 | 0.0 | 0.1 | 0.2 | 2.0 |
| $\beta_{zyy}$ | 0.0 | 0.0 | 0.0 | 0.0 | 0.0 | 0.0 | 0.9 |
| $\beta_{zzz}$ | 0.0 | 0.1 | 0.5 | 0.0 | 0.8 | 0.1 | 3.0 |
| $\beta_z$ | 0.0 | 0.0 | 0.2 | 0.0 | 0.3 | 0.1 | 2.0 |
| $\beta$ | 839.5 | 839.0 | 831.8 | 839.9 | 860.8 | 855.7 | 853.5 |
| $\Delta$E | | 0.1977 | | 0.1977 | | 0.1933 | 0.3652 |

[a]Ref. [215]

**Table** 5.11: Dipole moment, static polarizability, first hyperpolarizability and optical gap of N-methyl-2-methyl-4-nitroaniline (N-mtPNA-2)(in atomic units)

| | FF-BP86 | BP86 | FF-BPW91 | BPW91 | FF-BLYP | BLYP | FF-MP2[a] |
|---|---|---|---|---|---|---|---|
| $\mu_x$ | 3.506 | 3.506 | 3.502 | 3.503 | 3.522 | 3.522 | 3.097 |
| $\mu_y$ | -0.169 | -0.169 | -0.168 | -0.168 | -0.173 | -0.173 | -0.167 |
| $\mu_z$ | 0.0 | 0.0 | 0.0 | 0.0 | 0.0 | 0.0 | 0.0 |
| $\mu$ | 3.510 | 3.510 | 3.506 | 3.507 | 3.526 | 3.526 | 3.101 |
| $\alpha_{xx}$ | 205.11 | 205.08 | 204.09 | 203.96 | 206.66 | 206.73 | 179.84 |
| $\alpha_{yy}$ | 127.47 | 127.41 | 126.64 | 126.60 | 128.50 | 128.41 | 125.45 |
| $\alpha_{zz}$ | 67.59 | 67.57 | 66.80 | 66.87 | 68.61 | 68.60 | 66.80 |
| $\overline{\alpha}$ | 133.39 | 133.37 | 132.51 | 132.49 | 134.59 | 134.59 | 124.03 |
| $\lvert\Delta\alpha\rvert$ | 119.53 | 119.59 | 119.32 | 119.20 | 120.00 | 120.12 | |
| $\beta_{xxx}$ | 2675.3 | 2708.3 | 2659.5 | 2695.8 | 2718.8 | 2787.3 | 2534.9 |
| $\beta_{xyy}$ | -144.2 | -146.9 | -137.7 | -142.5 | -161.6 | -152.4 | -60.8 |
| $\beta_{xzz}$ | -45.1 | -50.4 | -52.2 | -47.5 | -49.1 | -50.6 | -13.6 |
| $\beta_x$ | 828.7 | 837.0 | 823.2 | 835.3 | 836.0 | 861.4 | 820.2 |
| $\beta_{yxx}$ | -69.6 | -54.0 | -76.7 | -57.1 | -78.2 | -64.6 | -102.6 |
| $\beta_{yyy}$ | 47.8 | 47.0 | 42.8 | 44.8 | 44.6 | 46.7 | 19.4 |
| $\beta_{yzz}$ | 38.5 | -2.6 | -18.3 | -3.4 | 15.7 | 5.1 | 10.2 |
| $\beta_y$ | 5.6 | -3.2 | -17.4 | -5.2 | -6.0 | 38.8 | -24.3 |
| $\beta_{zxx}$ | 0.1 | 0.1 | 0.1 | 0.1 | 0.1 | 0.1 | 3.3 |
| $\beta_{zyy}$ | 0.0 | 0.0 | 0.0 | 0.0 | 0.0 | 0.0 | 3.5 |
| $\beta_{zzz}$ | 0.0 | 0.0 | 0.1 | 0.0 | 0.0 | 0.0 | 3.7 |
| $\beta_z$ | 0.0 | 0.0 | 0.1 | 0.0 | 0.0 | 0.0 | 3.5 |
| $\beta$ | 828.7 | 837.0 | 823.4 | 835.3 | 836.0 | 862.3 | 820.6 |
| $\Delta$E | | 0.1882 | | 0.1885 | | 0.1842 | 0.3585 |

[a]Ref. [215]

**Table** 5.12: Dipole moment, static polarizability, first hyperpolarizability and optical gap of N-methyl-3-methyl-4-nitroaniline (N-mtPNA-3)(in atomic units)

| | FF-BP86 | BP86 | FF-BPW91 | BPW91 | FF-BLYP | BLYP | FF-MP2[a] |
|---|---|---|---|---|---|---|---|
| $\mu_x$ | 3.185 | 3.185 | 3.182 | 3.182 | 3.199 | 3.200 | 2.842 |
| $\mu_y$ | -0.103 | -0.104 | -0.101 | -0.101 | -0.107 | -0.107 | -0.127 |
| $\mu_z$ | 0.0 | 0.0 | 0.0 | 0.0 | 0.0 | 0.0 | 0.0 |
| $\mu$ | 3.187 | 3.187 | 3.184 | 3.184 | 3.201 | 3.201 | 2.845 |
| $\alpha_{xx}$ | 203.65 | 203.41 | 202.64 | 202.37 | 205.10 | 205.21 | 183.82 |
| $\alpha_{yy}$ | 129.25 | 129.02 | 128.36 | 128.16 | 130.41 | 130.16 | 126.71 |
| $\alpha_{zz}$ | 69.24 | 69.25 | 68.37 | 68.39 | 70.27 | 70.31 | 68.26 |
| $\overline{\alpha}$ | 134.04 | 133.90 | 133.13 | 132.98 | 135.26 | 135.24 | 126.27 |
| $\lvert\Delta\alpha\rvert$ | 116.74 | 116.56 | 116.61 | 116.39 | 117.12 | 117.22 | |
| $\beta_{xxx}$ | 2372.7 | 2400.7 | 2358.9 | 2392.2 | 2439.4 | 2466.5 | 2530.8 |
| $\beta_{xyy}$ | -226.0 | -220.6 | -213.7 | -213.0 | -214.7 | -222.7 | -154.7 |
| $\beta_{xzz}$ | -100.7 | -70.9 | -105.4 | -65.5 | -53.4 | -77.1 | -42.2 |
| $\beta_x$ | 682.0 | 703.1 | 679.9 | 704.6 | 723.8 | 722.2 | 778.0 |
| $\beta_{yxx}$ | -165.0 | -168.1 | -161.5 | -167.7 | -179.4 | -180.8 | -144.1 |
| $\beta_{yyy}$ | 67.8 | 66.4 | 62.3 | 63.9 | 80.5 | 62.5 | 49.9 |
| $\beta_{yzz}$ | -33.4 | -18.6 | -35.7 | -16.9 | 15.0 | -15.4 | 1.2 |
| $\beta_y$ | -43.5 | -40.1 | -45.0 | -40.2 | -28.0 | -44.6 | -31.0 |
| $\beta_{zxx}$ | 0.1 | 0.1 | 0.1 | 0.1 | 0.1 | 0.1 | 3.1 |
| $\beta_{zyy}$ | 0.0 | 0.0 | 0.0 | 0.0 | 0.0 | 0.0 | 1.2 |
| $\beta_{zzz}$ | 0.3 | 0.1 | 0.0 | 0.1 | 0.9 | 0.1 | 1.3 |
| $\beta_z$ | 0.1 | 0.1 | 0.0 | 0.1 | 0.3 | 0.1 | 1.9 |
| $\beta$ | 683.4 | 704.2 | 681.4 | 705.7 | 724.3 | 723.6 | 778.6 |
| $\Delta$E | | 0.2041 | | 0.2040 | | 0.1995 | 0.3711 |

[a]Ref. [215]

**Table** 5.13: Dipole moment, static polarizability, first hyperpolarizability and optical gap of N-methyl-5-methyl-4-nitroaniline (N-mtPNA-5)(in atomic units)

| | FF-BP86 | BP86 | FF-BPW91 | BPW91 | FF-BLYP | BLYP | FF-MP2[a] |
|---|---|---|---|---|---|---|---|
| $\mu_x$ | 3.146 | 3.146 | 3.143 | 3.143 | 3.161 | 3.161 | 2.807 |
| $\mu_y$ | -0.431 | -0.431 | -0.431 | -0.431 | -0.436 | -0.436 | -0.391 |
| $\mu_z$ | 0.0 | 0.0 | 0.0 | 0.0 | 0.0 | 0.0 | 0.0 |
| $\mu$ | 3.175 | 3.175 | 3.172 | 3.172 | 3.191 | 3.191 | 2.834 |
| $\alpha_{xx}$ | 205.05 | 204.13 | 203.84 | 203.82 | 206.41 | 205.81 | 184.69 |
| $\alpha_{yy}$ | 128.73 | 128.62 | 127.89 | 127.75 | 129.83 | 129.75 | 126.31 |
| $\alpha_{zz}$ | 69.22 | 69.22 | 68.31 | 68.31 | 70.25 | 70.29 | 68.29 |
| $\overline{\alpha}$ | 134.34 | 134.01 | 133.35 | 133.31 | 135.49 | 135.30 | 126.43 |
| $\lvert\Delta\alpha\rvert$ | 118.31 | 117.53 | 118.06 | 118.05 | 118.59 | 118.04 | |
| $\beta_{xxx}$ | 2434.6 | 2403.0 | 2417.4 | 2433.3 | 2446.9 | 2474.2 | 2540.5 |
| $\beta_{xyy}$ | -259.4 | -229.5 | -207.0 | -221.2 | -233.6 | -231.0 | -139.8 |
| $\beta_{xzz}$ | -75.1 | -75.6 | -57.1 | -69.0 | -60.6 | -82.0 | -33.4 |
| $\beta_x$ | 700.0 | 699.3 | 717.8 | 714.4 | 717.6 | 720.4 | 789.1 |
| $\beta_{yxx}$ | -81.4 | -82.4 | -81.0 | -82.1 | -91.4 | -88.8 | -138.3 |
| $\beta_{yyy}$ | 31.7 | -0.8 | 17.8 | 2.0 | -14.1 | 4.8 | -20.2 |
| $\beta_{yzz}$ | -57.7 | -57.4 | -59.1 | -51.7 | -26.0 | -59.5 | -57.6 |
| $\beta_y$ | -35.8 | -46.9 | -40.8 | -43.9 | -43.8 | -47.8 | -72.0 |
| $\beta_{zxx}$ | 0.1 | 3.5 | 0.1 | 0.3 | 0.1 | 0.3 | -0.8 |
| $\beta_{zyy}$ | 0.0 | -0.5 | 0.0 | 0.0 | 0.0 | 0.0 | 0.5 |
| $\beta_{zzz}$ | -0.1 | 0.2 | -1.4 | 0.1 | 0.1 | 0.1 | 0.9 |
| $\beta_z$ | 0.0 | 1.4 | 0.4 | 0.1 | 0.1 | 0.1 | 0.2 |
| $\beta$ | 700.9 | 700.9 | 718.9 | 715.7 | 718.9 | 721.9 | 792.4 |
| $\Delta$E | | 0.2027 | | 0.2026 | | 0.1980 | 0.3684 |

[a]Ref. [215]

**Table** 5.14: Dipole moment, static polarizability, first hyperpolarizability and optical gap of N-methyl-6-methyl-4-nitroaniline (N-mtPNA-6)(in atomic units)

| | FF-BP86 | BP86 | FF-BPW91 | BPW91 | FF-BLYP | BLYP | FF-MP2[a] |
|---|---|---|---|---|---|---|---|
| $\mu_x$ | 3.345 | 3.343 | 3.343 | 3.342 | 3.359 | 3.359 | 2.941 |
| $\mu_y$ | -0.498 | -0.498 | -0.496 | -0.496 | -0.498 | -0.498 | -0.454 |
| $\mu_z$ | 0.0 | 0.0 | 0.0 | 0.0 | 0.0 | 0.0 | 0.0 |
| $\mu$ | 3.382 | 3.380 | 3.380 | 3.379 | 3.396 | 3.396 | 2.976 |
| $\alpha_{xx}$ | 204.03 | 203.90 | 203.06 | 202.89 | 205.60 | 205.60 | 179.64 |
| $\alpha_{yy}$ | 130.58 | 130.41 | 129.74 | 129.57 | 131.69 | 131.60 | 128.07 |
| $\alpha_{zz}$ | 69.16 | 69.11 | 68.26 | 68.37 | 70.17 | 70.21 | 68.24 |
| $\overline{\alpha}$ | 134.59 | 134.49 | 133.69 | 133.62 | 135.82 | 135.82 | 125.32 |
| $\lvert\Delta\alpha\rvert$ | 117.07 | 117.04 | 117.01 | 116.80 | 117.56 | 117.60 | |
| $\beta_{xxx}$ | 2720.2 | 2760.5 | 2704.4 | 2749.9 | 2793.1 | 2852.7 | 2634.8 |
| $\beta_{xyy}$ | -163.7 | -165.2 | -160.0 | -161.2 | -191.9 | -178.8 | -77.5 |
| $\beta_{xzz}$ | -103.6 | -81.1 | -100.7 | -75.6 | -81.4 | -86.0 | -32.7 |
| $\beta_x$ | 817.6 | 838.1 | 814.6 | 837.7 | 839.9 | 862.6 | 841.5 |
| $\beta_{yxx}$ | -214.6 | -205.4 | -218.9 | -204.5 | -218.0 | -217.4 | -189.9 |
| $\beta_{yyy}$ | -1.2 | -5.2 | 4.0 | 0.2 | 15.1 | 13.9 | -5.7 |
| $\beta_{yzz}$ | -47.3 | -46.2 | -66.9 | -40.3 | -54.6 | -48.1 | -47.4 |
| $\beta_y$ | -87.7 | -85.6 | -93.9 | -81.5 | -85.8 | -83.9 | -81.0 |
| $\beta_{zxx}$ | 0.1 | 0.1 | 0.1 | 0.2 | 0.1 | 0.2 | 1.8 |
| $\beta_{zyy}$ | 0.1 | 0.0 | 0.0 | 0.0 | 0.0 | 0.0 | 3.4 |
| $\beta_{zzz}$ | 0.0 | 0.1 | 0.2 | 0.1 | 0.1 | 0.1 | 3.6 |
| $\beta_z$ | 0.1 | 0.1 | 0.1 | 0.1 | 0.1 | 0.1 | 2.9 |
| $\beta$ | 822.3 | 842.5 | 820.0 | 841.7 | 844.3 | 866.7 | 845.4 |
| $\Delta$E | | 0.1916 | | 0.1918 | | 0.1875 | 0.3598 |

[a]Ref. [215]

# References


[1] D. R. Hartree, *Proc. Cambridge Philos. Soc.* **24**, 89 (1928).

[2] V. Fock, *Z. Phys.* **61**, 126 (1930).

[3] A. Szabo and N. S. Ostlund, *Modern Quantum Chemistry: Introduction to Advanced Electronic Structure Theory*, 1st Rev. ed., McGraw-Hill, Inc., New York, (1989).

[4] L. H. Thomas, *Proc. Cambridge Philos. Soc.* **23**, 542 (1927).

[5] E. Fermi, *Z. Phys.* **48**, 73 (1928).

[6] N. H. March, *Self-Consistent Fields in Atoms*, Oxford: Pergamon (1975).

[7] J. A. Alonso and L. A. Girifalco, *J. Phys. Chem. Solids* **38**, 869 (1977).

[8] B. Jacob, E. K. U. Gross and R. M. Dreizler, *J. Phys. B* **11**, 22 (1978).

[9] E. K. U. Gross and R. M. Dreizler, *Phys. Rev. A* **20**, 1798 (1979).

[10] P. Gombs, *Die Statistische Theorie des Atomes and ihre Anwendungen*, Springer, Berlin (1949).

[11] N. H. March, *Adv. Phys.* **6**, 1 (1957).

[12] N. H. March, *Theor. Chem: A Specialist's Periodic Report* **4**, 92 (1981).

[13] E. H. Lieb and B. Simon, *Phys. Rev. Lett.* **31**, 681 (1973).

[14] E. H. Lieb, *Rev. Mod. Phys.* **48**, 553 (1976).

[15] E. H. Lieb, *Rev. Mod. Phys.* **53**, 603 (1981).

[16] E. H. Lieb and W. Thirring, In *Studies in Mathematical Physics*, ed. by, E. H. Lieb, B. Simon and A. S. Wightman, Princeton University, Princeton, New Jersey, p. 269 (1976).

[17] P. A. M. Dirac, *Proc. Cambridge Philos. Soc.* **26**, 376 (1930).

[18] C. F. von Weizsacker, *Z. Phys.* **96**, 431 (1935).

[19] J. C. Slater, *Phys. Rev.* **82**, 538 (1951).

[20] J. C. Slater, In *Adv. Quantum Chem.*, Ed. P. O. Lowdin, **6**, Academic, New York, p.1 (1972).

[21] K. H. Johnson, *Adv. Quantum Chem.* **7**, 143 (1973).

[22] J. W. D. Connolly, In *Semiempirical Methods of Electronic Structure Calculations, Part A: Techniques*, Ed. G. A. Segal, VI, Chapter 4, Plenum, New York (1977).

[23] J. C. Slater, *The Self-Consistent Field for Molecules and Solids: Quantum Theory of Molecules and Solids*, **4**, McGraw-Hill, New York (1974).

[24] J. C. Slater, *Int. J. Quantum Chem. Symp.* **9**, 7 (1975).

[25] R. Gasper, *Acta Physica Hungaria* **3**, 263 (1954).

[26] P. -O. Lowdin, *Phys. Rev.* **97**, 1474 (1955).

[27] R. McWeeny, *Rev. Mod. Phys.* **32**, 335 (1960).

[28] E. R. Davidson, *Reduced Density Matrices in Quantum Chemistry*, Academic Press, New York (1976).

[29] J. Coleman, *Rev. Mod. Phys.* **35**, 668 (1963).

[30] J. Coleman, In *The Force Concept in Chemistry*, Ed. B. M. Deb, Van Nostrand, Reinhold, p.418 (1981).

[31] J. K. Percus, *Int. J. Quantum Chem.* **13**, 89 (1978).

[32] R. Erdahl and V. H. Smith, Jr.,Eds., *Density Matrices and Density Functionals*, Reidel, Dordrecht (1987).

[33] R. G. Parr, R. A. Donnelly, M. Levy, W. E. Palke, *J. Chem. Phys.* **68**, 3801 (1978).

[34] T. L. Gilbert, *Phys. Rev. B* **12**, 2111 (1975).

[35] M. Berrondo, O. Goscinski, *Int. J. Quantum Chem. Symp.* **9**, 67 (1975).

[36] R. A. Donnelly, R. G. Parr, *J. Chem. Phys.* **69**, 4431 (1978).

[37] R. A. Donnelly, *J. Chem. Phys.* **71**, 2874 (1979).

[38] P. -O. Lowdin, *Phys. Rev.* **97**, 1490 (1955).

[39] P. Hohenberg and W. Kohn, *Phys. Rev.* **136**, B864 (1964).

[40] R. G. Parr and W. Yang, *Density Functional Theory of Atoms and Molecules*, Oxford University Press: Oxford, (1989).

[41] M. Levy, *Phys. Rev. A* **26**, 1200 (1982).

[42] E. H. Lieb, In *Physics as Natural Philosophy, Essays in Honor of Laszlo Tisza on his 75th Birthday.*, M. Fesgbach and A. Shimony, Eds., (MIT Press,

Cambridge), p. 111 (1982). [For a revised version, see *Int. J. Quantum Chem.* **24**, 243 (1983)].

[43] J. E. Harriman, *Phys. Rev. A* **24**, 680 (1980).

[44] M. Levy, *Proc. Natl. Acad. Sci. USA* **76**, 6062 (1979).

[45] M. Levy and J. P. Perdew, In *Density Functional Methods in Physics*, R. M. Dreizler and J. da Providência, Eds., NATO ASI Series, **123**, (Plenum, New York), p. 11 (1985).

[46] R. O. Jones, O. Gunnnarsson, *Rev. Mod. Phys.* **61**, 689 (1989).

[47] A. K. Rajagopal, *Adv. Chem. Phys.* **41**, 59 (1980).

[48] A. S. Bamzai and B. M. Deb, *Rev. Mod. Phys.* **53**, 95 (1981); **53**, 593(E) (1981).

[49] R. G. Parr, *Annu. Rev. Phys. Chem.* **34**, 631 (1983).

[50] W. Kohn and L. J. Sham, *Phys. Rev.* **140**, A1133 (1965).

[51] S.H. Vosko, L. Wilk, M. Nusair, *Can. J. Phys.* **58**, 1200 (1980).

[52] J. P. Dahl and J. Avery, Eds., *Local Density Approximations in Quantum Chemistry and Solid State Physics*, Plenum, New York (1984) and references therein.

[53] John P. Perdew, Stefan Kurth, Ales Zupan, and Peter Blaha, *Phys. Rev. Lett.* **82**, 2544 (1999).

[54] J. P. Perdew, *Phys. Rev. Lett.* **55**, 1668 (1985).

[55] D. C. Langreth and J. P. Perdew, *Phys. Rev. B* **21**, 5469 (1980).

[56] J.P. Perdew, Y. Wang, *Phys. Rev. B* **33**, 8800 (1986); **40**, 3399 (E) (1989).

[57] J.P. Perdew, *Phys. Rev. B* **33**, 8822 (1986); **34**, 7406 (E) (1986).

[58] J. P. Perdew, *Unified Theory of Exchange and Correlation Beyond the Local Density Approximation. Electronic Structure of Solids '91*, Ed., P. Ziesche and H. Eschrig, p 11-20 (1991).

[59] Y. Wang and J. P. Perdew, Spin scaling of the electron-gas correlation energy in the high-density limit. *Phys. Rev. B* **43**, 8911 (1991).

[60] J. P. Perdew, Y. Wang, *Phys. Rev. B* **45**, 13244 (1992).

[61] K. Burke, J. P. Perdew, and Y. Wang, *Derivation of a Generalized Gradient Approximation: The PW91 Density Functional. Electronic Density Functional Theory: Recent Progress and New Directions*, Ed., J. F. Dobson, G. Vignale and M. P. Das, p81-121, (1997).

[62] J. P. Perdew, K. Burke, and M. Ernzerhof, Generalized Gradient Approximation Made Simple. *Phys. Rev. Lett.* **77**, 3865 (1996).

[63] A. D. Becke, *J. Chem. Phys.* **84**, 4524 (1986).

[64] A. D. Becke, *J. Chem. Phys.* **96**, 2155 (1992).

[65] A. D. Becke, *J. Chem. Phys.* **97**, 9173 (1992).

[66] A. D. Becke, *J. Chem. Phys.* **98**, 5648 (1993).

[67] A. D. Becke, *J. Chem. Phys.* **104**, 1040 (1996).

[68] A. D. Becke, *J. Chem. Phys.* **107**, 8554 (1997).

[69] A. D. Becke, *J. Chem. Phys.* **98**, 1372 (1993).

[70] A. D. Becke, *Phys. Rev. A* **38**, 3098 (1988).

[71] C. Lee, W. Yang, R. G. Parr, *Phys. Rev.* **B37**, 785 (1988).

[72] R. Colle and D. Salvetti, *Theor. Chim. Acta.* **37**, 329 (1975).

[73] M. J. Frisch, G. W. Trucks, H. B. Schlegel, P. M. W. Gill, B. G. Johnson, M. W. Wong, J. B. Foresman, M. A. Robb, M. H.-Gordon, E. S. Replogle, R. Gomperts, J. L. Andres, K. Raghavachari, J. S. Binkley, C. Gonzales, R. L. Martin, D. J. Fox, D. L. Defrees, J. Baker, J. J. P. Stewart, and J. A. Pople, GAUSSIAN 92 ©. *Gaussian Inc.*, Pittsburgh, (1993).

[74] J. P. Perdew and A. Zunger, *Phys. Rev. B*, **23**, 5048 (1981).

[75] S.F. Boys, Electronic wavefunctions. I. A general method of calculation for stationary states of any molecular system. *Proc. Roy. Soc. [London]*, **A 200**, 542 (1950).

[76] I. N. Levine, *Quantum Chemistry*, 4th ed.; Prentice Hall, Upper Saddle River, p461 (2002).

[77] D. Buckingham, In *Advances in Chemical Physics*, J. O. Hirschfelder, Ed., **12**, Chapter 2, Interscience, New York (1967).

[78] H. Hellmann, *Einführung in die Quantenchemie*, Deuticke, Leipzig, p. 285 (1937).

[79] R. P. Feynman, *Phys. Rev.* **56**, 340 (1939).

[80] E. Wigner, *Math. Natur. Anz.* (Budapest) **53**, 477 (1935).

[81] J. Gerratt and I. M. Mills, *J. Chem. Phys.* **49**, 1719, 1730 (1968).

[82] J. A. Pople, R. Krishnan, H. B. Schlegel, J. S. Binkley, *Int. J. Quantum Chem. Symp.* **13**, 225 (1979).

[83] P. J. Pulay, *J. Chem. Phys.* **78**, 5043 (1983).

[84] G. C. Schatz, M. A. Ratner, *Quantum Mechanics in Chemistry*, Chapter 6, Prentice-Hall, Englewood Cliffs, NJ (1993).

[85] J. N. Murrell, A. J. Harget, *Semi-Empirical Self-Consistent-Field Molecular Orbital Theory of Molecules*, Wiley, London (1972).

[86] J. A. Pople, D. L. Beveridge, *Approximate Molecular Orbital Theory* McGraw-Hill, New York (1970).

[87] H. D. Cohen, C. C. J. Roothaan, *J. Chem.Phys.* **43**, S34 (1965).

[88] N. S. Hush, M. L. Williams, *Chem. Phys. Lett.* **5**, 507 (1970).

[89] J. E. Gready, G. B. Bacskay, N. S. Hush, *Chem. Phys.* **22**, 141 (1977).

[90] P. Pulay, *Mol. Phys.* **17**, 197 (1969).

[91] G. J. B. Hurst, M. Dupuis, E. Clementi, *J. Chem. Phys.* **89**, 385 (1988).

[92] C. E. Dykstra, P. G. Jasien, *Chem Phys. Lett.* **109**, 388 (1984).

[93] P. Jørgensen, J. Simons, Eds. *Geometrical Deriuatiues of Energy Surfaces and Molecular Properties* Reidel, Dordrecht (1986).

[94] D. J. Thouless, *Quantum Mechanics of Many Body Systems*, Academic, New York (1961).

[95] J. Linderberg, Y. Öhrn, *Propogators in Quantum chemistry*, Academic Press, London (1974).

[96] A. Dalgarno, G. A. Victor, *Proc. R. Soc. London Ser. A*, **291**, 291 (1966).

[97] D. R. Kanis, M. A. Ratner, T. J. Marks, *Chem. Rev.* **94**, 195 (1994).

[98] H. Sekino, R.J. Bartlett, *J. Chem. Phys.* **84**, 2726 (1986).

[99] H. Sekino, R. Bartlett, *J. Chem. Phys.* **94**, 3665 (1991).

[100] S. P. Karna, M. Dupuis, *J. Comput. Chem.* **12**, 487 (1991).

[101] J. E. Rice,R. D. Amos, S. M. Colwell, N. C. Handy, J. Sanz, *J. Chem. Phys.* 3, 8828 (1990).

[102] J.E. Rice and N.C. Handy, *J. Chem. Phys.* **94**, 4959 (1991).

[103] D.L. Yeager, J. Olsen and P. Jørgensen, *Intern. J. Quantum Chem. Symp.* **15**, 151 (1981).

[104] J. Oddershede and E.N. Svendsen, *Chem. Phys.* **64**, 359 (1982).

[105] H. Koch and P. Jørgensen, *J. Chem. Phys.* **93**, 3333 (1990).

[106] M. J. Stott, and E. Zaremba, *Phys. Rev. A* **21**, 12 (1980);**22**, 2293 (E) (1980).

[107] G. D. Mahan, *Phys. Rev. A* **22**, 1780 (1980).

[108] S. M. Colwell, C. W. Murray, N. C. Handy, R. D. Amos, *Chem Phys. Lett.* **210**, 261 (1993).

[109] B. M. Deb and S. K. Ghosh, *J. Chem. Phys.* **77**, 342 (1982).

[110] S. K. Ghosh and B. M. Deb *Chem. Phys.* **71**, 295 (1982).

[111] L. J. Bartlotti, *Phys. Rev. A* **24**, 1661 (1981).

[112] L. J. Bartlotti, *Chem. Phys.* **26**, 2243 (1982).

[113] S. Chakravarty, M. B. Fogel, and W. Kohn, *Phys. Rev. Lett.* **43**, 775 (1979).

[114] E. Runge and E. K. U. Gross, *Phys. Rev. Lett.* **52**, 997 (1984).

[115] E. K. U. Gross and W. Kohn, *Phys. Rev. Lett.* **55**, 2850 (1985); **57**, 923 (E) (1985).

[116] A. Zangwill, and P. Soven, *Phys. Rev. A* **21**, 1561 (1987).

[117] D. Mearns and W. Kohn, *Phys. Rev. A* **35**, 4796 (1987).

[118] E. K. U. Gross, and W. Kohn, *Adv. Chem. Phys.* **21**, 255 1990

[119] P. Duffy, D.P. Chong, M. E. Casida, D. R. Salahub, *Phys. Rev. A 50*, 4707 (1994).

[120] P. G. Jasien and G. Fitzgerald, *J. Chem. Phys.* **93**, 2554 (1990)

[121] F. Sim, D. R. Salahub, S. Chin, *Int. J. Quantum Chem.* **43**, 463 (1992).

[122] D. P. Chong, *J. Chin. Chem. Soc.* **39**, 375 91992).

[123] J. Guan, P. Duffy, J. T. Carter, D. P. Chong, K. C. Casida, M. E. Casida, M. Wrinn, *J. Chem. Phys.* 1993, **98**, 4753 (1993).

[124] J. Guan, M. E. Casida, A. M. Köster, D. R. Salahub, *Phys. Rev. B* **52**, 2184 (1995).

[125] D. P. Chong, . Phys. Lett. **217**, 539 (1994).

[126] A. M. Lee, S. M. Colwell, *J. Chem. Phys.* **101**, 9704 (1994).

[127] G. D. Mahan and K. R. Subbaswamy, *Local Density Theory of Polarizability*, Plenum Press, New York, NY (1990).

[128] M. Kamiya, H. Sekino, T. Tsuneda, K. Hirao, *J. Cem. Phys.* **122**, 234111 (2005).

[129] C. Jamorski, M. E. Casida, D. R. Salahub, *J. Chem. Phys.* **104**, 5134 (1996).

[130] M. E. Casida, In *Recent Developments and Applications of Modern Density Functional Theory*, Seminario M. J. (ed.), Elsevier, Amsterdam, p. 391 (1996).

[131] A. Ipatov, A. Fouqueau, C. P. del Valle, F. Cordova, M. E. Casida, A. M. Köster, A. Vela, C. J. Jamorski, *J. Mol. Struct. :THEOCHEM* **762**, 179 (2006).

[132] A. Banerjee, M. K. Harbola, *Pramana - J. Phys.* **49**, 455 (1997).

[133] M. E. Casida, C. Jamorski, F. Bohr, J. Guan, D. R. Salahub, *ACS Symposium Series* **628**, 145 (1996).

[134] M. E. Casida, T. A. Wesołowski, *Int. J. Quantum Chem.* **96**, 577 (2004).

[135] A. Görling, *Int. J. Quantum Chem.* **69**, 265 (1998).

[136] A. Görling, H. H. Heinze, S. Ph. Ruzankin, M. Staufer, N. Rösch, *J. Chem. Phys.* **110**, 2785 (1999).

[137] S.T. Epstein, *The Variation Method in Quantum Chemistry*, Academic Press, New York, (1974).

[138] Alain St-Amant, *Ph.D. Thesis*, University of Montreal (1992).

[139] A. St-Amant and D. R. Salahub, *Chem. Phys. Lett.* **169** 387 (1990).

[140] deMon-KS version 3.5, M. E. Casida, C. Daul, A. Goursot, A. Koester, L. G. M. Pettersson, E. Proynov, A. St-Amant, and D. R. Salahub principal authors, S. Chreties, H. Duarte, N. Godbout, J. Guan, C. Jamorski, M.

Leboeuf, V. Malkin, O. Malkina, M. Nyberg, L. Pedocchi, F. Sim, and A. Vela contributing authors, deMon Software (1998).

[141] A. M. Köster, P. Calaminici, R. Flores, G. Geudtner, A. Goursot, T. Heine, F. Janetzko, S. Patchkovskii, J. U. Reveles, A. Vela and D. R. Salahub, deMon2k, *The deMon developers*, Cinvestav, (2004).

[142] B. I. Dunlap, J. W. D. Connolly, J. R. Sabin, *J. Chem. Phys.* **71**, 4993 (1979).

[143] W. Mintmire, B. I. Dunlap, *Phys. Rev. A* **25**, 88 (1982).

[144] http://www.demon-software.com/public_html/support.html#manual

[145] K. B. Sophy and S. Pal, *J. Chem. Phys.* **118**, 10861 (2003).

[146] K. B. Sophy and S. Pal, *J. Mol. Struct.: THEOCHEM* **676**, 89 (2004).

[147] S. Pal and K. B. Sophy In *Lecture Series on Computer and Computational Sciences* **3**, p. 142, Brill Academic Publishers, Netherlands, (2005).

[148] K. B. Sophy, P. Calaminici, S. Pal *J. Chem. Theor. Comp.* (In press) (2007)

[149] C.E. Dykstra, *Ab Initio Calculations of the Structures and Properties of Molecules*, Elsevier, New York, (1988).

[150] A.E. Kondo, P. Piecuch, J. Paldus, *J. Chem. Phys.* **104**, 8566 (1996).

[151] H. Sekino, R.J. Bartlett, *J. Chem. Phys.* **98**, 3022 (1993).

[152] K.B. Ghose, P. Piecuch, S. Pal, L. Adamowicz, *J. Chem. Phys.* **104**, 6582 (1996).

[153] D.M. Bishop, J. Pipin, B. Lam, *Chem. Phys. Lett.* **127**, 377 (1986).

[154] G.H.F. Diercksen, A.J. Sadlej, *J. Chem. Phys.* **90**, 7300 (1989).

[155] V.E. Ingamells, M.G. Papadopoulos, N.C. Handy, A. Willetts, *J. Chem. Phys.* **109**, 1845 (1998).

[156] E.A. Salter, H. Sekino, R.J. Bartlett, *J. Chem. Phys.* **87**, 502 (1987).

[157] R.D. Amos, In, K.P. Lawley (Ed.), *Advances in Chemical Physics*, Ab Initio Methods in Quantum Chemistry, Vol. I, Wiley, New York, (1987).

[158] H. Sekino, R.J. Bartlett, *Int. J. Quantum Chem.* **S18**, 255 (1984).

[159] H. Koch, H.J.Aa. Jensen, P. Jørgensen, T. Helgaker, *J. Chem. Phys.* **93**, 3345 (1990).

[160] (a) S. Pal, *Phys. Rev. A*, **33**, 2240 (1986). (b) S. Pal, *Theor. Chim. Acta* **66**, 151 (1984). (c) S. Pal, *Phys. Rev. A* **39**, 39 (1989).

[161] H.J. Monkhorst, *Int. J. Quantum Chem.* **S11**, 421 (1977).

[162] K. Harbola, *Chem. Phys. Lett.* **217**, 461 (1994).

[163] R. Kobayashi, H. Koch, P. Jorgenson, T.J. Lee, *Chem. Phys. Lett.* **211**, 94 (1993).

[164] N. Godbout, D.R. Salahub, J. Andzelm, E. Wimmer, *Can. J. Phys.* **70**, 560 (1992).

[165] M. Dupuis, J.D. Watts, H.O. Villar, G.J.B. Hurst, *HONDO, version 7.0*, New York, (1987).

[166] S. J. A. van Gisbergen, F. Kootstra, P. R. T. Schipper, O. V. Gritsenko, J. G. Snijders, and E. J. Baerends, *Phys. Rev. A* **57**, 2556 (1998).

[167] N. Vaval, K.B. Ghose, S. Pal, *J. Chem. Phys.* **101**, 4914 (1994).

[168] N. Vaval, S. Pal, *Phys. Rev. A* **54**, 250 (1996).

[169] G. Maroulis, *J. Chem. Phys.* **105**, 8467 (1996).

[170] G. Maroulis, D. Xenides, U. Hohm, A. Loose, *J. Chem. Phys.* **115**, 7957 (2001).

[171] O. Quinet, V. Liegeois, B. Champagne, *J. Chem. Theory Comput.* **1**, 444, (2005).

[172] T. Bancewicz, Y. Le Duff, J. -L. Godet, *Adv. Chem. Phys.* **119**, 267 (2001).

[173] *Chem. Phys. Lett.* **259**, 645 (1996).

[174] R. D. Amos, *Chem. Phys. Lett.* **87**, 23 (1982).

[175] A. Elliasmine, J. -L. Godet, Y. Le Duff, T. Bancewicz, *Mol. Phys.* **90**, 147 (1997).

[176] H. Hoshina, T. Wakabayashi, T. Momose, T. J. Shida, *Chem. Phys.* **110**, 5728 (1999).

[177] T. Momose, M. Miki, T. Wakabayashi, T. Shida, M. -C. Chan, S. S. Lee, T. Oka, *J. Chem. Phys.* **107**, 7707 (1997).

[178] G. Maroulis, *J. Chem. Phys.* **108**, 5432 (1998).

[179] K. E. Laidig, *Can. J. Chem.* **74**, 1131 (1996).

[180] E. R. Batista, S. S. Xantheas, H. Jónsson, *J. Chem. Phys.* **111**, 6011 (1999).

[181] F. Torrens, J. Sánchez-Marín, I. Nebot-Gil, *Molecules* **4**, 28 (1999

[182] U. Hohm, *Vacuum* **58**, 117 (2000).

[183] A. Cartier, M. T. C. Martins-Costa, D. Rinaldi, *Int. J. Quantum Chem.* **60**, 883 (1996).

[184] U. Hohm, *Chem. Phys. Lett.* **425**, 242 (2006).

[185] U. Hohm, G. Maroulis, *J. Chem. Phys.* **124**, 124312 (2006)

[186] U. Hohm, G. Maroulis, *J. Chem. Phys.* **121**, 10411 (2004).

[187] A. V. Luzanov, L. N. Lisetskii, *J. Struc. Chem.* **42**, 544 (2001).

[188] T. Helgaker, P. Jørgensen, and J. Olsen, *Molecular Electronic-Structure Theory*, Wiley, Chichester, (2000).

[189] K. B. Wiberg, C. M. Hadad, T. J. LePage, C. M. Breneman, and M. J. Frisch, *J. Am. Chem. Soc.* **96**, 671 (1992).

[190] deMon2k (Version 2.2.4, July 2006) Copyright (C) by The International DeMon Developers Community, Authors: Andreas M. Köster, Patrizia Calaminici, Mark E. Casida, Roberto Flores-Moreno, Gerald Geudtner, Annick Goursot, Thomas Heine, Andrei Ipatov, Florian Janetzko, Jorge M. del Campo, Serguei Patchkovskii, J. Ulises Reveles, Alberto Vela and Dennis R. Salahub.

[191] R. Flores-Moreno, A. M. Köster *Static Density Response with Auxiliary Functions*, in preparation

[192] A.J. Sadlej, *Collection Czechoslovak Chem. Commun.* **53**, 1995 (1988).

[193] P. Calaminici, K. Jug, A. M. Köster, *J. Chem. Phys.* **111**, 4613 (1999).

[194] W. D. Knight, K. Clemenger, W. A. de Heer and W. A. Saunders, *Phys. Rev. B* **31**, 2539 (1985).

[195] R. W. Molof, T. M. Miller, H. L. Schwartz, B. Benderson, and J. T. Park, *J. Chem. Phys.* **61**, 1816 (1974).

[196] K. D. Bonin and V. V. Kresin, *Electric-Dipole Polarizabilities of Atoms, Molecules and Clusters*, World Scientific, Singapore, (1997).

[197] U. Kreibig and M. Vollmer, *Optical Properties of Metal Clusters*, Springer, Berlin, (1995).

[198] R. S. Berry and H. Haberland In *Chem. Phys. 52, Clusters of Atoms and Molecules: Theory, Experiment and Clusters of Atoms*, ed. by H. Haberland, Springer-Verlag, Berlin, Heidelberg (1994).

[199] J. A. Alonso, *Chem. Rev.* **100**, 637 (2000).

[200] M. Manninen, R. M. Nieminen and M. J. Puska, *Phys. Rev. B* **33**, 4289 (1986).

[201] I. Moullet, J. L. Martins, F. Reuse, and J. Buttet, *Phys. Rev. B* **42**, 11598 (1990).

[202] I. Moullet, J. L. Martins, F. Reuse, and J. Buttet, *Phys. Rev. Lett.* **65**, 476 (1990).

[203] M. Urban and A. J. Sadlej, *J. Chem. Phys.* **103**, 9692 (1995).

[204] I. A. Solov'yov, A. V. Solov'yov, and W. Greiner, *Phys. Rev. A* **65**, 053203 (2002).

[205] K. R. S. Chandrakumar, T. K. Ghanty, and S. K. Ghosh, *J. Chem. Phys.* **120**, 6487 (2004).

[206] G. Maroulis, *J. Chem. Phys.* **121**, 10519 (2004).

[207] D. Rayane, A. R. Allouche, E. Benichou, R. Antoine, M. Aubert-Frecon, Ph. Dugourd, M. Broyer, C. Ristori, F. Chandezon, B. A. Huber, and C. Guet, *Eur. Phys. J. D* **9**, 243 (1999).

[208] W. A. de Heer, *Rev. Mod. Phys.* **65**, 611 (1993).

[209] D. S. Chemla, J. Zyss, *Nonlinear Optical Properties of Organic Molecules and Crystals*, Vol.1, Academic Press, New York (1987).

[210] B. Champagne, B. Kirtman, *Handbook of Advanced Electronic and Photonic Materials*, H. S. Nalwa, Ed.,Vol 9, Chapter 2, p. 63, Academic,San Deigo (2001).

[211] J. Morley, *J. Chem. Soc. Perkin Trans.* **2**, 177 (1995); *J. Phys. Chem.* **98**, 11818 (1994).

[212] D. M. Bishop, *Adv. Chem. Phys.* **104**, 1 (1998).

[213] F. Sim, S. Chin, M. Dupuis, J. E. Rice, *J. Phys. Chem.* **97**, 1158 (1993).

[214] C. Daniel, M. Dupuis, *Chem. Phys. Lett.* **171**, 209 (1990).

[215] D. Davis, K, Sreekumar, Y. Sajeev, S. Pal, *J. Phys. Chem. B* **109**, 14093 (2005).

[216] H. Årgen, O. Vahtras, H. Koch, P. Jørgensen, *J. Chem Phys.* **98**, 6417 (1993).

[217] K. V. Mikkelsen, Y. Luo, H. Årgen, P. Jørgensen, *J. Chem. Phys.* **102**, 9362 (1994).

[218] B. Champagne, E. A. Perpete, D. Jacquemin, S. J. A. van Gisbergen, E. -J. Baerends, C. Soubra-Ghaoui, K. A. Robins, B. Kirtman, *J. Phys. Chem. A* **104**, 4755 (2000).

[219] B. Champagne, *Chem. Phys. Lett.* **261**, 57 (1996).

[220] O. Quineta, B. Champagne, B. Kirtman, *J. Mol. Struct.:THEOCHEM* **633**, 199 (2003).

[221] R. M. Dreisler and E. K. U. Gross, *Density Functional Theory*, Springer, Berlin, (1990).

[222] A. M. Köster, P. Calaminici, R. Flores-Moreno, G. Geudtner, A. Goursot, T. Heine, A. Ipatov, F. Janetzko, J. Martin del Campo, S. Patchkovskii, J.U. Reveles, D.R. Salahub, A. Vela, *The deMon Developers*, Mexico (2006).

[223] A. M. Köster, R. Flores-Moreno, J.U. Reveles, *J. Chem. Phys.* **121**, 681 (2004).

[224] C. C. J. Roothaan, *Rev. Mod. Phys.* **23**, 69 (1951).

[225] J.U. Reveles, A.M. Köster, *J. Comput. Chem.* **25**, 1109 (2004).

[226] H.-J. Werner, W. Meyer, *Mol. Phys.* **31**, 855 (1976).

[227] G.D. Zeiss, W.R. Scott, N. Suzuki, D.P. Chong, S.R. Langhoff, *Mol. Phys.* **37**, 1543 (1979).

[228] M. Jaszu'nski, B.O. Roos, *Mol. Phys.* **52**, 1209 (1984).

[229] B.O. Roos, A.J. Sadlej, *Chem. Phys.* **94**, 43 (1985).

[230] M. Krack, *private communication.*

[231] C. Møller, M. S. Plesset, *Phys. Rev.* **46**, 618 (1934).

[232] M. W. Schmidt, K. K. Baldridge, J. A. Boatz, S. T. Elbert, M. S. Gordon, J. H. Jensen, S. Koseki, N. Matsunaga, K. A. Nguyen, S. J. Su, T. L. Windus, M. Dupius, J. A. Montgomery, *J. Comput. Chem.* **14**, 1347 (1993).

[233] J. L. Martins, J. Buttet, and R. Car, *Phys. Rev. B* **31**, 1804 (1985).

[234] G. Herzberg, *Molecular Spectra and Molecular Structure, I. Spectra of Diatomic Molecules*, Van Nostrand Reinhold, New York, (1950).

[235] K. K. Verma, J. T. Bahns, A. R. Rajaei-Rizi, W. C. Stwalley, and W. T. Zemke, *J. Chem. Phys.* **78**, 3599 (1983).

[236] T. A. Dahlseid, M. M. Kappes, J. A. Pople, and M. A. Ratner, *J. Chem. Phys.* **96**, 4924 (1992).

[237] P. Sykes, *A guide book to mechanism in inorganic chemistry*, Orient Longman, New Delhi (1986).

## List of Publications

1. *Ab initio and density functional studies of response electric properties of para-nitroaniline (PNA) and its derivatives*,
   **K. B. Sophy** and S. Pal
   *In preparation.*

2. *Density functional static polarizability and first-hyperpolarizability calculations of $Na_n$ (n=2,4,6,8) clusters using an approximate CPKS method and its comparison with MP2 calculations*,
   **K. B. Sophy**, P. Calaminici and S. Pal
   J. Chem. Theory and Comp. *In Press.*

3. *Density functional response approach for electric properties of molecules*,
   S. Pal and **K. B. Sophy**
   In *Lecture Series on Computer and Computational Sciences*, Brill Academic Publishers: Netherlands **3**, 142-151 (2005).

4. *Electric properties of BH, CO and H2O molecules by density functional response approach*,
   **K. B. Sophy** and S. Pal
   J. Mol. Struc.: THEOCHEM **676**, 89-95 (2004).

5. *Density functional response approach for the linear and nonlinear electric properties of molecules*,
   **K. B. Sophy** and S. Pal
   J. Chem. Phys. **118**, 10861-10866 (2003).